



Institute of Biomechanics
Center of Biomedical Engineering
Kronesgasse 5-I
8010 Graz, Austria

Diploma Thesis

**Biaxial mechanical investigation of human
ventricles myocardium**

to achieve the degree of
Dipl.Ing.

Author: Kresnik Roland

Supervisor: Gerhard Sommer, Dipl.-Ing. Dr.techn.

Head of Institute: Professor Gerhard A. Holzapfel, PhD

April 27, 2012

Contents

1	Introduction	1
1.1	Soft tissue biomechanics in general	1
1.2	Motivation	2
1.2.1	Anatomy of the heart	4
1.2.2	Structure of the heart tissue	6
1.2.2.1	Cardiomyocytes	6
1.2.2.2	Heart muscle fibers	6
1.2.2.3	Stiffness of the passive heart muscle	8
1.2.2.4	Contour length and persistence length	10
1.2.2.4.1	Formal description of contour length	10
1.2.2.4.2	Formal description of persistence length	10
1.2.2.5	Referring from contour length and persistence length to the stiffness of the specific filaments of the heart tissue	10
1.2.2.6	Collagen of the human myocardium	11
1.2.2.6.1	Cardiac collagen changes in health and disease	12
1.2.3	Chronological history of conducted biaxial tensile tests and occurred problems in the literature	13
1.2.4	Summary of the facts - What is still required?	14
1.2.4.1	Status quo of the human heart tissue	14
1.2.4.2	Status quo of the mechanical behavior of human heart tissue	14
1.2.4.3	Theoretical material modeling of human myocardium	15
2	Material and methods	17
2.1	Materials	17
2.1.1	Origin of the myocardial tissue	17
2.1.2	Porcine heart tissue	17
2.1.3	Human myocardial tissue from the Institute for Pathology	18
2.1.4	Human myocardial tissue from the Clinical Department of Transplantation Surgery	18
2.2	Methods	21
2.2.1	Transport and storage of the myocardial tissue	21
2.2.1.1	Storage and transport of Porcine heart tissue	21
2.2.1.1.1	Storage in PBS - solution	21
2.2.1.1.2	Storage in 'standard cardioplegical solution'	21

2.2.1.2	Storage and transport of human myocardial tissue from the Institute of Pathology	22
2.2.1.2.1	Storage and autolysis	22
2.2.1.3	Storage and transport of human myocardial tissue from the Clinical Department of Transplantation Surgery . .	22
2.2.1.3.1	Importance of storage method according to prevent activation of tissue	22
2.2.2	Biaxial testing device and test equipment	23
2.2.2.1	Principle of measuring with the biaxial testing device .	23
2.2.2.2	Carriage device, hooks and cords	25
2.2.2.3	Overview of the solutions used for the biaxial tensile tests	27
2.2.2.3.1	PBS solution	27
2.2.2.3.2	Cardioplegical solution	28
2.2.2.3.3	Potassium buffered cardioplegical solution . .	28
2.2.2.3.4	Potassium buffered Ringer solution	29
2.2.3	Preparing the specimen	30
2.2.3.1	Tools for specimen preparation	30
2.2.3.2	Method of specimen separation	31
2.2.3.2.1	Porcine heart	31
2.2.3.2.1.1	Separating the ventricles and the septum	32
2.2.3.2.1.2	Consistence of porcine myocardium tissue	32
2.2.3.2.1.3	Specimen separation for the combined biaxial tensile test and triaxial shear test	32
2.2.3.2.2	Human heart tissue	33
2.2.3.2.2.1	Consistence of the human myocardial tissue	34
2.2.4	Setup and mounting the specimen into the biaxial testing device .	35
2.2.4.1	Attaching the hooks to the specimen	35
2.2.4.2	Marker and marker position	36
2.2.4.3	Inserting the specimen into the testing device and calibration of the optical measuring system for the marker detection	36
2.2.5	Measurement and loading protocol	37
2.2.5.1	Loading protocol for biaxial tensile tests	37
2.2.6	Data acquisition, data analysis and mathematical background . . .	37
2.2.6.1	Data analysis and smoothing	38
2.2.6.1.1	Stretch-controlled protocol	39
2.2.6.1.2	Cauchy-stress calculation	39
2.2.6.2	Data analysis with Matlab	40

3	Results	43
3.1	Porcine myocardium	44
3.1.1	Porcine hearts at fresh state	46
3.1.2	Frozen porcine hearts	46
3.1.3	Representative plot with different ratios and overall plot	46
3.2	Human heart tissue	55
3.2.1	Human hearts from the Clinical department of Transplantation Surgery	55
3.2.1.1	Heart with the index Transplant# 1	55
3.2.1.2	Heart with the index Transplant# 2	55
3.2.1.3	Heart with the index Transplant# 3	56
3.2.1.4	Heart with the index Transplant# 4	57
3.2.2	Human heart tissue from the Institute of Pathology	58
3.2.3	Heart with the index MYO 1/12	59
3.2.4	Heart with the index MYO 2/12	59
3.2.5	Heart with the index MYO 3/12	69
3.2.6	Calculating tables for human hearts	70
3.2.6.1	Calculating table of Heart with the index Transplant#1	71
3.2.6.2	Calculating table of Heart with the index Transplant#2	71
3.2.6.3	Calculating table of Heart with the index Transplant#3	72
3.2.6.4	Calculating table of Heart with the index Transplant#4	73
3.2.6.5	Calculating table of Heart with the index Myo1/12	73
3.2.6.6	Calculating table of Heart with the index Myo2/12	74
3.2.6.7	Calculating table of Heart with the index Myo3/12	74
4	Discussion	79
4.1	Porcine myocardial tissue	79
4.2	Human myocardial tissue	80
4.2.1	Result and comparison of the different datasets	81
4.2.2	Autolysis and activation	83
4.2.3	Heart related diseases and age related changes in structure	84
5	Appendix	85
5.1	Ethics applicant	86
5.1.1	Ethics comission humble	99

List of Figures

1.1	General arrangement of subepicardial fibers over the ventricles (Greenbaum et al., 1981)	3
1.2	Orientation of the fibers shown on a removed block from the human myocardium showing the fiber angles taken from Greenbaum et al. (1981)	3
1.3	3D-model showing the fibers and sheets direction in the heart taken from Rohmer et al. (2006)	4
1.4	Principle schematic of a human heart including formal directions (Texas-Heart-Institute, 2012)	4
1.5	Layers in the heart wall (Medic on Web, 2012)	5
1.6	Schematic of a typical eucaryotic cell with organelles (Holzapfel, 2010)	6
1.7	Components of the muscle sacromere. The A-band comprises thick filaments (TF) and the I-band comprises thin filaments (tf). The (z-line, Z-band, and the label Z) forms the sacromere boundary and is at the center of the I-band. The H-zone (H) is the central A-band region taken from The-Cardio-Researched-Web-Project (2012)	7
1.8	Sliding filament model of muscle contraction. Defined positions of titin, myosin, and actin inside the sacromere of a muscle fiber Richfield (2008)	8
1.9	Connective tissue skeleton of human heart sectioned transversely. Its organization is similar to a honeycomb. The perimysium (P) envelops groups of myocytes. The endomysium, as final arborization of the perimysium, supports and connects individual cells. The endomysial weave (W) envelops each individual myocyte and is connected to adjacent myocytes by lateral struts (s) presenting branches of variable size and extension. The range of length and diameter of these struts is very broad. Collagen struts also connect myocytes to interstitial microvessels (blue arrow) or perimysium (red arrow) (Rossi et al., 1998)	9
1.10	Schematic of thermally fluctuating filaments of contour lengths L_c at two points t_1 and t_2 in time: : the more rigid the filament the larger the persistence length and the smaller the curvature. For a flexible filament ($lp \ll L_c$) the conformational entropy dominates so that the orientational order is destroyed (top). Balance between thermal fluctuations and stiffness is characteristic for a semi-flexible filament ($lp \sim L_c$) (middle), while for a rigid filament the thermal energy is not sufficient to introduce a bend in its contour ($lp \gg L_c$) (Holzapfel, 2010).	11
2.1	Picture of a porcine heart, anterior view, including aorta valves, atriums and ventricles	18
2.2	Picture from the left ventricles of a pathological human heart. Left ventricles is cut into half from basal to apical direction (standard pathological surgery cut) after the pathological investigation.	19
2.3	Picture from the left ventricles free wall tissue (right) and tissue from the septum (left) of a human heart from the Clinical Department of Transplantation Surgery.	20
2.4	Schematic of the biaxial testing device from Yin et al. (1987) including optical detection system, bath for testing solution and the motor controlled carriage system. The specimen is placed in the middle of the bath and connected with each slide using silk cords.	23
2.5	Principle of the data acquisition and data collection according to the biaxial testing device developed by the Institute of Biomechanics and the Messphysik company	24
2.6	Non-linear stress force on the cords according to the carriage device depending on the attachment of the cords. The diagram shows the undiserable traverse force F_t , which occurs as a non-homogeneous force displacement on the specimen.	25
2.7	New developed carriage device with almost 'linear' forces. The new attachment system also provides the detach of the cords during the measurement cycles.	26
2.8	Picture of the surgery cords and fishing hooks used for fitting the specimen into the biaxial testing device.	26
2.9	The defined regions for specimen separations including reference axis and directions for the exactly description of the origin of the specimen extraction. For human myocardial tissue the thickness of the ventricles is too small to separate the heart wall into the 3 defined layers (epicardial, endocardial, and central), so the separated specimens removed from human hearts are generally defined as procured from central location.	30
2.10	This picture shows the different steps of specimen preparation from the PIG Heart #3 for the biaxial tensile tests. The different steps are signed with numbers from one to six. Step 1: cutting axes for apex and atriums; Step 2: cutting of the right ventricles (a) from the septum and left ventricles (b) using the cutting axes; Step 3: cutting axes for separating the left ventricles (c) from the septum (d); Step 4: separated parts of the heart as described; Step 5: extracted tranches from the left ventricles of the PIG Heart #3; Step 6: separating of one specimen for the biaxial tensile test out of one tranche extracted in step 5.	31
2.11	This figure shows a basal to apical cutting plain(2) for the extraction of myocardial tissue (1) used for the combined triaxial shear test of the left ventricles of Pig Heart#3, chronological between the steps four and five shown in Fig. 2.10, and the extracted slice (3)	33

2.12	Preparation sequence of pathological heart Myo3/12; Steps of separation shown chronological from one to five; Step 1: Picture of the frontal left ventricles freewall anterior (definition see Fig. 2.9) received from the Department of Pathology with the index Myo3/12; Step 2: Separated LAD - coronary artery (a) and the cutting-plane for removing the pericard and the tranche from the myocard using the cutting axes shown in Fig. 2.13. Step 3: picture of separated pericard (b), tranche for specimen extraction (c) and the epicardial tissue (d) including the axis for mean fiber direction. The violet arrows shows inhomogeneous regions of the tranche ; Step 4 and 5: Region for specimen separation depending on the available size of the tissue and the compromise choosing the TDMFD (Tissue depending mean-fiber direction) instead of the MFD (Mean-fiber direction) showing the deviation angle β .	34
2.13	Cutting sequence for separating the tranche for the specimen out of the pathological tissue of Myo3/12.	35
2.14	Cutting sequence for separating the slice for the specimen out of the pathological tissue of Myo3/12.	36
2.15	Schematic of different loadings according to the loading protocols. The pictures a) to e) show the different stretch ratios between the fiber direction and the cross-fiber direction. A ratio of 1 : 1 means a stretch ratio of 100% in f_0 axis and 100% in f_x axis [fiber direction : cross-fiber direction]. Different loadings: a) $f_0 : f_x = 1 : 1$; b) $f_0 : f_x = 1 : 0.75$; c) $f_0 : f_x = 1 : 0.5$; d) $f_0 : f_x = 0.75 : 1$; e) $f_0 : f_x = 0.5 : 1$	38
2.16	GUI (Graphical User Interface) created in Matlab 2009a for data analysis of data received from the biaxial testing system. The plotted data are from a porcine heart with the index PigHeart#4 left ventricles epicardial, showing the different stretch ratios from the stretch protocol at five percent stretch. MFD (Mean-fiber direction) and CFD (Cross-fiber direction) are plotted separately in the left two plots, and an overlapping plot of both for analyzing the mechanical behavior in the center of the GUI.	40
2.17	Stress-Strain plot for 7.5% stretch protocol with different ratios of pathological heart PatoTU1/12; Plots are shown as unfiltered in section A, filtered in section B and afferent part only in section C.	41
2.18	Schematic diagram of: (a) the left ventricle and a cutout from the equator; (b) the structure through the thickness from the epicardium to the endocardium; (c) five longitudinal circumferential sections at regular intervals from 10 to 90 per cent of the wall thickness from the epicardium showing the transmural variation of layer orientation; (d) the layered organization of myocytes and the collagen fibers between the sheets referred to a right-handed orthonormal coordinate system with fiber axis f_0 , sheet axis s_0 and cross-fiber axis n_0 ; and (e) a cube of layered tissue with local material coordinates (X_1, X_2, X_3) serving as the basis for the geometrical and constitutive model (Holzapfel and Ogden, 2009).	42
3.1	Stress-stretch datasets from porcine hearts at fresh state. The plotted datasets are measured at a stretch level of 7.5% at a Stretch ratio from 1:1 (see Chapt. 2.2.5.1). All plotted datasets are listed in Tab. 3.1 with its origin, the heart number and specimen number according to their legend index.	46
3.2	Stress-stretch datasets from fresh state. The plotted datasets are measured at a stretch level of 10% at a Stretch ratio from 1:1 (see Chapt. 2.2.5.1). All plotted datasets are listed in Tab. 3.1 with its origin, the heart number and specimen number according to their legend index. Because of the large amount of data, the datasets are plotted as loading path.	47
3.3	Stress-stretch datasets from porcine hearts at fresh state. The plotted datasets are measured at a stretch level of 15% at a Stretch ratio from 1:1 (see Chapt. 2.2.5.1). All plotted datasets are listed in Tab. 3.1 with its origin, the heart number and specimen number according to their legend index. Because of the large amount of data, the datasets are plotted as loading path.	49
3.4	Stress-stretch datasets from porcine hearts at fresh state. The plotted datasets are measured at a stretch level of 10% at a stretch ratio from 1:1 (see Chapt. 2.2.5.1). All plotted datasets are listed in Tab. 3.1 with its origin, the heart number and specimen number according to their legend index. Because of the large amount of data, the datasets are plotted as loading path.	50
3.5	Stress-stretch datasets from porcine hearts at fresh state. The plotted datasets are measured at a stretch level of 15% at a Stretch ratio from 1:1 (see Chapt. 2.2.5.1). All plotted datasets are listed in Tab. 3.1 with its origin, the heart number and specimen number according to their legend index.	51
3.6	Stress-stretch datasets from porcine hearts at fresh state. The plotted datasets are measured at a stretch level of 15% at a Stretch ratio from 1:1 (see Chapt. 2.2.5.1). All plotted datasets are listed in Tab. 3.1 with its origin, the heart number and specimen number according to their legend index. Because of the large amount of data, the datasets are plotted as loading path.	52
3.7	Stress-stretch datasets from porcine hearts at fresh state. The plotted datasets are measured at a stretch level of 7.5% at a Stretch ratio from 1:1 (see Chapt. 2.2.5.1). All plotted datasets are listed in Tab. 3.1 with its origin, the heart number and specimen number according to their legend index.	53
3.8	All datasets from porcine hearts at fresh state.	54
3.9	Stress-stretch datasets from porcine heart with the index PIG# 4. The plotted representative datasets are measured at a stretch level of 10% at different stretch ratios (see Chapt. 2.2.5.1).	54
3.10	Stress-stretch datasets from Heart Transplant#1 at a stretch level of 5% including all different ratios (see Chapt. 2.2.5.1).	56
3.11	Stress-stretch datasets from Heart Transplant#1 at a stretch level of 7.5% including all different ratios (see Chapt. 2.2.5.1).	57
3.12	Stress-stretch datasets from Heart Transplant#2 at a stretch level of 5% including all different ratios (see Chapt. 2.2.5.1).	58
3.13	Stress-stretch datasets from Heart Transplant#2 at a stretch level of 7.5% including all different ratios (see Chapt. 2.2.5.1).	58
3.14	Stress-stretch datasets from Heart Transplant#3 at a stretch level of 5% including all different ratios (see Chapt. 2.2.5.1).	60
3.15	Stress-stretch datasets from Heart Transplant#3 at a stretch level of 7.5% including all different ratios (see Chapt. 2.2.5.1).	60
3.16	Stress-stretch datasets from Heart Transplant#3 at a stretch level of 10% including all different ratios (see Chapt. 2.2.5.1).	61
3.17	Stress-stretch datasets from Heart Transplant#3 at a stretch level of 12.5% including all different ratios (see Chapt. 2.2.5.1).	61

3.18 Stress-stretch datasets from Specimen #1 of the Heart Transplant#4 at a stretch level of 5% including all different ratios (see Chapt. 2.2.5.1).	63
3.19 Stress-stretch datasets from Specimen #1 of the Heart Transplant#4 at a stretch level of 7.5% including all different ratios (see Chapt. 2.2.5.1).	63
3.20 Stress-stretch datasets from Specimen #1 of the Heart Transplant#4 at a stretch level of 10% including all different ratios (see Chapt. 2.2.5.1).	64
3.21 Stress-stretch datasets from Specimen #1 of the Heart Transplant#4 at a stretch level of 12.5% including all different ratios (see Chapt. 2.2.5.1).	64
3.22 Stress-stretch datasets from Specimen #2 of the Heart Transplant#4 at a stretch level of 5% including all different ratios (see Chapt. 2.2.5.1).	65
3.23 Stress-stretch datasets from Specimen #2 of the Heart Transplant#4 at a stretch level of 7.5% including all different ratios (see Chapt. 2.2.5.1).	65
3.24 Stress-stretch datasets from Specimen #2 of the Heart Transplant#4 at a stretch level of 10% including all different ratios (see Chapt. 2.2.5.1).	66
3.25 Stress-stretch datasets from the Heart with the index Myo 1/12 at a stretch level of 12.5% including all different ratios (see Chapt. 2.2.5.1).	67
3.26 Stress-stretch datasets from the Heart with the index Myo 1/12 at a stretch level of 15% including all different ratios (see Chapt. 2.2.5.1).	68
3.27 Stress-stretch datasets from the Heart with the index Myo 2/12 at a stretch level of 5% including all different ratios (see Chapt. 2.2.5.1).	69
3.28 Stress-stretch datasets from the Heart with the index Myo 2/12 at a stretch level of 7.5% including all different ratios (see Chapt. 2.2.5.1).	69
3.29 Stress-stretch datasets from the Heart with the index Myo 2/12 at a stretch level of 10% including all different ratios (see Chapt. 2.2.5.1).	70
3.30 Stress-stretch datasets from the Heart with the index Myo 2/12 at a stretch level of 12.5% including all different ratios (see Chapt. 2.2.5.1).	70
3.31 Stress-stretch datasets from the Heart with the index Myo 3/12 at a stretch level of 10% including all different ratios (see Chapt. 2.2.5.1).	71
3.32 Stress-stretch datasets from the Heart with the index Myo 3/12 at a stretch level of 12.5% including all different ratios (see Chapt. 2.2.5.1).	72
3.33 Stress-stretch datasets from the Heart with the index Myo 3/12 at a stretch level of 15% including all different ratios (see Chapt. 2.2.5.1).	72

List of Tables

1.1	Thickness of the myocardium depending on species and location	5
1.2	Stiffness of different filaments in the heart tissue according to their persistence length l_p and their contour length L_c . Data references: aktin and microtubuli by Gittes et al. (1993), collagen by Sun et al. (2004), spectrin by Li et al. (2005) and Svoboda et al. (1992), elastin by Baldock et al. (2011), GAG by Ng L. (2005), hyalauron by Fujii et al. (2002), intermediate filaments by Hohenadl et al. (1999)	12
2.1	Recipe of PBS solution used for solution bath	27
2.2	Recipe of 'standard cardioplegical solution' used for solution bath	28
2.3	Recipe of potassium buffered Ringer-'Fresenius' solution used for solution bath	29
3.1	Index of the hearts for the biaxial tensile tests, including origin and state	43
3.3	Calculating table for the porcine hearts tensile test from the LV at a stretch value of 7.5% .This table includes the calculated data for the hysteresis areas HA within the stress-stretch curve and the maximum forces for each direction (fiber direction FD and cross-fiber direction CFD) from the dataset shown in Fig. 3.1.	47
3.4	Calculating table for the porcine hearts tensile test from the LV at a stretch value of 10% .This table includes the calculated data for the hysteresis areas HA within the stress-stretch curve and the maximum forces for each direction (fiber direction FD and cross-fiber direction CFD) from the dataset shown in Fig. 3.2.	48
3.5	Calculating table for the porcine hearts tensile test from the LV at a stretch value of 15% .This table includes the calculated data for the surface areas SA within the stress-stretch curve and the maximum forces for each direction (fiber direction FD and cross-fiber direction CFD) from the dataset shown in Fig. 3.3.	49
3.6	Calculating table for the porcine hearts tensile test from the septum at a stretch value of 10%. This table includes the calculated data for the hysteresis areas HA within the stress-stretch curve and the maximum Cauchy stresses for each direction (fiber direction FD and cross-fiber direction CFD) from the dataset shown in Fig. 3.4.	50
3.7	Calculating table for the porcine hearts tensile test at defrosted state from the LV at a stretch value of 10% .This table includes the calculated data for the hysteresis areas HA within the stress-stretch curve and the maximum Cauchy stresses for each direction (fiber direction FD and cross-fiber direction CFD) from the dataset shown in Fig. 3.5.	51
3.8	Calculating table for the porcine hearts tensile test at defrosted state from the LV at a stretch value of 15% .This table includes the calculated data for the hysteresis areas HA within the stress-stretch curve and the maximum Cauchy stresses for each direction (fiber direction FD and cross-fiber direction CFD) from the dataset shown in Fig. 3.6.	52
3.9	Calculating table for the porcine hearts tensile test at defrosted state from the LV at a stretch value of 7.5% .This table includes the calculated data for the surface areas within the stress-stretch curve and the maximum Cauchy stresses for each direction (fiber direction FD and cross-fiber direction CFD) from the dataset shown in Fig. 3.7.	53
3.10	Information about the donors according to the heart indexes, including the used solution during the tests. The index Pa stands for the additive of potassium, RFS for Ringer- Fresenius solution, SCS for standard cardioplegical solution, hypo for hypotrophy, ad for adipose, ddf for dyastolic dysfunction, sc for coronar sclerose.	55
3.11	Index of plotting curves of human heart with the heart index Transplant#1.	56
3.12	Index of plotting curves of human heart with the heart index Transplant#2.	57
3.13	Index of plotting curves of human heart with the heart index Transplant#3.	59
3.14	Index of plotting curves of human heart with the heart index Transplant#4.	62
3.15	Information about the donors according to the heart indexes, including the used solution during the tests. The index Pa stands for the additive of potassium, RFS for Ringer- Fresenius solution, SCS for standard cardioplegical solution, hypo for hypotrophy, ad for adipose, ddf for dyastolic dysfunction, sc for coronar sclerose.	66
3.16	Index of plotting curves of human heart with the heart index Myo 1/12.	67
3.17	Index of plotting curves of human heart with the heart index Myo 2/12.	68
3.18	Information about the donors according to the heart indexes, including the used solution during the tests	71
3.19	Calculating table for the datasets of specimen #1 of the heart with the index Transplant#1. This table includes the calculated data for the surface areas within the stress-stretch curve and the maximum Cauchy stresses for each direction (fiber direction FD and cross-fiber direction CFD) from the datasets listed in Tab. 3.11.	73
3.20	Calculating table for the datasets of specimen #1 of the heart with the index Transplant#2. This table includes the calculated data for the hysteresis areas HA within the stress-stretch curve and the maximum Cauchy stresses for each direction (fiber direction FD and cross-fiber direction CFD) from the datasets listed in Tab. 3.12.	73
3.21	Calculating table for the datasets of specimen #1 of the heart with the index Transplant#3. This table includes the calculated data for the surface areas within the stress-stretch curve and the maximum Cauchy stresses for each direction (fiber direction FD and cross-fiber direction CFD) from the datasets listed in Tab. 3.13.	74

3.22	Calculating table for the datasets of specimen #1 of the heart with the index Transplant#4. This table includes the calculated data for the hysteresis areas HA within the stress-stretch curve and the maximum Cauchy stresses for each direction (fiber direction FD and cross-fiber direction CFD) from the datasets listed in Tab. 3.14.	75
3.23	Calculating table for the datasets of specimen #2 of the heart with the index Transplant#4. This table includes the calculated data for the hysteresis areas HA within the stress-stretch curve and the maximum Cauchy stresses for each direction (fiber direction FD and cross-fiber direction CFD) from the datasets listed in Tab. 3.14.	76
3.24	Calculating table for the datasets of specimen #1 of the heart with the index Myo1/12. This table includes the calculated data for the hysteresis areas HA within the stress-stretch curve and the maximum Cauchy stresses for each direction (fiber direction FD and cross-fiber direction CFD) from the datasets listed in Tab. 3.24.	76
3.25	Calculating table for the datasets of specimen #1 of the heart with the index Myo2/12. This table includes the calculated data for the hysteresis areas HA within the stress-stretch curve and the maximum Cauchy stresses for each direction (fiber direction FD and cross-fiber direction CFD) from the datasets listed in Tab. 3.17.	77
3.26	Calculating table for the datasets of specimen #1 of the heart with the index Myo3/12. This table includes the calculated data for the hysteresis areas HA within the stress-stretch curve and the maximum Cauchy stresses for each direction (fiber direction FD and cross-fiber direction CFD) from the datasets listed in Tab. 3.18.	78
4.1	Mean value (mean) and standard deviation (SD) of datasets from porcine heart tissue separated from the LV at fresh state according to their maximum values for each direction and hysteresis areas HA.	80
4.2	Mean value (mean) and standard deviation (SD) of datasets from porcine heart tissue separated from the septum at fresh state according to their maximum values for each direction and hysteresis areas HA.	80
4.3	Relevant datasets from hearts of the Department of Transplant Surgery showing their maximum values for each direction and hysteresis areas HA.	81
4.4	Relevant datasets from Hearts of the Institute of Pathology showing their maximum values for each direction and hysteresis areas HA.	82
4.5	Mean value (mean) and standard deviation (SD) of datasets from Transplant heart tissue according to their maximum values for each direction and hysteresis areas HA.	82

Abstract

These days, one of the most common reason for mortality in our world are heart related diseases, such as cardiac fibrillation. According to the WHO report of 2012, the mortality rate related to those diseases is about 17.3 million and increasing every year. The pathophysiology of such issues seems to be directly related to the changes of elastic components in the tissue of the myocardium.

This Diploma Thesis treats the hardly explored area of the biomechanics of human myocardium. To better understand how such diseases can occur, its necessary to get more information about the structure and the mechanical behavior, which is closely linked with the electrophysiology of the heart tissue. This thesis is the first one, where biaxial tensile tests are done on human myocardium tissue, according to the existing literature up to now. The collected data in this thesis, in addition with data collected from triaxial shear test, should give digestion about the mechanical behavior of the human myocardium tissue, and with the addition of electrophysiology components, it should be able to create a realistic model of the human heart for further scientific findings.

The human myocardial tissue for the biaxial tensile tests was obtained from two different departments (Department of Transplant Surgery and Department of Pathology of the Medical University of Graz), so it was possible to perform test on myocardial tissue in 'dead' state and in 'deactivated' state. The tensile test are executed at different stretch levels while using a specified test protocol (with different ratios). According to the different tissue directions (fiber direction and mean-fiber direction) a relationship of both was defined. The tensile test were performed using different solutions for holding the tissue at an passive state. The specimens were separated from the left ventricle and the septum as a defined block of $2.5\text{cm} \times 2.5\text{cm} \times 3\text{mm}$. As basic data for the evaluation of the myocardial tissue, the calculated Cauchy-stress in order to the stretch level yield as significant data.

Evaluating the data from the biaxial tensile test, new scientific findings were made referring to appropriate use of cardioplegical solution in their use, as well as age related mechanical behavior of myocardial tissue. Furthermore important correlations between the anisotropic mechanical behavior of the tissue due the autolysis were detected.

Zusammenfassung

Eine der häufigsten Todesursachen der heutigen Zeit stellen Herzkrankheiten wie der Herzinfarkt dar. Laut dem WHO Bericht von 2012 liegt die Sterberate verursacht durch Herzkrankheiten bei 17.3 Millionen und diese Zahl nimmt auf Grund der stark alternden Bevölkerung jedes Jahr drastisch zu. Um diesem Trend entgegen zu wirken ist es notwendig neue Erkenntnisse im Bereich der Pathophysiologie solcher Erkrankungen zu erlangen. Es wird vermutet, dass diese Erkrankungen direkt im Zusammenhang mit den Änderungen der elastischen Komponenten des Myokards zusammenhängen.

Ziel dieser Arbeit ist es, den kaum erforschten Myokard anhand seiner biomechanischen Eigenschaften durch biaxiale Zugversuche zu untersuchen. Mit Hilfe der experimentell ermittelten Daten aus den biaxialen Zugversuchen, als auch triaxialen Scherversuchen, soll später in Verbindung mit dem Wissen der Elektrophysiologie, ein realistische Finite Elemente Methoden Simulation des Herzen realisiert werden.

Anfangen mit Gewebeproben vom Schwein, wurden nach genehmigter Ethik (durch die Ethikkommission der Medizinische Universität Graz), Humanproben des Myokards von zwei unterschiedlichen Institutionen (Institut für Pathologie, Klinische Abteilung für Transplantationschirurgie der Medizinischen Universität in Graz) für die Bestimmung der mechanischen Eigenschaften herangezogen. Dadurch war es erstmals möglich myokardiales Humangewebe im passiven und teilaktiven Zustand zu testen. Die Versuche wurden unter Berücksichtigung der unterschiedlichen Orientierungen (Faserrichtung und Querfaserrichtung) gemessen und deren Relation zueinander bestimmt. Hierfür wurden unterschiedliche Lösungen verwendet um das Gewebe in einem definierten passiven Zustand zu halten. Die separierte Probengröße beträgt $2.5\text{cm} \times 2.5\text{cm} \times 3\text{mm}$. Als Bewertungsgrundlage für die mechanischen Eigenschaften dient der Cauchy-Spannung der in Abhängigkeit des ausgeübten Dehnungen (Streckungen) betrachtet wird.

Die Evaluierung der gesammelten Daten ergab neue Erkenntnisse im Bezug auf den Einsatz kardioplegischer Lösungen, sowie auch die altersabhängige Veränderung des mechanischen Verhaltens des Myokards. Weitere Erkenntnisse über die Änderung des anisotropen Verhalten des Myokardgewebes im Zuge der Autolyse wurden erkannt.

Acknowledgment

I would like to phrase my thankfulness to all people, who supported me during this thesis. First of all i acknowledge my supervisor and friend Dipl.-Ing. Dr.techn. Gerhard SOMMER for his great support.

I also acknowledge the honest Head of the Institute of Biomechanics at the technical University of Graz Univ.-Prof. Dipl.-Ing. Dr.techn. Gerhard A. HOLZAPFEL for providing the test equipment and the appliance during this thesis.

I also want to thank Michaela SCHWARZ, MD, Michael SACHERER, MD and Aris VAFIADIS for providing human samples from the Clinical Department of Transplant Surgery (LKH-University Clinic Graz) and Peter REGITNIG, MD as well as Christian VIERTLER, MD from the Institute of Pathology (Medical University, Graz) and their professional advice during this thesis.

So und jetzt in German:

Ich bedanke mich vor allem bei meinen Eltern f'r das ermöglichen des Studiums und vor allem dafür, dass sie mich mit aller Kraft unterstützt haben und auch in schwierigen Zeiten immer zur Seite gestanden sind. Ein eben so grosser Dank gebührt meinem Schatzi Regina, die mich die letzten Jahre aushalten musste, und mir immer mit Rat und Tat zur Seite stand. Und nicht zu vergessen alle meine Freunde, vor allem meinen Leidensgenossen Michi alias MasterKuz, der mir bei der endlosen Arbeit im Labor immer zu guter Laune verholfen hat. Wahrscheinlich hab ich in meiner Hektik gerade einige Leute vergessen, war sicher keine Absicht, ich danke euch allen.

1 Introduction

1.1 Soft tissue biomechanics in general

Biomechanics is the study of the structure and function of biological systems, which tries to attempt the mechanical connection of both. The main aim of soft tissue biomechanics is to create models which try to describe the behavior of any biological system. It is necessary to describe the mechanical behavior of such a system to find out how the inner working of a cell and the mechanical properties of soft tissue interact. One of the most remarkable characteristic of biomaterials is their hierarchical structure. This requires especially a deep understanding of the hierarchical structure of biological materials. Rohmer et al. (2006) said that the necessary main division of soft tissue biomechanics is the continuum mechanics, which deals with the analysis of the kinematics and the mechanical behavior of materials, modelled as a continuous mass rather than as discrete particles.

Another motivating statement for the necessary of soft tissue biomechanics is given by Humphrey (2002):

‘Because of the complexity of tissue structure and behavior, there is a need for sophisticated theoretical ideas; because of a continuing lack of data, there is a need for new, clever experiments; because of the geometric complexity of cells, tissues and organs, there is a need for robust computational methods; and because of the morbidity and mortality that results from disease and injury, there is a need for improved modalities for diagnosis and treatment’.

Structure knowledge and continuum mechanics are tools, which are needed to create a working constitutive model. This model describes the essential mechanical behavior in a way, that other sciences, for example the tissue engineering, can be based on those results to develop tissue equivalents. So in fact, biomechanics is the necessary basic research in biological systems - based on mechanical conditions- so that constitutive material models can be developed and FEM (finite element methods) simulations performed.

1.2 Motivation

This Diploma Thesis treats the hardly explored area of human myocardium. Nowadays, one of the most common reason for mortality in our world are heart related diseases, such as cardiac fibrillation. The pathophysiology of such issues seems to be directly related to the changes of elastic components in the tissue of the myocardium. In this regard Yin (1981) stated:

‘Quantification of ventricles wall stress is necessary for an understanding of both normal and pathological ventricles mechanics. At present there are no reliable means to measure, directly, wall stresses in the intact ventricle. Thus, we must rely on mathematical models to predict these stresses, knowing that the predictions cannot be validated directly’.

To better understand how such diseases can occur, its necessary to get more information about the structure and the mechanical behavior, which is closely linked with the electrophysiology of the heart tissue. So there is a need to do more fundamental research to understand the complex cardiac functionality of the human heart. An appropriate way to find out how this highly complex tissue of the human ventricles myocardium mechanics behave, is to perform biaxial tensile tests and also triaxial shear-testing. This is a quite effective way to determine the mechanical behavior of the tissue under stress, which act further as relevant data for a mathematical material model. We have to note, that the only ‘true’ biaxial experiment ever with different loadings in the two direction, performed on myocardium, was conducted over 23 years ago from Yin et al. (1987) - under former technical possibilities. Also only one shear experiment on porcine myocardial tissue exists in the literature from Dokos et al. (2002).

In this thesis, planar biaxial extension tests under state-of-the-art conditions should be offer new scientific findings. A basic for further considerations is the ‘fiber orientated schematic’ from Greenbaum et al. (1981) based on the inspection of cavity shape and subepicardial fiber orientation seen in Fig. 1.1 and the schematics for a separated block from the myocardium tissue in Fig. 1.2. The more complex fiber and sheet model developed from Rohmer et al.(2006) while using the DTMRT technology (Diffusion Tensor Magnetic Resonance Imaging) shown in Fig. 1.3 is also a basic model, and it has introduced the term of ‘sheet-direction’ in biomechanics. It is quite common, that the fibers are present in specific layers, called sheets, but their distribution in the human myocardium is still not scientifically established.

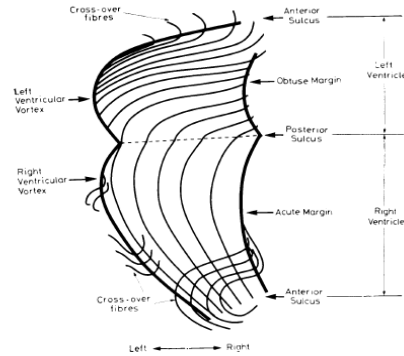


Figure 1.1: General arrangement of subepicardial fibers over the ventricles (Greenbaum et al., 1981)

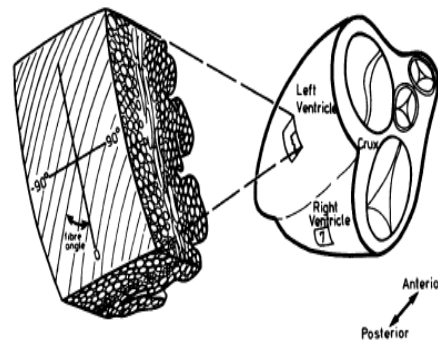


Figure 1.2: Orientation of the fibers shown on a removed block from the human myocardium showing the fiber angles taken from Greenbaum et al. (1981)

The aim of this study is the combination of biaxial tensile test and triaxial shear to get a better validity according to the mechanical behavior of the myocardium. Biaxial test data with different loading protocols and shear test data at different specimen orientations allows to adequately capture the direction-dependent material response. With these complete sets of mechanical data, combined with structural data, an appropriate material model and associated material parameters can be defined for the description of the mechanical behavior. Furthermore, these data give more insight in the function and influence of the muscle sheets in the myocardium.

The collected data in this Diploma Thesis should offer new information about the cardiac assembly of the human heart in several parts. These should be the basic for further scientific investigations.

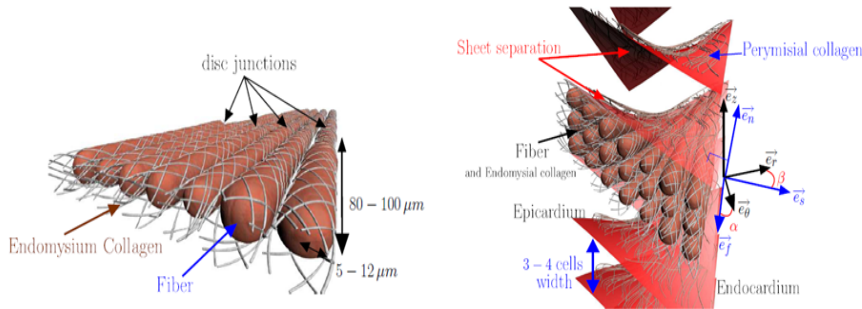


Figure 1.3: 3D-model showing the fibers and sheets direction in the heart taken from Rohmer et al. (2006)

1.2.1 Anatomy of the heart

The heart is the main part of the cardiovascular system. For the vertebrate organism the function of the heart is -for all species- nearly the same. It is a myogenic muscular organ with the main task to circulate the blood through the body. In this subsection only the human and the pig heart are considered because they have similar size; and the knowledge of the basic structure is essentially for understanding the importance of the experiments and their results according to this thesis. Fig. 1.4 shows the principle structure of the human heart.

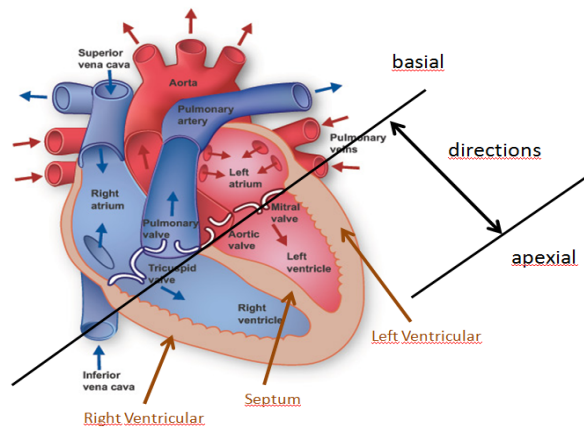


Figure 1.4: Principle schematic of a human heart including formal directions (Texas-Heart-Institute, 2012)

Generally the heart can be divided into four main chambers; the left ventricles and atrium, which belongs to the body-blood-circle and the right ventricles and atrium which is a part of the pulmonary-blood-

circle are the vena cava superior, the vena cava inferior and the pulmonary artery. The addition and disposals from the body-blood-circle are described as aorta and pulmonary vein. The heart also has an internal blood-circle-system, to supply the human heart muscle with nutrients and oxygen. Those blood vessels are called the coronary arteries. They also play a major role when inactivating the human heart muscle with specific solutions which will be explained in chapter refsusbubsec:kapitelsimulation-einfuehrung . At this point it is necessary to define significant directions to be more precisely when talking about different locations in the heart as seen in Fig. 1.4. Another necessary part for the the further experiments is to determine the different wall layers of the myocardium. There are three different layers; the endocardium which is the innerst layer; the myocardium (intermediate layer) , and the epicardium which is the outermost tissue layer of the heart wall. A schematic of the layersystem is shown in Fig. 1.5. In this figure, the individual wall components can

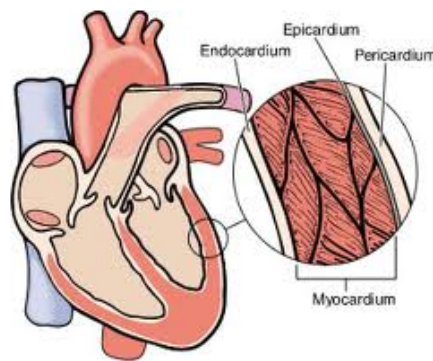


Figure 1.5: Layers in the heart wall (Medic on Web, 2012)

be distinguished. The outer smooth pericard with the embedded blood vessels, and the subepicardial adipose tissue follow the muscular layer of the heart wall, the myocardium. The inner layer is the endocardium. The fibers, which are individually directed outward to the apical heart direction, encircle both chambers - the left and the right ventricle. They are the basis of the myocardium, which is the the focus of the biaxial tensile test. There are several differences between the thickness of the myocardium depending on the different locations listed in Tab. 1.1.

Table 1.1: Thickness of the myocardium depending on species and location

	Left ventricles [mm]	Septum [mm],	Right ventricles [mm]
Human Heart	13 – 17	8 – 13	5 – 8
Pig Heart	16 – 30	15 – 25	6 – 13

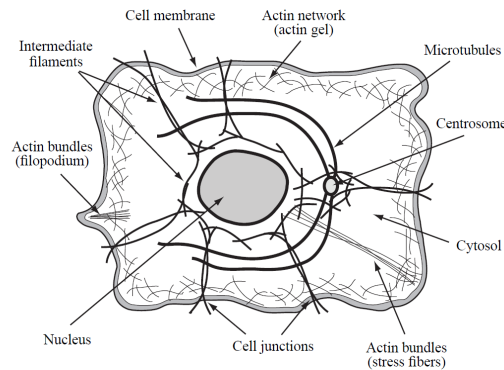


Figure 1.6: Schematic of a typical eucaryotic cell with organelles (Holzapfel, 2010)

1.2.2 Structure of the heart tissue

1.2.2.1 Cardiomyocytes

To understand the mechanical behavior of the heart tissue, it is important to look into the microscopic layer, to the smallest part - the eucaryotic cells. There are some essential components which are necessary for the functionality of such a eucaryotic cell (we are talking now of any cell). The main parts can be described as cytoskeleton (containing of the actin filaments, the intermediate filaments, the microtubules and spectrin), the cytosol, the cell membrane (consists of a semipermeable lipid bilayer with embedded proteins) and the cell junctions (relevant for the interaction of the cells). The cell is surrounded by the extracellular matrix (consists of protein, glycosaminoglycans, proteoglycans, collagen, elastin, adhesion proteins, integrins, macrophages and water).

Fig. 1.6 shows the principle assembly of an eucaryotic cell. Actin filaments (or thin filaments in muscle cells) are major constituents of the cytoskeletal network found in virtually all eukaryotic cells, and are essential mechanical components in a variety of cellular processes. Actin filaments are bundled in so-called stress fibers, and connect the intermediate filaments with the extracellular matrix of the cell. Those are the cytoskeletal filaments that have the structural size between the thin actin filaments and the thick microtubules. They have the property to increase the density in response to increased mechanical stress which can be applied to the eucaryotic cell. Now let's get more specific, talking about cardiovascular muscle cells. This specific eucaryotic cells are known as cardiomyocyte. At a more macroscopic layer we are talking now of 'heart muscle fibers'.

1.2.2.2 Heart muscle fibers

Cardiomyocytes are often branched, and contain one nucleus but many mitochondria, which provide the energy required for contraction. A feature of cardiac muscle is the presence of irregularly-spaced dark bands between myocytes. These are known as inter-

calated discs, and are due to areas where the membranes of adjacent myocytes come very close together. From a mechanical standpoint, intercalated discs are the glue that enables contractile force to be transmitted from one cardiomyocyte to another. Force generated by the motor protein myosin in the A-band thick filaments of cardiomyofibrils (about $2.5 \mu\text{m}$ long, $1 \mu\text{m}$ in diameter) is transmitted along the actin filaments in the I-bands to the Z-discs at the ends of the sarcomere shown in Fig. 1.7, and hence along adjacent myofibrills until the force reaches the intercalated discs membranes at ends of the cell (The-Cardio-Researched-Web-Project, 2012).

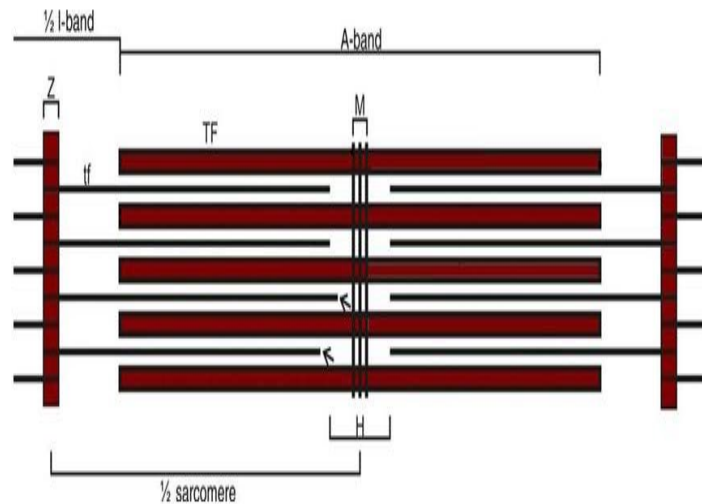


Figure 1.7: Components of the muscle sacromere. The A-band comprises thick filaments (TF) and the I-band comprises thin filaments(tf). The (z-line, Z-band, and the label Z) forms the sacromere boundary and is at the center of the I-band. The H- zone (H) is the central A-band region taken from The-Cardio-Researched-Web-Project (2012)

In this thesis, the precise detailing of this individual components are not being discussed, because this will exceed the scope of this work. However, important for understanding the mechanical behavior at this point, is the task of the proteins, which play a major role when talking about mechanical behavior of the myocardic muscle fibers. Stretched muscle fibers develop a resistive force, similar to an elastic band. For the magnitude of this resistive force some specific proteins are responsible. Perhaps the most important is titin, a fibrous protein that links the ends of the myosin molecule to the Z disks on either side, also keeping the myosin centered within the sarcomere. In Fig. 1.8 the placement of myosin, actin and titin inside the myocardic sacromere are mapped. All three are members of the intermediate filaments - where myosin and actin are the so called ‘motor proteins’. The connection of myosin to the actin filaments can be described as a motor unit - the interaction of both is essential for the muscle contraction (at this microscopic layer). The myosin filaments have at their border so-called ‘myosin heads’, which connect to the actin filaments under the

phosphorylation of ATP (Adenosine TriPhosphate), and walk along the actin filaments while reducing the ATP to ADP (Adenosine DiPhosphate). This occurs under normal condition - the cardiac muscle sarcomere is activated by signal proteins (interneurons) and the contraction follows (this is only a very simple description of the highly complex process).

We try to prevent the contraction of the fibers during the mechanical tests, because we want to determine the mechanics behavior under passive conditions (inactivated). Therefore, we use special solutions in which the cardiac tissue is inactivated during transport and mechanical testing. For the inactivated state the passive muscle fibers play the major role. When talking about passive muscle fibers, collagen, elastin, proteoglycans, glycosaminoglycans, same as the proteins titin, actin and myosin act as structure protein.

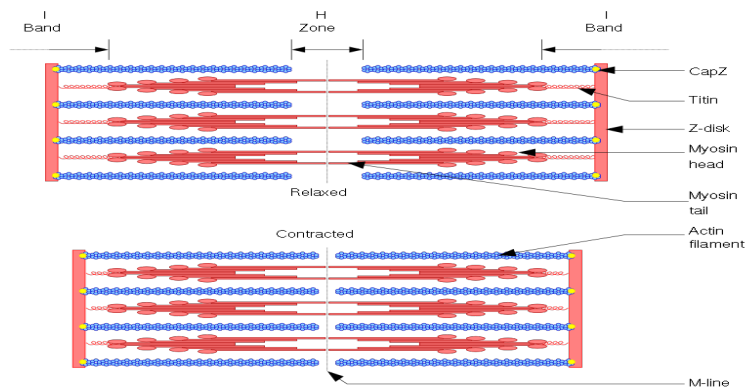


Figure 1.8: Sliding filament model of muscle contraction. Defined positions of titin, myosin, and actin inside the sarcomere of a muscle fiber Richfield (2008)

1.2.2.3 Stiffness of the passive heart muscle

Mainly responsible for the stiffness of passive heart fibers at a microscopic level are the structure proteins of the cytoskeleton and the extracellular matrix. The three types of filaments that make up the cytoskeleton are actin filaments, intermediate filaments, and microtubules. The interactive behavior of the three types of filaments significantly contributes to the mechanical behavior of the cell. But what is about the cell surroundings, the connective tissue between the cells - talking about tissue including the ECM (extracellular matrix) not only from cells?

Weber et al. (1993) introduced, that the extracellular tissue matrix - the 'stroma' of the heart - maintains the structure of the myocardium, determining tissue tensile strength and stiffness. So the main responsibility for the stiffness of the heart tissue depends on the connective tissue skeleton of the heart. Rossi et al. (1998) examined the stroma of the heart and divided the stroma into a three dimensional configuration of the cardiac collagen - which is mainly responsible for the stiffness of the tissue - by doing electron microscopy scans of the stroma. Rossi et al. (1998) defined the hierarchy as follows:

'The epimysium envelops the entire cardiac muscle; the perimysium, which is an extension of the epimysium, serves to enwrap groups of myocytes; and the endomysium, as final arborization of the perimysium, supports and connects individual cells. The endomysial weave envelops each individual myocyte and is connected to adjacent myocytes by lateral struts'.

He dissolved the cellular parts of the myocardial tissue and examined the non-cellular matrix - as a result he got a three dimensional picture of the collagen fibrils within the heart tissue shown in Fig. 1.9.

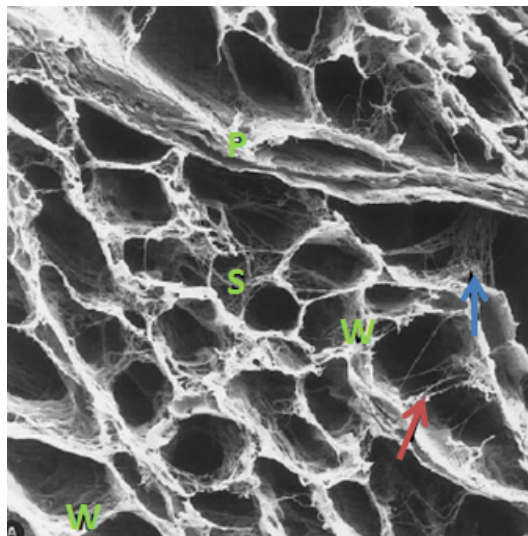


Figure 1.9: Connective tissue skeleton of human heart sectioned transversely. Its organization is similar to a honeycomb. The perimysium (P) envelops groups of myocytes. The endomysium, as final arborization of the perimysium, supports and connects individual cells. The endomysial weave (W) envelops each individual myocyte and is connected to adjacent myocytes by lateral struts (s) presenting branches of variable size and extension. The range of length and diameter of these struts is very broad. Collagen struts also connect myocytes to interstitial microvessels (blue arrow) or perimysium (red arrow) (Rossi et al., 1998)

This arrangement of the cardiomyocytes and the fibrous components of the stroma - the collagen - are representative for the stiffness of the muscle tissue. Now lets have a look at the physiological properties and the mechanical behavior of this filaments.

1.2.2.4 Contour length and persistence length

A good starting point for theoretical analysis of the viscoelastic properties of semiflexible filaments is to refer to the two significant quantities, the persistence length and the contour length. Those are for all filaments different and they can be used to find a inference between the different filament types and their stiffness. In this thesis no specific mathematical description will be done for the persistence length and the contour length; they are treated as already determined sizes known from further experiments. There are simple formal description of the contour length and the persistence length below, to understand what they are in general (Holzapfel, 2010).

1.2.2.4.1 Formal description of contour length

The contour length L_c is the total length of a filament, i.e. the length of the filament between two tie points or junctions. It is the filament length at the maximum physically possible extension. The contour length can be determined by the use of technologies like the ATM (Atomic Force Microscope) for each different filament.

1.2.2.4.2 Formal description of persistence length

The persistence length, say l_p , relates to a mechanical property quantifying the structural stiffness of the filaments. It is defined as:

$$l_p = \frac{K}{k_B * T} \quad E = I * K$$

E is the Young-modulus, I the area moment of inertia of the filament, k_B is the Boltzmann constant and T is the temperature (in Kalvin). The persistence length is determined when the bending energy equals the thermal energy. The persistence length is the maximum length over which the filament will appear straight in the presence of constant Brownian forces. It experiences in a medium at finite temperature.

1.2.2.5 Referring from contour length and persistence length to the stiffness of the specific filaments of the heart tissue

Single filaments may be categorized by three types, flexible, semi-flexible and rigid shown in Fig. 1.10, while each filament may be characterized by the contour length L_c and the persistence length l_p . A filament is considered as flexible when the the persistence length is much smaller than the contour length ($l_p \ll L_c$). The stiffness of different filaments in the heart tissue is shown in Tab. 1.2.

So referring to the experimental data, appending on the persistence length and contour length of the several filaments listed in Tab. 1.2, we can probably formulate some conclusion about the filaments behavior during biaxial tensile tests. As described in 1.2.2.3, the most relevant filament for tissue stiffness at a macroscopic layer is the collagen from the extracellular matrix of the cardiomyocytes. However, some filaments from the cytoskeleton, like the GAG and Actin (microscopic cell layer) have a much higher stiffness. The

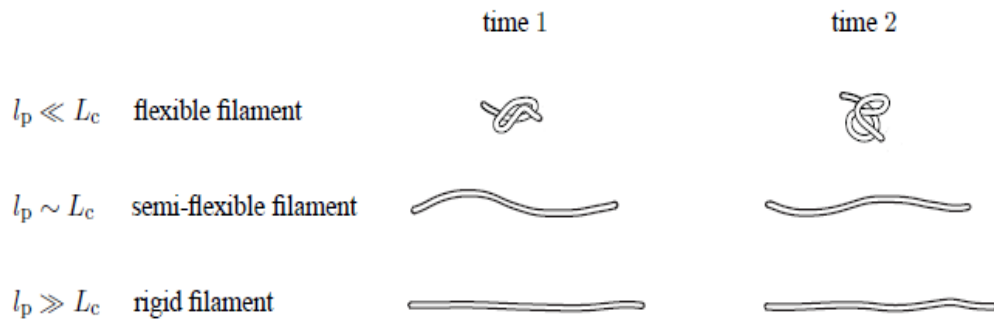


Figure 1.10: Schematic of thermally fluctuating filaments of contour lengths L_c at two points t_1 and t_2 in time: : the more rigid the filament the larger the persistence length and the smaller the curvature. For a flexible filament ($l_p \ll L_c$) the conformational entropy dominates so that the orientational order is destroyed (top). Balance between thermal fluctuations and stiffness is characteristic for a semi-flexible filament ($l_p \sim L_c$) (middle), while for a rigid filament the thermal energy is not sufficient to introduce a bend in its contour ($l_p \gg L_c$) (Holzapfel, 2010).

interaction and relevance of those filaments is up to now not clarified.

The results of the biaxial tensile test of the human myocardium is one step in the basic research for more insight, according to further studies about the interaction of all filaments and their mechanical behavior.

1.2.2.6 Collagen of the human myocardium

Weber (1989) examined the collagen structure of the human myocardium. Synthesized by cardiac fibroblasts, this fibrillar collagen supports and tether myocytes to maintain their alignment, whereas their respective tensile strength and resilience resist the deformation, maintain the shape and thickness, prevent the rupture and contribute to the passive and active stiffness of the myocardium. He also defined the main function of the cardiac collagen as follows:

‘Collagen fibers, the major structural protein of the interstitium, serve several functions: 1) they provide a scaffold that supports muscle cells and blood vessels; 2) they act as lateral connections between cells and muscle bundles to govern architecture while coordinating the delivery of force, generated by myocytes, to the ventricles chamber; and 3) their respective tensile strength and resilience are important determinants of diastolic and systolic myocardial

Table 1.2: Stiffness of different filaments in the heart tissue according to their persistence length l_p and their contour length L_c . Data references: aktin and microtubuli by Gittes et al. (1993), collagen by Sun et al. (2004), spectrin by Li et al. (2005) and Svoboda et al. (1992), elastin by Baldock et al. (2011), GAG by Ng L. (2005), hyalauron by Fujii et al. (2002), intermediate filaments by Hohenadl et al. (1999)

Filament	persistence length [l_p]	contour length [L_c]	stiffness [$l_p : L_c$]
Collagen	11.2 nm	295.8 nm	$l_p < L_c$
Actin	17.7 μm	22.7 μm	$l_p \sim L_c$
Microtubuli	5.2 nm	100 μm	$l_p \ll L_c$
Spectrin	7.5 nm	100 nm	$l_p < L_c$
Elastin	0.36 nm	166 nm	$l_p \ll L_c$
GAG	93 nm	110 nm	$l_p \sim L_c$
Hyalauron	4.5 nm	110 nm	$l_p < L_c$
Intermediate filaments	17 nm	110 nm	$l_p < L_c$

stiffness and serve to resist myocardial deformation, maintain shape and wall thickness and prevent ventricles aneurysm and rupture’.

Referring to the mechanical behavior of the human myocardium, it also means that an increase or decrease of collagen in the interstitium - the sona - of the myocard, or changing collagen fiber thickness during a cardiac disease (e.g. hypertrophy) would highly influence the stiffness of the myocardium. With the data from the biaxial tensile tests, and the pathological information about common diseases of the contributor, it is possible to infer the changes of the mechanical behavior referring to the injury.

1.2.2.6.1 Cardiac collagen changes in health and disease

When talking about injuries, which affects even the myocardium, we are always talking about dilated cardiomyopathy, hypertrophic cardiomyopathy and restrictive cardiomyopathy. All other structural heart diseases - like valve stenosis or coronary artery disease- are precursors. Weber (1989) described this circumstances as a physical or biochemical abnormality of collagen tethers, responsible for the respective regional or global transformation in myocardial architecture, including its thinning, impaired contractility and enlargement of the ventricles chamber. This thesis is also the first part of a prolonged study, to get the

knowledge about the collagen network deformation depending on each heart disease.

1.2.3 Chronological history of conducted biaxial tensile tests and occurred problems in the literature

In the work of Holzapfel and Ogden (2009) a main problem in developing an adequate constitutive model is the shortage of experimental data suitable for detailed parameter estimation in specific functional forms. Early contributions to gathering such data are contained in the work of Demer and Yin (1983) in which data from biaxial tests were obtained. However, data from biaxial tests alone are not enough to characterize the passive response of myocardium because such data suggest that the material is transversely isotropic. That this is not the case has been demonstrated clearly in the more recent work by Dokos et al. (2002), which, on the basis of shear tests conducted on cube-shaped specimens from different orientations within the myocardium, highlighted the orthotropic behavior of the material. It remains the case, however, that there is a need for more comprehensive sets of data to be obtained. Holzapfel and Ogden (2009) defined the key features of the morphology and structure of the myocardium and described the passive mechanical response of myocardial tissue on the basis of the available biaxial and shear test data.

At this point it is necessary to mention, that all results published up to now, are tensile test results from non human species. In the past, mainly equibiaxial tensile tests have been carried out on thin sections of myocardial tissue removed from the left ventricle of a canine heart (e.g., Demer and Yin (1983); Yin et al. (1987); Humphrey et al. (1990); Novak et al. (1994)). Also mainly equibiaxial tensile tests on hearts from mongrel dogs were performed by Demer and Yin (1983), Yin et al. (1987), Humphrey et al. (1990), Novak et al. (1994) and Sacks and Chuong (1993).

For myocardial tissue such tests do not yield sufficient quantitative information to formulate a reliable constitutive law. Dokos et al. (2002) demonstrated this fact clearly by the results of simple shear tests on passive ventricles myocardium from porcine hearts. That work highlighted the orthotropic behavior of myocardial tissue. Moreover, myocardial tissues undergo complex patterns of tensile, compressive, and, in particular, shear deformations throughout the cardiac cycle. For this case Holzapfel and Ogden (2009) recognized, that the data from biaxial test alone is not enough to characterize the passive response of orthotropic materials, such as the myocardium. Up to now, only Yin et al. (1987) performed 'true' biaxial test with different ratios on the myocardium of mongrel dogs, which offered quite more responsible data for the mechanical behavior of the myocardium.

There is a need to extend the test protocol in a way that its possible to formulate more accurate statements. Therefore Holzapfel and Ogden (2009) found a solution to demonstrate the mechanical behavior of the myocardial tissue. A combination of biaxial test data with different loading protocols and shear test data at different specimen orientations should solve the problem, to capture adequately the direction-dependent nonlinear material response. Therefore the biaxial tensile test are done under specific loading conditions.

1.2.4 Summary of the facts - What is still required?

In the sections above, the terms of heart components and stiffness are illustrated quite well, so that we can understand the general problems in soft tissue biomechanics. To get a conclusion about what is already done, and what is still required, it would be instructive to sum up the facts, or let's say to define the status quo. Therefore it is necessary to separate the term of soft tissue biomechanics according to this thesis into three main terms.

Chronological it would be useful to start with the tissue, then go on with the mechanical behavior, and after all finish with the term of theoretical material model.

1.2.4.1 Status quo of the human heart tissue

Up to now, the tissue components of the myocardium are anatomically and physiologically explored quite well. There are some models present, that try to describe the structure of the myocardium with all its constituents. The medical research on the microscopic layer has proceeded to a level, that the filament components of the tissue are developed in their composition summarized in chapter 1.2.2. The medicine can also understand, how the components (e.g. filaments) interact referring to a level in chemical manner, to provide a self-contained system depending on the physiological point of view. Most of the areas in the human heart tissue are explored quite well in the matter of the chemical behavior. But to understand the chemical exchange of the constituent parts is not sufficient to understand the mechanical behavior of myocardial soft tissue. Up to now there are only few data that describe the mechanical backlash of the filaments in the human myocardium. Moreover, only a few data exists according to non-human myocardium (e.g. from pigs or dogs). Therefore, there is a pressing need for more basic research about human myocardium, as done in this thesis.

1.2.4.2 Status quo of the mechanical behavior of human heart tissue

The global mechanical behavior of the myocardium can only be guessed, according to the already known data from the tissue components. As shown in chapter 1.2.2.5 every filaments is very specific in its length and stiffness. Fact is, that just to know, that the different filaments with their specific mechanical behavior exist in the tissue, is insufficient to make a meaningful statement about the global mechanical properties of the human myocardium. There are too many factors that are not uniquely determined yet, such as the concentration of each filament in the myocardium. Also not exactly declared is, how the individual filaments are closely coupled with each other, and how the influence of the different coupling mechanism affect the mechanical behavior of the soft tissue. This fact is another reason, why it is necessary to collect biaxial mechanical tensile data about the highly complex overall system.

1.2.4.3 Theoretical material modeling of human myocardium

Up to now, there are some theoretical models about the human ventricles geometry and the fiber organization like the mathematical representation from Nielsen et al. (1991). There are also non-human models existing, that couples the mechanical behavior of the heart with the electro-physical components, to simulate the action of the heart, like the model from Hooks (2007) based on pig hearts. It is possible to describe the human heart behavior with the anatomically similar pig heart model, however, only approximately. Describing the exact behavior of the human heart presuppose exact knowledge of the human heart structure, mechanically and physio-electrically. There is still a long way to a functioning and representative model of the human heart. With the help of the data collected in this thesis, it is possible to do a big step for understanding the mechanical behavior of the human heart soft tissue.

2 Material and methods

In order to yield high quality measurement results it is necessary to define a strict approach for the specimen's origin and the measurement data acquisition. In addition also a defined setup and a well structured test protocol are required. This chapter describes exactly the steps from the origin of the samples, transport and transport conditions, the storage of the tissue, preparation and processing and the data analysis. To stay on top of things, the steps from the specimen's origin up to the data analysis, are documented chronological in the following sections.

2.1 Materials

2.1.1 Origin of the myocardial tissue

Relevant tissue types for the biaxial tensile test in this thesis are myocardial tissue from porcine heart, and of course tissue from the human myocardium. It is highly recommended to define a precise operation sequence from the pick-up and the transport to the laboratory where the tests take place. In general there is one main rule: The fresher the heart tissue, the more meaningful the results from the tests according to the in-body milieu. The tissues used for the biaxial tensile tests on porcine hearts were obtained directly from the slaughterhouse Marcher, whereas the human samples are obtained from two different institutions: the Institute of Pathology and the Clinical Department of Transplantation Surgery. Contrary to the heart tissue obtained from the Slaughterhouse Marcher, where the hearts are picked up immediately after slaughter. The time span between the death of the donor and the storage of the separated human myocardial tissue in the specific solution during the pick up play a major role.

2.1.2 Porcine heart tissue

Generally the porcine heart has to be evaluated by a veterinarian. During this evaluation the porcine heart is getting truncated and would be unusable for further specimen extraction. Due an arrangement with the abattoir Marcher it was possible to get porcine hearts in a fresh condition without this truncate cut. The porcine hearts were separated directly after the death of the donor, so that there was an effective time duration of about one hour from the separation, the pick-up and the transport to the laboratory. Figure 2.1 shows a porcine heart in a cleaned untreated state.

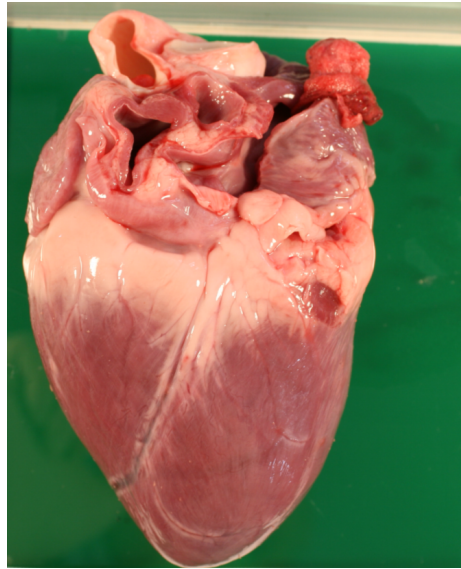


Figure 2.1: Picture of a porcine heart, anterior view, including aorta valves, atriums and ventricles

2.1.3 Human myocardial tissue from the Institute for Pathology

The main problem depending on pathological hearts is the fact, that the time duration between the donors death and the arrival of the donor at the Institute for Pathology is quite long. Until the pathological investigation are completed and the heart is separated for the test purposes, the minimal progress of autolysis is about 14 hours. For the biaxial tensile test the maximum duration of autolysis progress should not extend 24 hours. Normally, the pathological tissue is stored in formalin (an aqueous solution of formaldehyde that is 37 percent by weight) after the removal for further pathological investigations to stop the autolysis and to conserve the specimen. For our tests this conservation would make the tissue unsuitable. So there was a need to minimize the time duration over all. Figure 2.2 shows the left ventricles of a pathological human heart with the pathological surgery cut done from the pathologist during pathological investigation.

2.1.4 Human myocardial tissue from the Clinical Department of Transplantation Surgery

The myocardial tissue from the Department of Transplantation Surgery for the tensile test is derived from hearts that are declared as non-transplantable. There are some factors playing a major role for defining a heart as non-transplantable. The most common reason is the too advanced age of the donor. Generally transplantable hearts should be as young as possible and must not exceed an age of 60 years.

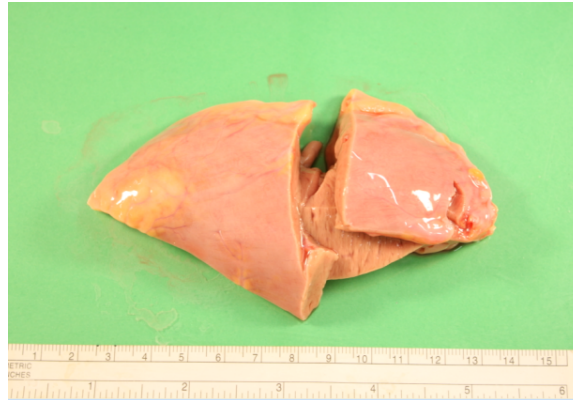


Figure 2.2: Picture from the left ventricles of a pathological human heart. Left ventricles is cut into half from basal to apical direction (standard pathological surgery cut) after the pathological investigation.

The reason for this is, that the long-term survival of the patient who gets the heart transplanted is decreasing strongly with the increasing age of the donor's heart. Further important reasons are the duration of cold ischemia, the damage of the heart during the cold ischemia, coronary graft sclerosis and the number of rejections. Occurred heart diseases like a hypotrophy, cardiomyopathy, circumferential akinesia or circumferential dyskinesia make a heart also unusable for transplantation, and these are the circumstances for releasing a heart at an age below 60 years for scientific research.

The clinical characterization of the declared non-transplantable heart is done with cardiac ultrasound investigation. With the results of the cardiac ultrasound it is possible to define a non-transplantable heart as 'failing heart' or 'non-failing heart'. The basic assessment for defining a heart as non-failing or failing are the data from the cardiac ultrasound, referring to the hearts ejection fraction (it refers to the performance of cardiac output of the left and right ventricles). With increasing age of the donor, the EF (ejection fraction) is decreasing as a result of normal aging of the cardiac system. So in fact, all hearts that have not an age related EF (the criteria for non-failing is a ratio between 55% and 60%) are declared as failing hearts. From a scientific view, however, both types are relevant, and used for the biaxial tensile tests.

There is a strict sequence extracting the specimens from the non-transplantable heart. The donors heart is getting deactivated directly after the extraction using Custadiol with BDM (2,3-butanedione monoxime, which is known to inhibit cross-bridge activity and prevents contracture arising from cutting injury). It is a highly specific cardioplegical solution to keep the heart tissue in an inactivated state.

Fig. 2.3 shows two of the received specimens (a part of the left ventricles free wall and a part of the septum) from a human heart after the separation by the surgeon at the Clinical Department of Transplantation Surgery.

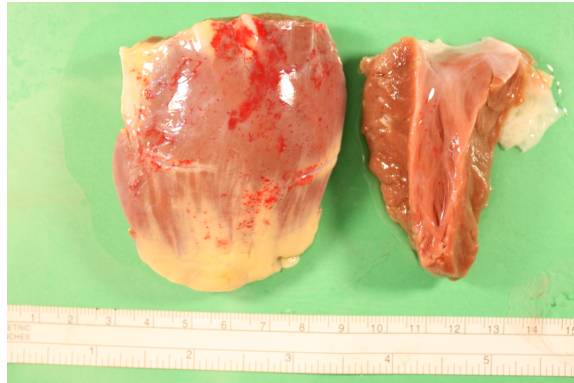


Figure 2.3: Picture from the left ventricles free wall tissue (right) and tissue from the septum (left) of a human heart from the Clinical Department of Transplantation Surgery.

2.2 Methods

2.2.1 Transport and storage of the myocardial tissue

Generally it is necessary to store the tissue at cold temperature, to effect a nearly inactivation of the metabolism; to prevent the germ-infect in the contaminated environment after the tissue removal; and to keep the tissue in a fresh state. Therefore the samples were stored in a cooling box after receiving. In this study three different solution were used for the storage during the transport: PBS (Phosphate buffered saline); a ‘standard cardioplegical solution’ from a pharmacy in Salzburg; and Celsior (a very specific cardioplegical solution used for the storage during transplant surgery). Another reason for cooling the tissue is the fact that cardioplegical solutions have their optimized operating temperature at 4°C.

2.2.1.1 Storage and transport of Porcine heart tissue

The porcine hearts were handed over from the abattoir Marcher in a fresh state with a temperature of 37°C (porcine body temperature). There was a need to cool down the porcine heart tissue rapidly, to provide a slow blood coagulation.

2.2.1.1.1 Storage in PBS - solution

Phosphate buffered saline is a buffer water-salt solution containing potassium chloride and potassium phosphate, as well as sodium chloride and sodium phosphate. The phosphates of the PBS provide a constant pH score of 7.4 and have a specific osmolarity and ion concentration, which match with the milieu of the human body. The porcine heart gets inlayed into a vessel with PBS and is stored at 4°C during the transport to the laboratory. Because PBS is not a cardioplegical solution, there is no need to inject the solution into the coronary arteries.

2.2.1.1.2 Storage in ‘standard cardioplegical solution’

The ‘standard cardioplegical solution’ used for our biaxial tensile tests is composed from a pharmacy in Salzburg. The solution consists of calcium chloride, potassium chloride, magnesium chloride, sodium chloride and procaine hydrochloride, where potassium plays the main role for the inactivation of the heart tissue. The cardioplegical solution is directly injected into the coronary arteries locally at the abattoirs place, before the transport to the laboratory. For the transport the tissue is stored in a vessel with ‘standard cardioplegical solution’ at a temperature of 4°C in a cooling box.

2.2.1.2 Storage and transport of human myocardial tissue from the Institute of Pathology

In general the pathological tissue is very susceptible against high temperature. Referring to the important time duration, as mentioned in chapter 2.1.3, the continuous decay of the cardiomyocytes is usually at an advanced state. According to this, it is highly recommended that the time span between storage and transport is as short as possible.

2.2.1.2.1 Storage and autolysis

The pathological heart tissue is separated by the dissection personal at a not cooled state (at room temperature at about 21°C). After investigation from the pathologist, the tissue is stored in 'standard cardioplegical solution' at the temperature of 4°C until the pick up. As a result of the operations done at not cooled state, autolysis it getting proceeded. The continuous decay of the cardiomyocytes represents a major problem for the biaxial tensile tests, because the tissue stability is decreasing and as a result the data from the biaxial tensile test are getting falsified. Due to this, the refrigeration chain must not be interrupted during the storage and transport, to minimize the softening of the pathological myocardial tissue.

2.2.1.3 Storage and transport of human myocardial tissue from the Clinical Department of Transplantation Surgery

Immediately after tissue separation from the human heart, the tissue is very susceptible against temperature. Due the extraction of the tissue from the human heart, the cooling chain must not be interrupted and the tissue has to be supplied with sufficient Custadiol+BDM solution to prevent the activation of the tissue.

2.2.1.3.1 Importance of storage method according to prevent activation of tissue

For the transport issue two different solutions were used: Celsior (a high specific clinical proven solution for the storage of transplantable solid organs) and the 'standard cardioplegical solution'. During several transports of heart tissues from the Transplant Surgery Department with both cardioplegical solutions it turned out, that there is no need to use Celsior for the transport, because there was no difference between the use of Celsior solution and the 'standard cardioplegical solution' according to the mechanical behavior during preparation and our tests (purchasing Celsior is quite a problem, because of its special kind of use and the high price). The tissue received from the Clinical Department of Transplant Surgery is inlayed directly after the handover into the prepared vessel including cardioplegical solution. Transport occurs in a cooling box at a temperature of 4°C.

2.2.2 Biaxial testing device and test equipment

Biaxial tensile tests are done with a measurement device developed by the Institute of Biomechanics from the Technical University of Graz in cooperation with the Messphysik company (a division of Zwick and Roell). The developed testing device is based on the principle of the testing system developed by Yin et al. (1987). In general the machine consists of 4 main parts: four independently controlled traverses with independent loading cells for each traverse, a vessel system including a heating circuit, the optical detection system consisting of a video extensometer and the computer-based measurement data acquisition. A schematic of the system developed by Yin et al. (1987) is shown in Fig. 2.4. The new biaxial testing device used for biaxial tensile tests was specially designed for mechanical testing of natural and artificial elastic tissues. The four high-resolution linear actuators can be controlled independently by position, force or elongation (stress) using a stretch controlled testing algorithm. The position control is handled by an individual computing and control unit for each traverse.

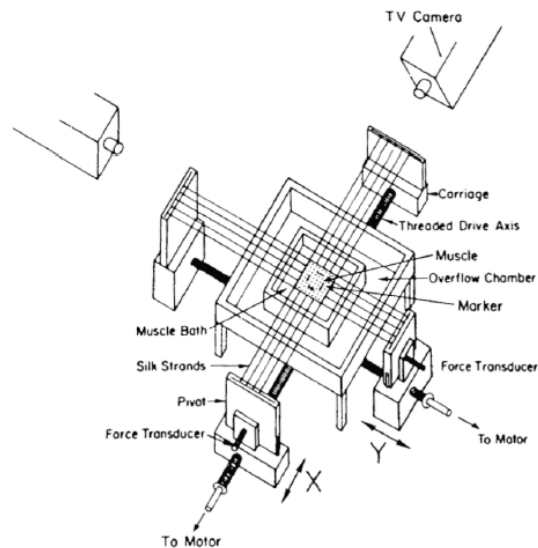


Figure 2.4: Schematic of the biaxial testing device from Yin et al. (1987) including optical detection system, bath for testing solution and the motor controlled carriage system. The specimen is placed in the middle of the bath and connected with each slide using silk cords.

2.2.2.1 Principle of measuring with the biaxial testing device

The specimen is equipped with four markers before fitted into the testing device. After the fitting the video extensometer gets calibrated according to the specimens location and the markers positions on the specimen. After the calibration of the video detection the zero position is getting defined. The zero position defines the distance between the markers at

a not loaded state of the specimen and the starting position for each of the four sledges. During the measurement cycle the video extensometer detects the position of the markers located on the specimen and compares the position with the different force informations from the loading cells of the four traverses. The Doli software is calculating the position data for the control unit of each linear actuator using a stretch controlled protocol. This stretch controlled protocol makes it possible to define the parameters for the traverse speed in a form, that the stretch ratios for each axis (x-axis and y-axis) are kept at a constant defined level. A principle of the biaxial measurement device is shown in Fig. 2.5.

A measuring cycle consists of two different parts: a loading curve, and a strain relief curve. The form of the curves will be explained in Chapt. 3. The advantage of this measuring method is the real-time acquisition of all relevant data, which is necessary for a high quality measurement result. The data is stored in form of an excel-sheet, including the forces collected from the loading cell of each traverse (F1, F2, F3, F4), the position of the four traverses (according to the defined zero-position), the distance of the markers at zero-position and the sampling time for each data point.

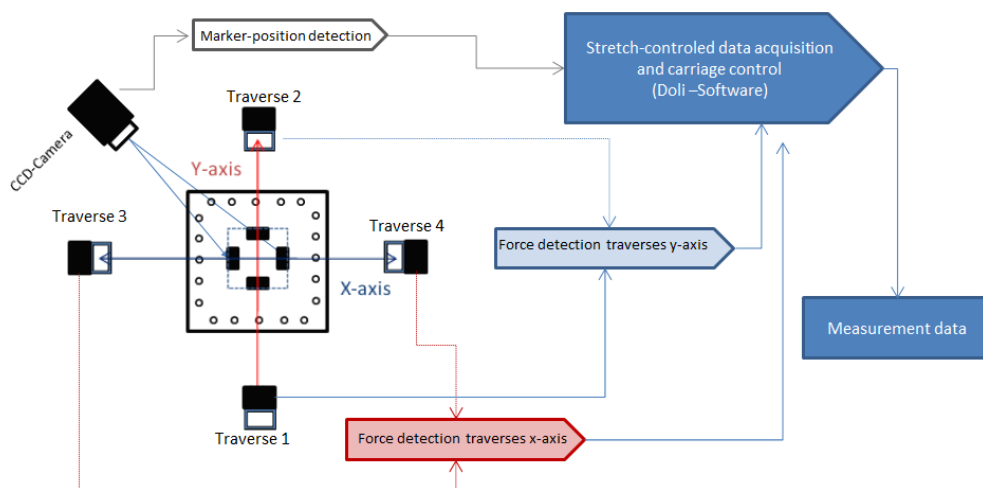


Figure 2.5: Principle of the data acquisition and data collection according to the biaxial testing device developed by the Institute of Biomechanics and the Messphysik company

2.2.2.2 Carriage device, hooks and cords

Depending on the softness of the tested myocardial tissue, the carriage device, the hooks and cords play a major role. According to the slight deformation and ductility of myocardial tissue, residual stresses and elasticity of the cords are highly undesirable and would occur a falsification of the test resulting data. Another problem are the traverse ‘non-linear’ forces according to the form of the carriage device depending on the attachment of the cords onto the provided bolts of the carriage devices. As demonstrated in Fig. 2.6 the cords provide forces along the traverse axis because of their assembly on the carriage. These traverse forces prevent a linear force distribution on the specimen during the tensile testing. To counteract these shear forces, new carriage devices were developed, to get more linear tensile forces. As shown in Fig. 2.7, the traverse forces in contrast to the standard carriage devices shown in Fig. 2.6 are much smaller. Another problem during the biaxial tensile tests is the loosening of the cords from the anchorage. With the new anchorage the cords are fixed with the bolt to prevent this.

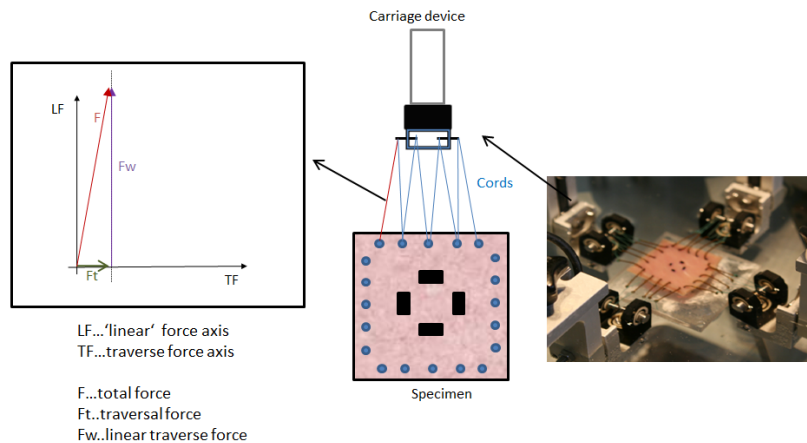


Figure 2.6: Non-linear stress force on the cords according to the carriage device depending on the attachment of the cords. The diagram shows the undesirable traverse force F_t , which occurs as a non-homogeneous force displacement on the specimen.

The cords which fasten the specimen to the carriages should not be stretchable. A stretchable cord would hardly falsify the results of the tensile tests because the expansion of the cords would be included into the measured data. Therefore a surgery cord was used. A surgery cord has the advantage, that it provides an even good stress behavior during

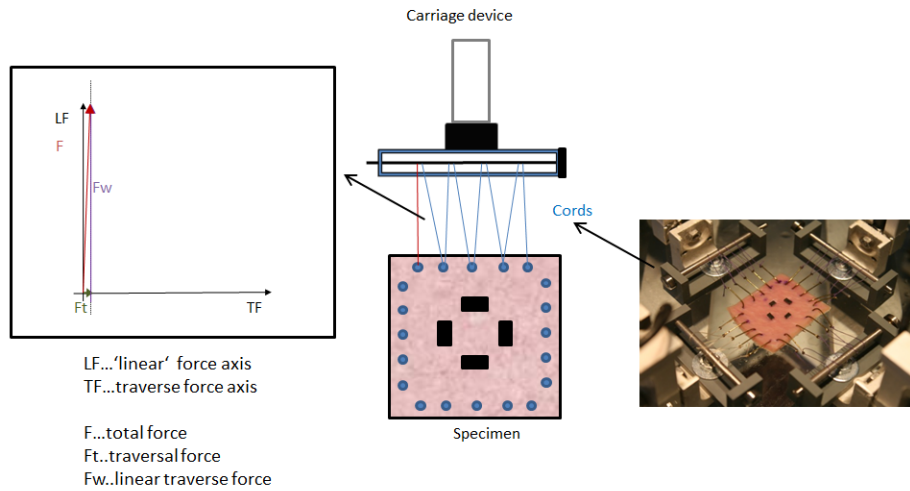


Figure 2.7: New developed carriage device with almost 'linear' forces. The new attachment system also provides the detach of the cords during the measurement cycles.



Figure 2.8: Picture of the surgery cords and fishing hooks used for fitting the specimen into the biaxial testing device.

the tensile tests with nearly being unstretchable. The hooks used were commercially used fishhooks which were strung on the cords for the fitting of the specimen into the biaxial measuring device. A picture of the surgical cord and the hooks for testing setup is shown in Fig. 2.8.

2.2.2.3 Overview of the solutions used for the biaxial tensile tests

According to the biaxial tensile test and the highly specific behavior of the tissue at a non-body milieu, the use of specific solutions are recommended. The main target is to seek a nearly similar milieu as given in the body of the donor with consideration to the inactivated state of the myocardial tissue. To ensure that, during this thesis different solutions were used, to get as realistic measurement data as possible.

2.2.2.3.1 PBS solution

The PBS solution (Phosphate buffered saline) is a buffer solution which is used during biological research. The solution offers a similar Ph-value (7.2PH) as the one in the human body's milieu. As mentioned in chapter 2.2.1.1.1 this solution is a water-based salt solution containing potassium chloride and potassium phosphate and sodium chloride. This solution is isotonic and non-toxic to cells. A list of all components included in the PBS solution is shown in Tab. 2.1. Potassium chloride is an essential salt in the bodies cell life-circle. Due to its antiseptic property, it is capable of fighting germs. It can even prevent the decay of body tissue. Potassium phosphate and sodium phosphate are essential salts that are used for human body ph-value regulation and play several roles as addition in the ATP cycle and as components in several cell membranes.

Table 2.1: Recipe of PBS solution used for solution bath

Component	Formula weight [g*mol ⁻¹]	Amount [g]	Weight [g]
Sodium phosphate ($NaH_2PO_4 * 2H_2O$)	178.01	1.44	
Potassium phosphate (KH_2PO_4)	136.09	0.24	
Potassium chloride (KCL)	74.55	0.2	
dissolve in distilled water			1000

PBS is a very good buffer solution for tests at an defined ph-value. For the tests, the solution was heated to body temperature at 37°C. Because PBS solution has no cardioplegical components, which are required for testing the myocardium at a passive state, PBS was only used for the first biaxial tensile tests done with porcine myocardial tissue. From previous tests, attempted on porcine myocardium tissue, this solution was already proved, and there were no activations of the porcine myocardial tissue detectable during the biaxial tensile tests at this defined temperature.

2.2.2.3.2 Cardioplegical solution

Contrary to PBS solution described in chapter 2.2.2.3.1, the ‘standard cardioplegical solution’ used for transport and for the bath during the test has special components, that should prevent the activation of the heart tissue during the tests. The components of the ‘standard cardioplegical solution’ for our tests are shown in Tab. 2.2. Additionally to the PH regulating components in this solution Procaine hydro-chloride and the large amount of potassium play the major role as cardioplegical components of this ‘standard cardioplegical solution’. They prove an inactivity of the myocardial tissue, which is necessary for keeping the myocardial tissue at an passive state.

Table 2.2: Recipe of ‘standard cardioplegical solution’ used for solution bath

Component	Formula weight [g*mol ⁻¹]	Amount [g]	Weight [g]
Calcium chloride ($CaCl_2 * 2H_2O$)		0.176	
Potassium chloride (KCL)		0.24	
Magnesium chloride ($MgCl_2$)		3.252	
Sodium chloride ($NaCl$)		6.429	
Procaine hydro-chloride ($C_{13}H_{20}N_2O_2$)		0.267	
Potassium (K)	16		
Sodium (Na)	110		
Calcium (Ca)	1.2		
Magnesium (Mg)	16		
Chlorine (Cl)	160		
dissolve in distilled water			1000

2.2.2.3.3 Potassium buffered cardioplegical solution

According to the concentration of potassium and procaine hydro-chloride it can be assumed, that at testing temperatures from 37°C an activation of the human myocardial tissue would occur. Especially in intact myocardial tissue this would cause problems holding the tissue at a passive state. Therefore, the concentration of cardioplegical components have to be increased. To the already given amount of 16g/l potassium, an amount of 20g*mol⁻¹ was added.

2.2.2.3.4 Potassium buffered Ringer solution

The Ringer-‘Fresenius’ solution is a infusion solution that is mostly used for short-term volume replacement and for the replacement of extracellular fluid (isotonic and hypotonic dehydration). The main components of the Ringer-‘Fresenius’ solution are sodium chloride, potassium chloride, calcium chloride and sodium bicarbonate. They have a similar function as the chloride and phosphate components of the PBS solution, regulating the Ph value to a body-similar milieu (at 7.2). The Ringer-‘Fresenius’ solution includes also other additions like chemical fuel sources for cells, including ATP and dextrose, as well as antibiotics and antifungals. The receipt of the Ringer-‘Fresenius’ solution is shown in Tab. 2.3. The Ringer-‘Fresenius’ solution at normal condition has only an amount of $4\text{g}\cdot\text{mol}^{-1}$ potassium acting as cardioplegical component. At the department of transplant surgery this Ringer-‘Fresenius’ solution is refined to a Cancer-Ringer-‘Fresenius’ solution, that is highly specific and used for storing the hearts during transplantation. Refining the ringer solution to a cancer ringer solution is highly specific and complex. After consultation with the Institute of Transplant Surgery, for our purposes an increased potassium concentration should give the same results. To the given concentration of $4\text{g}\cdot\text{mol}^{-1}$ potassium, an amount of $20\text{g}\cdot\text{mol}^{-1}$ of potassium was added, to be sure that there is no activation of the myocardial tissue during the biaxial tensile test.

Table 2.3: Recipe of potassium buffered Ringer-‘Fresenius’ solution used for solution bath

Component	Formula weight [$\text{g}\cdot\text{mol}^{-1}$]	Amount [g]	Weight [g]
Calcium chloride ($\text{CaCl}_2 * 2\text{H}_2\text{O}$)		0.33	
Potassium chloride (KCL)		0.30	
Sodium chloride (NaCl)		8.6	
Potassium (K)	24 (4+20)		
Sodium (Na)	147.20		
Calcium (Ca)	2.25		
Chlorine (Cl)	155.70		
dissolve in distilled water			1000

The testing temperature was set to 37°C at body temperature.

2.2.3 Preparing the specimen

For the biaxial tensile tests the location of specimen separation is very important. The possibilities for the procurement of the specimen are strongly dependent on the available myocardial tissue which is provided from the different departments. Especially the demand for human tissue is very high, and therefore the received tissue pieces are not always separated from the same defined position of the ventricle. Contrary to the quite small amount of human myocardial tissue, a precise specimen separation from porcine heart is quite easy, because of the large available amount of myocardial tissue. In Fig. 2.9 the regions for removal of the specimen are shown.

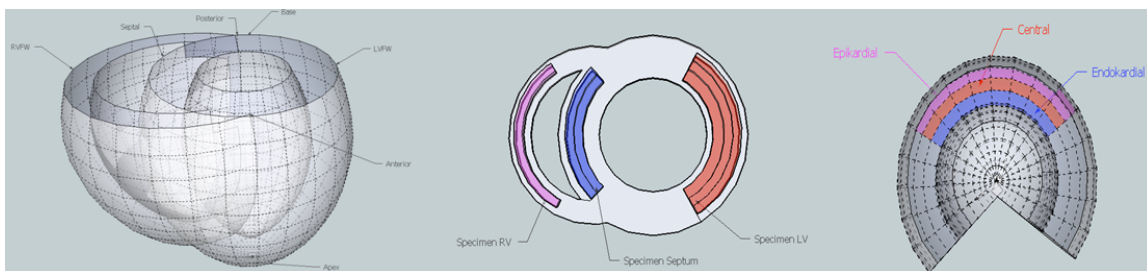


Figure 2.9: The defined regions for specimen separations including reference axis and directions for the exactly description of the origin of the specimen extraction. For human myocardial tissue the thickness of the ventricles is too small to separate the heart wall into the 3 defined layers (epicardial, endocardial, and central), so the separated specimens removed from human hearts are generally defined as procured from central location.

2.2.3.1 Tools for specimen preparation

The myocardial tissue has to be disassembled to tranches with a thickness of 3mm. This sections are done with a common commercial slicer. The press arm of the slicer for fixing the tissue during the cut, got modified in a way, so it was possible to cut myocardial tissue at a very thin state (about 5mm thickness). This was necessary because of the small wall thickness of the human ventricles tissue as listed in Tab. 1.1 received from the several departments (Department for Pathology and Department for Transplantation Surgery). For separating the cuboid out of the tranches, surgery blades were used (special trimming blade material: carbon steel; blade length: 130mm; manufacturer: FEATHER CO., LTD). The surgery blades have the advantage to cut very precise while using small expense pressure during the cutting process. The sensitive myocardial tissue would be easily crushed by too high pressure during the cutting process, and this would harm the tissue. Another problem is, that the deformation during the cutting process according to too high expense pressure would make it impossible to cut specimens from tissue tranches with defined dimension.

2.2.3.2 Method of specimen separation

2.2.3.2.1 Porcine heart

The chronological procedure of specimen preparation is shown in Fig. 2.10. The preparation occurs in six different steps. After the transport from the abattoir the heart is getting washed, to remove the blood from the outer layer of the heart. In the first step the atrium and the apex are cut away. For the biaxial tensile tests only the ventricless and the septum are of interest. Cutting away the apex has the advantage, that the blood from the ventricless can be flushed out using the solution the tissue should be tested with. No tap-water should be used for this step, because of the Ph sensitive tissue and the risk of tissue-activating. This means, that if testing with cardioplegical solution, the washing solution should be the same.



Figure 2.10: This picture shows the different steps of specimen preparation from the PIG Heart #3 for the biaxial tensile tests. The different steps are signed with numbers from one to six. Step 1: cutting axes for apex and atriums; Step 2: cutting of the right ventricles (a) from the septum and left ventricles (b) using the cutting axes; Step 3: cutting axes for separating the left ventricles (c) from the septum (d); Step 4: separated parts of the heart as described; Step 5: extracted tranches from the left ventricles of the PIG Heart #3; Step 6: separating of one specimen for the biaxial tensile test out of one tranche extracted in step 5.

2.2.3.2.1.1 Separating the ventricles and the septum

The second step shown in Fig. 2.10 is the dissection of the right ventricles from the porcine heart. The first cutting axis for separating the right ventricles is along the LAD-coronary arteries (left anterior descending coronary arteries), the second one is the junction axis between the right ventricles and the septum at the posterior layer. In the third step the cutting axis between the left ventricles (c) and the septum (d) is illustrated. The cut is done from basal to apical direction referring to the axis definition shown in Fig. 2.9. After the dissection of the relevant parts (left ventricles, right ventricles and septum shown in step four), the parts are disassembled to tranches. Part five of Fig. 2.10 shows the tranches extracted from the left ventricles of PIG Heart #3. The common thickness of the tranches should be 3 mm. For each tranche the fiber-axis and the cross-fiber-axis has to be determined. Therefore the main-fiber-direction of the epicardial surface and the endocardial surface of the tranches are elicited, and the mean-fiber-direction of both is getting defined. The final step (step 6 in Fig. 2.10) is the extracting of the specimen for the test purposes in dependence of the determined mean-fiber-direction. The dimension of the cuboid for porcine myocardial tissue is 30mm \times 30mm \times 3mm (length \times width \times thickness).

2.2.3.2.1.2 Consistence of porcine myocardium tissue

In general the myocardial tissue from porcine hearts has a stiff, solid structure. This is a result of the short lifespan of a pig from birth to slaughter for food purposes. Because of the short growth and life (normally three months) time of the heart, the hearts consists almost no visible fat storages in the myocardial heart tissue. The walls of the ventricles and the septum are, assigned to the rapid growth, very thick in comparison to the human heart.

2.2.3.2.1.3 Specimen separation for the combined biaxial tensile test and triaxial shear test

To provide meaningful measurement data, biaxial tensile tests and triaxial shear tests are done from the same part of heart. The origin of the separated specimens should be the same, to be able to reference the measured data from the triaxial shear test and the biaxial tensile test according to the mechanical properties. Therefore, a new separation method was developed. Between the steps four and five shown in Fig. 2.10 the tissue for the triaxial shear tests is removed. Therefore one slice with a thickness of about five to seven millimeters is separated from the left ventricles as shown in Fig. 2.11. This method makes it possible to compare the results of the different testing methods because of extracting the specimen of nearly the same region.

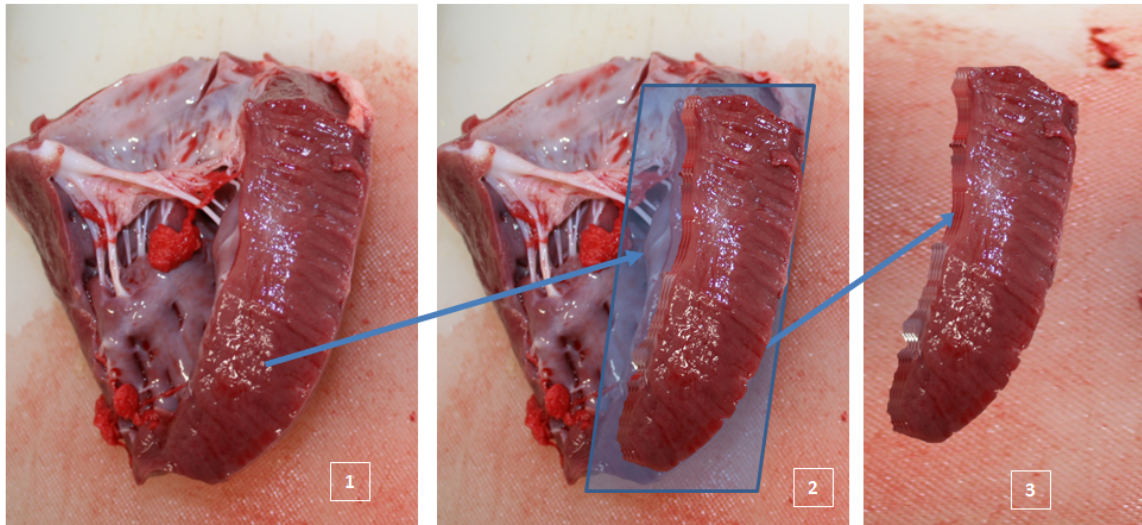


Figure 2.11: This figure shows a basal to apical cutting plain(2) for the extraction of myocardial tissue (1) used for the combined triaxial shear test of the left ventricles of Pig Heart#3, chronological between the steps four and five shown in Fig. 2.10, and the extracted slice (3)

2.2.3.2.2 Human heart tissue

In general the preparing process for human myocardial tissue is nearly the same as for porcine hearts (described in chapter 2.2.3.2.1.1). In comparison to the tensile test on porcine hearts, where the whole heart was available for research purposes, the amount of tissue received for human myocardial research is rather small. Due to the small amount of available tissue, the specimen preparation is quite complicated, and the specimen dimensions for the biaxial tensile tests are reduced to $25\text{mm} \times 25\text{mm} \times 3\text{mm}$ (length x width x thickness). There was a need to find a compromise between the available tissue size and the choosing of the defined directions (cross-fiber direction and fiber direction) to obtain specimens with the required size for the biaxial tensile tests over all.

In Fig. 2.12 the extraction process is shown chronological from step one to step five from the pathological human heart with the heart index Myo3/12. Before cutting the tranches as shown in step 3, the tissue for the triaxial shear test is separated as shown in Fig. 2.11.

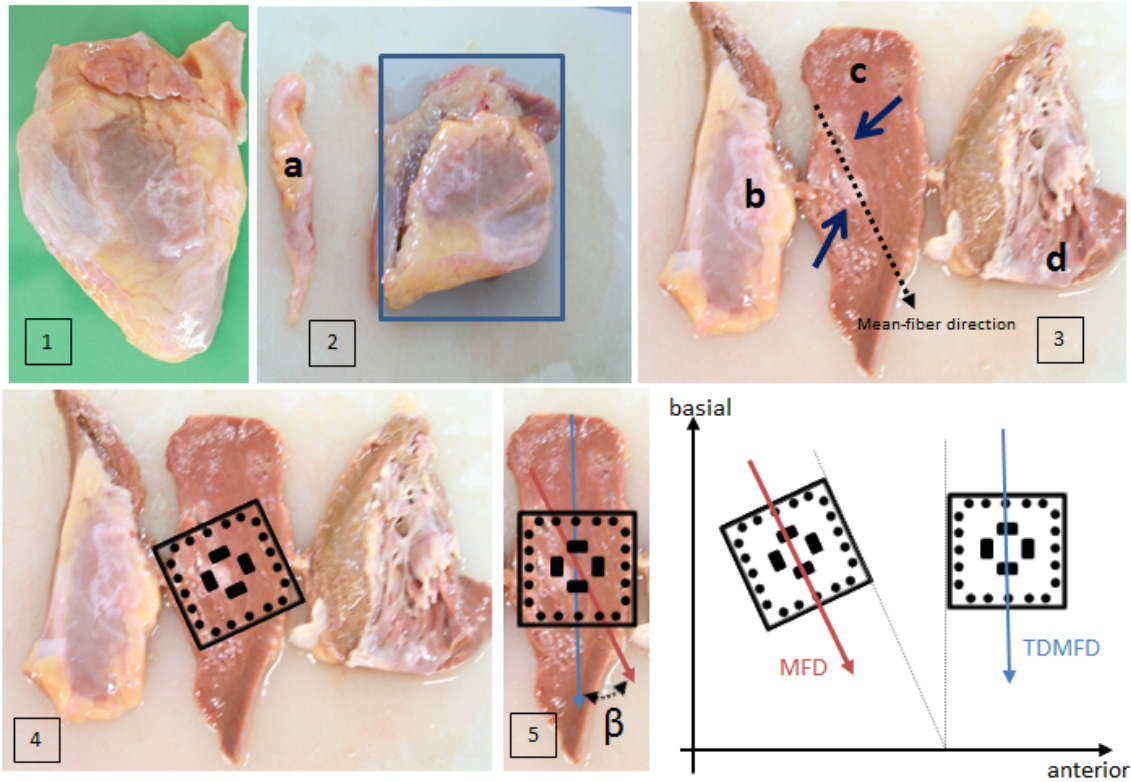


Figure 2.12: Preparation sequence of pathological heart Myo3/12; Steps of separation shown chronological from one to five; Step 1: Picture of the frontal left ventricle freewall anterior (definition see Fig. 2.9) received from the Department of Pathology with the index Myo3/12; Step 2: Separated LAD - coronary artery (a) and the cutting-plane for removing the pericard and the tranche from the myocard using the cutting axes shown in Fig. 2.13. Step 3: picture of separated pericard (b), tranche for specimen extraction (c) and the epicardial tissue (d) including the axis for mean fiber direction. The violet arrows shows inhomogeneous regions of the tranche ; Step 4 and 5: Region for specimen separation depending on the available size of the tissue and the compromise choosing the TDMFD (Tissue depending mean-fiber direction) instead of the MFD (Mean-fiber direction) showing the deviation angle β .

2.2.3.2.2.1 Consistence of the human myocardial tissue

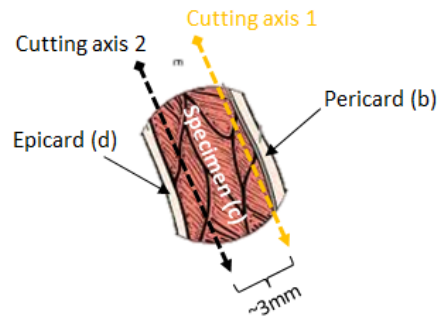


Figure 2.13: Cutting sequence for separating the tranche for the specimen out of the pathological tissue of Myo3/12.

In comparison to the porcine myocardial tissue, the human myocardial tissue is very soft and easily deformable. According to the long lifetime of the human heart in the body of the donor, the tissue stores fat into the myocardial tissue. As shown in step 3 in Fig. 2.12, there are inhomogeneous regions (violet arrows), which we tried to prevent for specimens tissue separation. However, this is usually not possible because of the small amount of human myocardial tissue received for the biomechanical study. Depending on this, it is assumed, that fat storages are biological artifacts. Fat storages are common in nearly every human heart and should not falsify the measurements results particularly.

2.2.4 Setup and mounting the specimen into the biaxial testing device

To allow a clamping of the myocardial tissue to the testing device for the biaxial tensile tests, the carrier cords are attached to the specimen. One carrier cord consists of a surgery cord where five hooks are strung on it (used cords and hooks are shown in Fig. 2.8). For high quality measurement results this step must be done very carefully, because influences like false pretension of the specimen between the four carrier devices or false hook position falsify the received data strongly.

2.2.4.1 Attaching the hooks to the specimen

The positioning of the hooks on the specimen plays a major role. It is important that the implementation of the hooks into the specimen is carefully set according to the marked positions from the template, in order to achieve a nearly homogeneous distribution of the tensile forces during the biaxial tensile tests Yin et al. (1987). Picture 1 of Fig. 2.14 shows the solaced hooks onto the specimen from human myocardial tissue of a pathological heart with the index Myo3/12. Because of the softness of the myocardial tissue, the attachment of the hooks to the specimen onto the marked positions is not exactly possible as seen in picture one of Fig. 2.14.

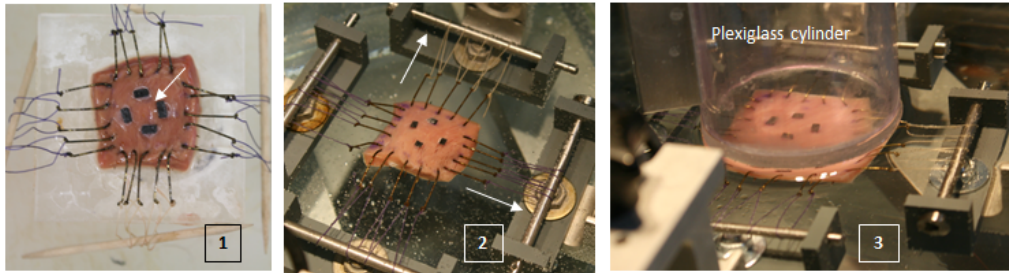


Figure 2.14: Cutting sequence for separating the slice for the specimen out of the pathological tissue of Myo3/12.

2.2.4.2 Marker and marker position

As material for the markers black foam rubber with a thickness of 0.5mm is used. This material was chosen because of its good contrast according to the optical detection by the CCD-camera. The marker dimension should be about 2.5mm \times 1mm (length \times width), because with this size the amount of lost markers by the the video extensometer during the biaxial test study was minimized. The markers are glued onto the specimen at the marked positions from the template. The region between the markers represents the homogeneous area to which the measured data from the tensile tests are referred (the white arrow of picture one in Fig. 2.14 shows the glued markers defining the homogeneous region).

2.2.4.3 Inserting the specimen into the testing device and calibration of the optical measuring system for the marker detection

The inserting of the specimen into the biaxial testing device requires a lot of experience. During the fixing of the specimen using the carrier cords between the carriage devices, the tissue may not be injured by excessive stretching forces. Excessive stretching of the tissue would damage the tissue before the biaxial tensile tests and would render the tissue as useless. It is also important to place the specimen exactly central between the carriage devices to provide linear traction forces during the tensile tests. The selection of the proper preload of the cords stretch is also very essential for defining a non-loaded state for the specimen at zero position for biaxial tensile testing setup as shown in picture two of Fig. 2.14.

Since the optical marker detection is very sensitive to surface contamination of the solution bath, a transparent plexiglass cylinder was used to avoid them. Because of the dissolve of the fat deposits in the human myocardial tissue due to the temperature of the solution bath, there was fat floating on the solution baths surface and caused a loss of the markers. The plexiglass cylinder is a hollow cylinder that is dipped into the solution bath to prevent artifacts according to the reflection of solution surface contamination, which can be responsible for a loss of the marker by the video detection system during the tensile tests. The setup for the cylinder above the specimen is shown in picture three of Fig. 2.14.

After defining the zero position for the specimen and the cylinder, the video extensometer system gets calibrated, using a film with defined marked intervals placed on the specimens surface.

2.2.5 Measurement and loading protocol

2.2.5.1 Loading protocol for biaxial tensile tests

According to the structural schematic of the passive myocardium as shown in Fig. 2.18, the loading protocol has to be extended in a form, that the structural behavior can be established, dependent on the part of the specimen's location of fibers and sheets. To capture adequately the direction-dependent nonlinear material response it is insufficient to use a test protocol that is collecting data only from the fiber direction -fiber axis f_0 , and the cross fiber direction f_x at a similar stretch ratio for each axis f_0 and f_x . Much more instructive is a loading protocol with different ratios, such as used during the biaxial tensile test done in this thesis. From this additional received information about the mechanical behavior, referring to different loading conditions, it is possible to get a much higher spatial resolution according to the direction-dependent nonlinear mechanical material response of the myocardium. However, the biaxial tensile tests are not able to formulate an exact statement according to the position and direction of the sheets as shown in Fig. 1.3 and Fig. 2.18, because the testing method is two dimensional (fiber and cross-fiber direction). To find out how the sheets layers are, a third dimension would be needed. Therefore the tests are done as a combination between biaxial tensile test and triaxial shear test. This makes it possible to take all three dimensions into account. Further informations about the triaxial combination test will be explained in chapter 4.

Because of this, the stretch protocol was extended with four more ratios as shown in Fig. 2.15. The stress-strain-curves of all stretch ratios give a meaningful statement about the mechanical properties in the homogeneous region of the specimen. The homogeneous region of the specimen is defined as the region between the markers, where it is possible to assume nearly linear tensile forces.

2.2.6 Data acquisition, data analysis and mathematical background

Actuator control and data acquisition is achieved by using the software Test&Motion Version 2:0 by 2.4 Section 2 41 'Doli' Elektronik GmbH, Munich, Germany. For the non-contacting strain-measurements the software Laser Speckle Extensometer Version 2:23:3:0 by MESSPHYSIK Materials Testing, Fuerstenfeld, Austria was used. The analysis of data obtained from the biaxial tensile tests are realized by the use of a custom-written Matlab application for the used stretch protocol. The application includes computation, smoothing algorithm and a plotting option for calculated data. The assessment of the data occurs, using plots, showing the calculated Cauchy-stress σ depending on the measured stretch λ for each specimen during the biaxial tensile tests under different loading conditions.

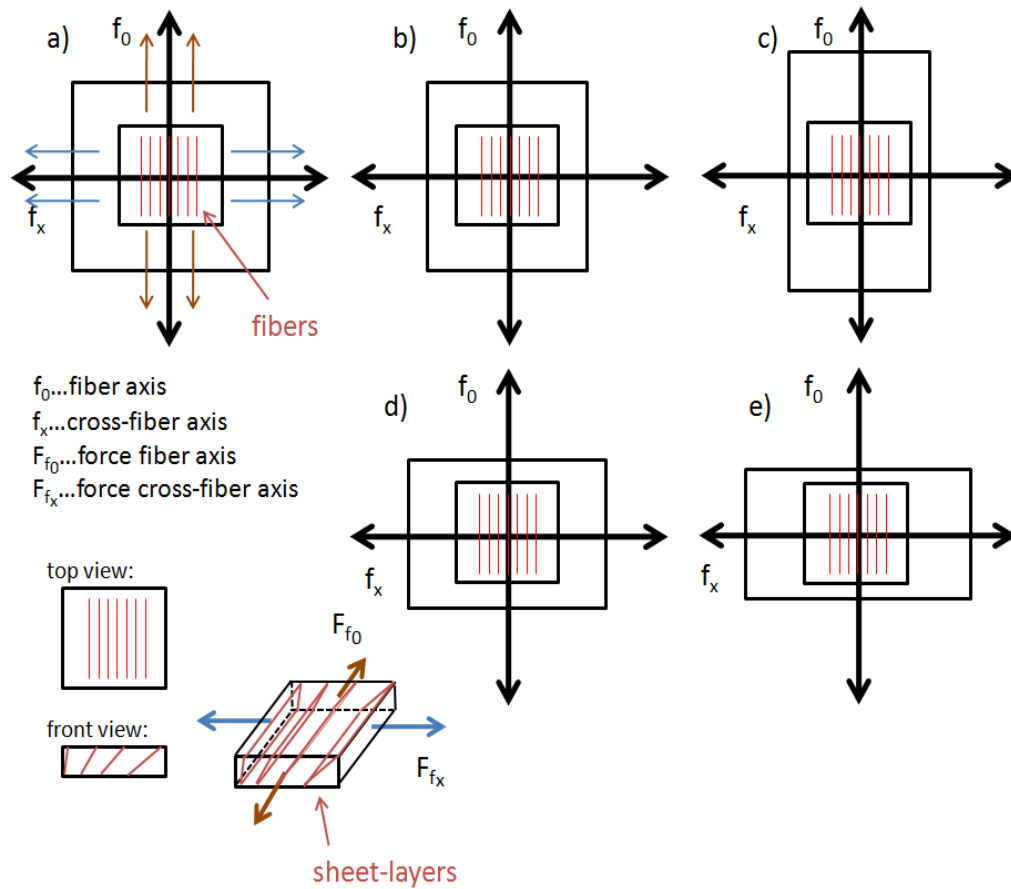


Figure 2.15: Schematic of different loadings according to the loading protocols. The pictures a) to e) show the different stretch ratios between the fiber direction and the cross-fiber direction. A ratio of 1 : 1 means a stretch ratio of 100% in f_0 axis and 100% in f_x axis [fiber direction : cross-fiber direction]. Different loadings: a) $f_0 : f_x = 1 : 1$; b) $f_0 : f_x = 1 : 0.75$; c) $f_0 : f_x = 1 : 0.5$; d) $f_0 : f_x = 0.75 : 1$; e) $f_0 : f_x = 0.5 : 1$

2.2.6.1 Data analysis and smoothing

Biological tissue, like the myocard shows a non-linear stress behavior and is assumed to be incompressible, anisotropic and viscoelastic. Non-linear stress behavior means that the stiffness of the myocardial tissue is increasing due the increasing stress exerted on the tissue. The reason for this behavior refers to the microscopic structure of the myocardial tissue (see chapter 1.2.2). Due the assumption of incompressibility, the volume of myocardial tissue, according to the stress-strain relation is constant.

2.2.6.1.1 Stretch-controlled protocol

While using a stretch-controlled measurement protocol, the regulating values are the stretch ratios of the different axis (fiber axis and cross-fiber axis), where the stretch ratio for x-direction is written as λ_x and in y-direction as λ_y . The stretch ratios are calculated as shown in equations 2.1 from the collected measuring data.

$$\lambda_x = \frac{x_x^*}{X_x} \quad \lambda_y = \frac{x_y}{X_x} \quad (2.1)$$

Here X_x and X_y are the defined marker distances for each direction (X_x in cross-fiber direction and X_y in fiber direction) which include the homogeneous area and x_y and x_x are the measured distance changes between the markers on the specimen according to the stretch acting on the specimen for each direction. For each protocols as described in 2.2.5.1 the stretch ratios λ_x and λ_y are held constant depending on the ratio.

2.2.6.1.2 Cauchy-stress calculation

In order to quantify the mechanical behavior of myocardial tissue, the Cauchy-stress ('true stress') is used as significant value. The Cauchy-stress σ can be calculated for each direction by the formula shown in 2.2 where t is the mean thickness of of the tissue in the current configuration and x_x and y_y indicates the current dimensions of the specimen for the x-direction and y-direction of the specimen according to the traverse position in dependence of the defined zero-position of the biaxial testing device.

$$\sigma_{xx} = \frac{f_x}{t * x_y} \quad \sigma_{yy} = \frac{f_y}{t * x_x} \quad (2.2)$$

Because of the assumed incompressibility of the myocardial tissue, the volume during deformation is constant. For this incompressible state of the myocardial tissue the values from the undeformed configuration t, x_x, y_y and the deformed configuration T, X_x, X_y can be written as shown in Eq. 2.3.

$$t * x_x * x_y = T * X_x * X_y \quad (2.3)$$

$$\sigma_{xx} = \frac{f_x * \lambda_x}{T * X_y} \quad \sigma_{yy} = \frac{f_y * \lambda_y}{T * X_x} \quad (2.4)$$

The tissue stretches are defined as λ_x for x-direction and λ_y for y-direction, shown in Eq. 2.1, whereas the Cauchy stress can be rewritten from Eq. 2.2, Eq. 2.3 and Eq. 2.1 to Eq. 2.4. The optical marker detection system and the loading cells of each traverse provide the relevant data for the Cauchy-stress calculation.

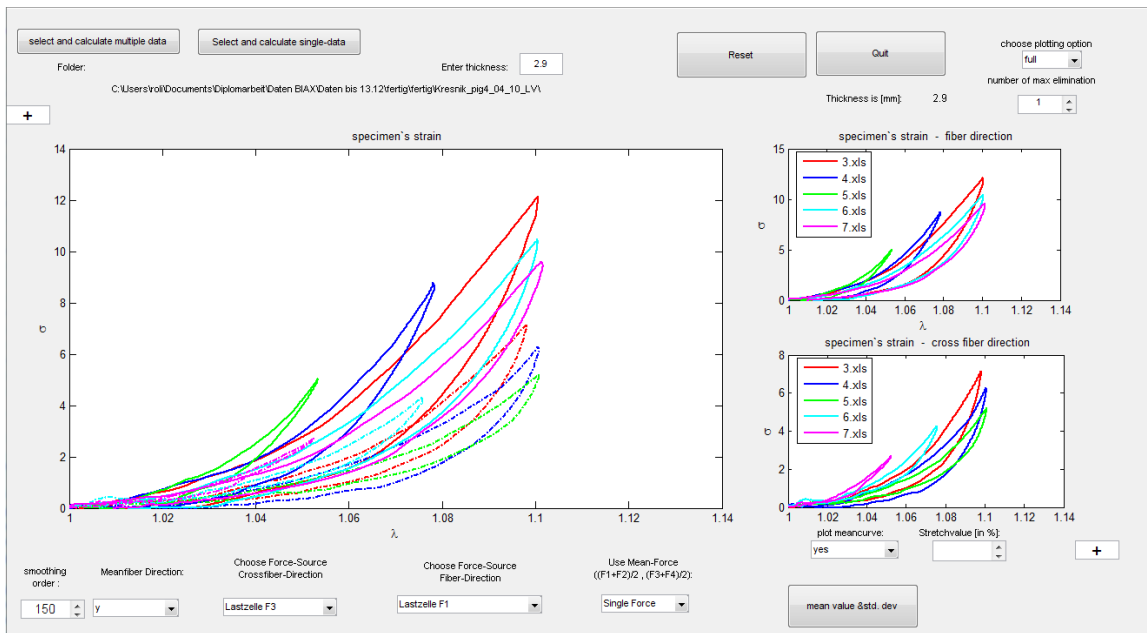


Figure 2.16: GUI (Graphical User Interface) created in Matlab 2009a for data analysis of data received from the biaxial testing system. The plotted data are from a porcine heart with the index PigHeart#4 left ventricles epicardial, showing the different stretch ratios from the stretch protocol at five percent stretch. MFD (Mean-fiber direction) and CFD (Cross-fiber direction) are plotted separately in the left two plots, and an overlapping plot of both for analyzing the mechanical behavior in the center of the GUI.

2.2.6.2 Data analysis with Matlab

The data calculation is done with an individually designed program, including fitting algorithm, offset correction and plotting option. It offers the possibility to overlay multiple curves simultaneously, or to plot a single curve for data analysis. The main problem getting meaningful data for plotting are the artifacts from the loading cells since the loads are in the very lower measuring range. This noise falsify the measured data achieved from the loading cells, and cause very noisy plots. Specially during the biaxial tensile test of the human myocardium tissue, which consistence is very soft, the magnitudes of the residual stresses of the cords are relatively high in comparison to the calculated stress-strain components. Therefore a variable smoothing filter was implemented. Fig. 2.16 shows a screen shot of the GUI (Graphical User Interface) for data analysis.

Because the maximum of the plotted curves represents a significant value for the assessment of the mechanical behavior of the myocardial tissue, it must not be falsified during smoothing process. So it is necessary to find an optimum configuration for smoothing the plots, to provide a non-tampering of the minimum and maximum. Therefore an algorithm was implemented, that prevents an accurate reference. Fig. 2.17 shows the very noisy unfiltered plot (section A) from the human pathological heart with the index PatoTU1/12 and the filtering of relevant data out of this signal. In this case, only the smoothing of the plots (section B) would make a qualitative assessment of the curves impossible. To plot only the afferent parts (section C) is much more informative for the assessment. The red circles mark the maximum positions of the cross-fiber direction magnitudes and the blue circles mark the maximum positions of the mean-fiber magnitudes for each stretch ratio (stretch ratio explained in chapter 2.2.5.1)

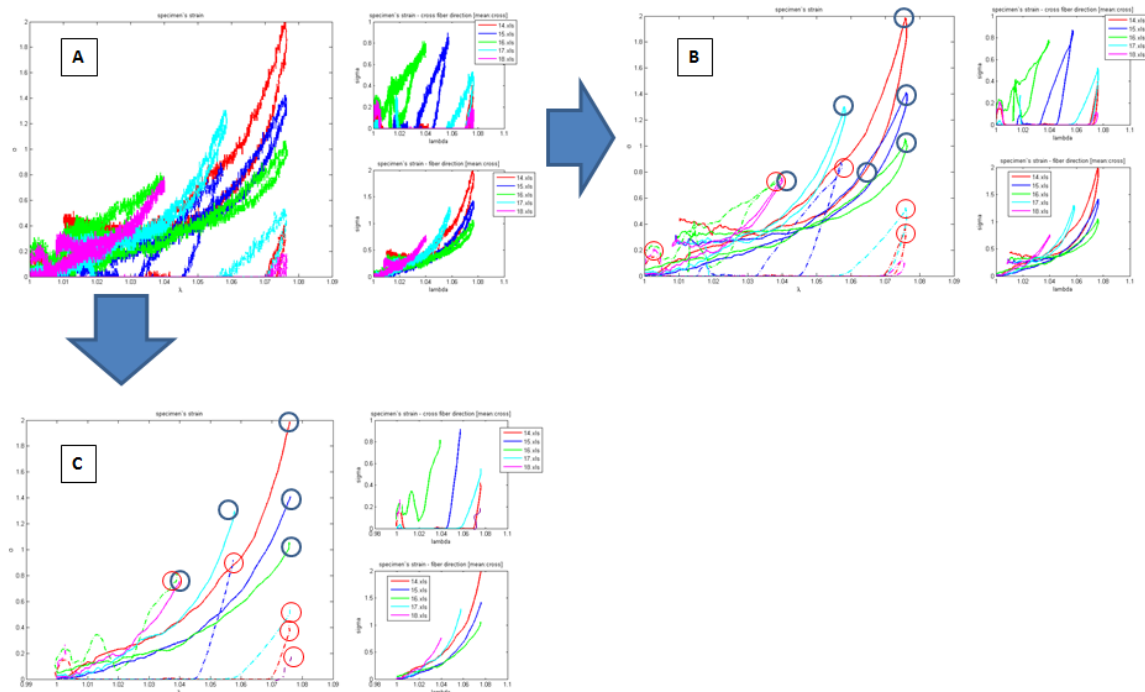


Figure 2.17: Stress-Strain plot for 7.5% stretch protocol with different ratios of pathological heart PatoTU1/12; Plots are shown as unfiltered in section A, filtered in section B and afferent part only in section C.

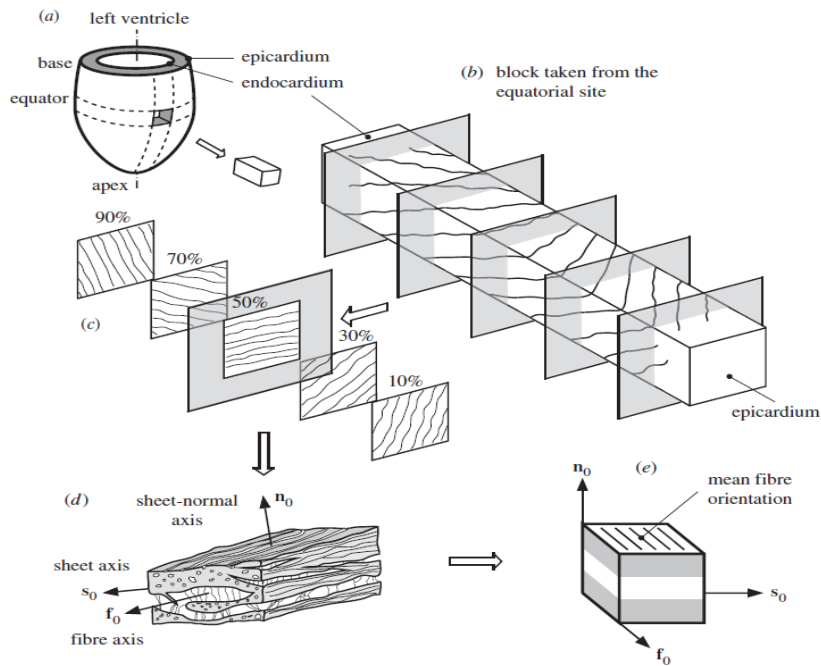


Figure 2.18: Schematic diagram of: (a) the left ventricle and a cutout from the equator; (b) the structure through the thickness from the epicardium to the endocardium; (c) five longitudinal-circumferential sections at regular intervals from 10 to 90 per cent of the wall thickness from the epicardium showing the transmural variation of layer orientation; (d) the layered organization of myocytes and the collagen fibers between the sheets referred to a right-handed orthonormal coordinate system with fiber axis f_0 , sheet axis s_0 and cross-fiber axis n_0 ; and (e) a cube of layered tissue with local material coordinates (X_1, X_2, X_3) serving as the basis for the geometrical and constitutive model (Holzapfel and Ogden, 2009).

3 Results

The mechanical behaviors of the different myocardium types are quite different. So, the results from the biaxial tensile test data at porcine myocardium are quite different according to the human myocardium types.

Table 3.1: Index of the hearts for the biaxial tensile tests, including origin and state

Heart Number	Heart index	Origin	State
PIG #1	PIG #1	Abattoir	fresh
PIG #2	PIG #2	Abattoir	frozen
PIG #3	PIG #3	Abattoir	fresh
PIG #4	PIG #4	Abattoir	fresh
PIG #5	PIG #5	Abattoir	fresh
PIG #6	PIG #6	Abattoir	frozen
PIG #7	PIG #7	Abattoir	fresh
PIG #8	PIG #8	Abattoir	fresh
PIG #9	PIG #9	Abattoir	fresh
Human #1	Transplant# 1	Clinical Department of Transplantation Surgery	passive state (2 h after separation)
Human #2	Myo 1/12	Institute of Pathology	28 hours of autolysis
Human #3	Myo 2/12	Institute of Pathology	20 hours of autolysis
Human #4	Myo 3/12	Institute of Pathology	18 hours of autolysis
Human #5	Transplant# 2	Clinical Department of Transplantation Surgery	passive state (2 h after separation)
Human #6	Transplant# 3	Clinical Department of Transplantation Surgery	frozen
Human #7	Transplant# 4	Clinical Department of Transplantation Surgery	passive state (1 h after separation)

Another fact is, that depending on the location of the specimen separation (left ventricular, right ventricular and septum) different results can be expected. This means that from the septum a higher stiffness is awaited than from the ventricles. In the following sections the results from porcine and human myocardial tensile test are shown, referring to the specimens destinations. In addition, different bath solutions (see Chapt. 2.2.2.3) should also take affect on the measured data, since the different solution components influence the mechanical behavior of the myocardium. The amount of hearts for the biaxial tensile tests include nine pig hearts and seven human hearts. The indexes for each heart are shown in Tab. 3.1.

3.1 Porcine myocardium

In this thesis tensile tests from nine different porcine hearts are performed. As a basic for the qualitative evaluation of the biomechanical behavior of porcine hearts the stress-stretch curves at different stretch levels are relevant. In Tab. 3.2 the separated specimen are listed according to the defined heart index shown in Tab. 3.1.

Table 3.2: Index of plotting curves depending on the heart index, the specimen number, the part of heart and specimen separation area.

Heart index	Specimen	Origin	Layer	Curve index	Thickness
Pig #1	# 1	LV	epicardial	<i>III</i> LV 10% <i>III</i> LV 15% <i>III</i> LV 20%	3.1mm
Pig #2	# 1	LV	central	<i>I</i> LV 10% <i>I</i> LV 15%	3.1mm
	# 2	Septum	endocardial	<i>I</i> Sept 10% <i>I</i> Sept 15%	2.9mm
	# 3	Septum	epicardial	<i>II</i> Sept 10% <i>II</i> Sept 15%	2.9mm
Pig #3	# 1	LV	epicardial	<i>IV</i> LV 10% <i>IV</i> LV 15%	3.1mm
	# 2	LV	central	<i>V</i> LV 10% <i>V</i> LV 15%	3mm
Pig #4	# 1	LV	central	<i>IV</i> LV 10% <i>III</i> LV 15%	2.8mm
	# 2	Septum	central	<i>VI</i> Sept 20%	2.9mm
Pig #5	# 1	LV	central	<i>VII</i> LV 10% <i>VII</i> LV 15%	3.1mm

Table 3.2: Index of plotting curves depending on the heart index, the specimen number, the part of heart and specimen separation area.

Heart index	Specimen	Origin	Layer	Curve index	Thickness
Pig #6	# 1	LV	epicardial	<i>VII</i> LV 7.5% <i>VII</i> LV 10%	3.1mm
	# 2	LV	central	<i>VIII</i> Sept 7.5% <i>VIII</i> Sept 10% <i>VIII</i> Sept 15%	2.9mm
	# 3	LV	endocardial	<i>X</i> LV 7.5% <i>X</i> LV 10%	3mm
	# 4	Septum	central	<i>III</i> Sept 7.5%	2.9mm
Pig #7	# 2	LV	endocardial	<i>XI</i> LV 7.5% <i>XI</i> LV 10% <i>XI</i> LV 15%	2.7mm
	# 2	LV	central	<i>XII</i> Sept 7.5% <i>XII</i> Sept 10% <i>XII</i> Sept 15%	3.1mm
	# 2	LV	epicardial	<i>XIII</i> Sept 7.5% <i>XIII</i> Sept 10% <i>XIII</i> Sept 15%	2.9mm
Pig #8	# 1	LV	endocardial	<i>XIII</i> LV 7.5% <i>XIII</i> LV 10% <i>XIII</i> LV 15%	3.1mm
	# 2	Septum	epicardial	<i>XV</i> Sept 10% <i>XV</i> Sept 15%	2.9mm
Pig #9	# 1	LV	endocardial	<i>XVI</i> LV 7.5% <i>XVI</i> LV 10%	3.1mm
	# 2	LV	epicardial	<i>XVII</i> LV 7.5% <i>XVII</i> LV 10% <i>XVII</i> LV 15%	2.9mm
	# 3	Septum	central	<i>IV</i> LV 7.5%	3mm

For each heart region (left ventricular and septum) the datasets are arranged in one plot at different stretch levels. The main informations from this plots are the mean average of the maximum strain from the plotted curves and the area within the hysteresis curve. The datasets are presented for fresh porcine hearts and frozen porcine hearts separately, same as datasets for the different heart regions (left ventricle and septum). Because of the large amount of datasets at some stretch levels several data are only plotted as loading curve.

3.1.1 Porcine hearts at fresh state

Datasets from the biaxial tensile tests are plotted from porcine hearts at fresh state. For each dataset the maximum value and the region area is calculated.

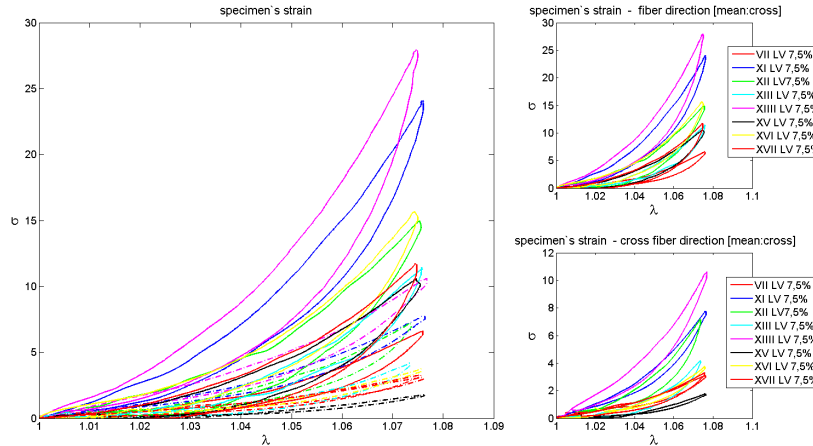


Figure 3.1: Stress-stretch datasets from porcine hearts at fresh state. The plotted datasets are measured at a stretch level of 7.5% at a Stretch ratio from 1:1 (see Chapt. 2.2.5.1). All plotted datasets are listed in Tab. 3.1 with its origin, the heart number and specimen number according to their legend index.

To ensure a better overview about the large amount of datasets in Fig. 3.2 and Fig. 3.3, only the loading part of the stress-stretch curve was plotted. The area of the stress-stretch curves for both directions were calculated using the trapezoidal method. Because of the interpolation of the measurement data to an expanded set of 20.000 measuring points for each axis, the calculation errors according to the trapezoidal method could be minimized.

3.1.2 Frozen porcine hearts

The test results for the two porcine hearts with the index PIG#2 and PIG#6 (as listed in Tab. 3.1) are shown in Fig. 3.5, 3.6 and 3.7. In Tab. 3.8, Tab. 3.7 and Tab. 3.9 the relevant values are calculated.

3.1.3 Representative plot with different ratios and overall plot

All specimens from porcine hearts were tested under different ratios.

Because the main part of this thesis are the results from the biaxial tensile tests of human myocardium, only one representative plot at different ratios is shown in Fig. 3.8 from the

Table 3.3: Calculating table for the porcine hearts tensile test from the LV at a stretch value of 7.5% .This table includes the calculated data for the hysteresis areas HA within the stress-stretch curve and the maximum forces for each direction (fiber direction FD and cross-fiber direction CFD) from the dataset shown in Fig. 3.1.

Curve index	maximum CFD [kPa]	maximum FD [kPa]	HA CFD [J/m ³]	HA FD [J/m ³]
VII LV 7.5%	3.1051	6.614	0.0159	0.0632
XI LV 7.5%	7.7221	24.066	0.0409	0.1827
XII LV 7.5%	7.164	14.9254	0.0495	0.1665
XIII LV 7.5%	4.1862	11.4257	0.0296	0.0612
XIII LV 7.5%	10.6326	27.8966	0.0791	0.2555
XV LV 7.5%	1.7607	10.5855	0.0016	0.1179
XVI LV 7.5%	3.7358	15.6655	0.0103	0.1485
XVII LV 7.5%	3.32	11.732	0.0319	0.1541
Mean	5.2034	15.364	0.0324	0.1435
SD	2.9918	7.1831	0.0247	0.0623

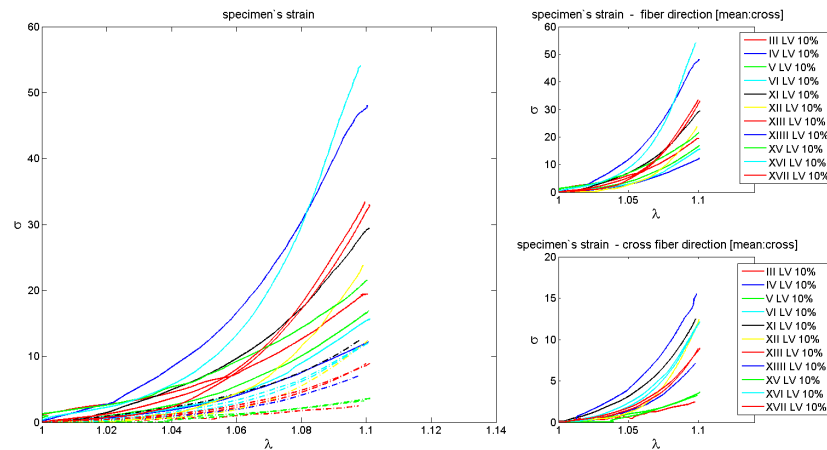


Figure 3.2: Stress-stretch datasets from fresh state. The plotted datasets are measured at a stretch level of 10% at a Stretch ratio from 1:1 (see Chapt. 2.2.5.1). All plotted datasets are listed in Tab. 3.1 with its origin, the heart number and specimen number according to their legend index. Because of the large amount of data, the datasets are plotted as loading path.

Table 3.4: Calculating table for the porcine hearts tensile test from the LV at a stretch value of 10% .This table includes the calculated data for the hysteresis areas HA within the stress-stretch curve and the maximum forces for each direction (fiber direction FD and cross-fiber direction CFD) from the dataset shown in Fig. 3.2.

Curve index	maximum CFD	maximum FD	HA CFD	HA FD
	[kPa]	[kPa]	[J/m ³]	[J/m ³]
III LV 10%	2.503	19.394	0.016	0.2192
IV LV 10%	7.163	12.142	0.0656	0.1695
V LV 10%	3.262	16.891	0.0340	0.1939
VI LV 10%	11.736	15.616	0.1111	0.1651
VII LV 10%	9.239	21.918	0.111	0.2795
XI LV 10%	12.493	29.353	0.1038	0.3317
XII LV 10%	12.395	23.745	0.0649	0.2615
XIII 10%	8.925	32.965	0.0859	0.2851
XIII 10%	15.574	48.028	0.1897	0.9580
XV LV 10%	3.650	21.527	0.0237	0.3039
XVI LV 10%	12.106	53.872	0.0474	0.5409
XVII LV 10%	8.945	33.336	0.0728	0.3949
Mean value [\bar{X}]	8.9917	27.4109	0.0745	0.3419
SD	4.1701	12.8814	0.0525	0.2206

porcine heart with the index PIG# 4 at different ratios (see Chapt. 2.2.5.1). In Fig. 3.9 all datasets derived from porcine hearts at fresh state are shown.

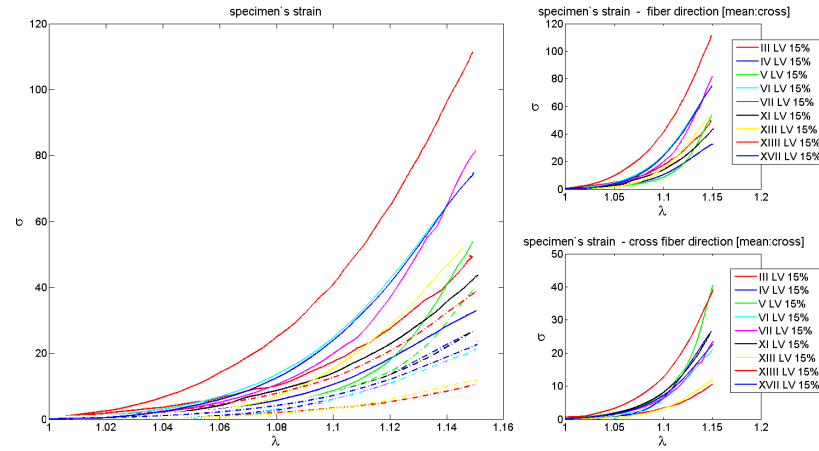


Figure 3.3: Stress-stretch datasets from porcine hearts at fresh state. The plotted datasets are measured at a stretch level of 15% at a Stretch ratio from 1:1 (see Chapt. 2.2.5.1). All plotted datasets are listed in Tab. 3.1 with its origin, the heart number and specimen number according to their legend index. Because of the large amount of data, the datasets are plotted as loading path.

Table 3.5: Calculating table for the porcine hearts tensile test from the LV at a stretch value of 15%. This table includes the calculated data for the surface areas SA within the stress-stretch curve and the maximum forces for each direction (fiber direction FD and cross-fiber direction CFD) from the dataset shown in Fig. 3.3.

Curve index	maximum CFD [kPa]	maximum FD [kPa]	HA CFD [J/m ³]	HA FD [J/m ³]
III LV 15%	10.599	49.568	0.0738	0.854
IV LV 15%	25.946	32.843	0.4086	0.6346
V LV 15%	40.530	53.749	0.4035	0.6530
VI LV 15%	21.337	74.52	0.1553	1.4681
VII LV 15%	23.555	81.371	0.3234	1.4090
XI LV 15%	26.588	43.722	0.3664	0.9056
XIII LV 15%	11.889	51.965	0.1368	0.9345
XIV LV 15%	39.156	111.327	0.5977	2.1072
XVII LV 15%	22.731	74.769	0.3957	1.5799
Mean	24.7039	63.7538	0.3159	1.1768
SD	10.2722	23.9999	0.1609	0.4936

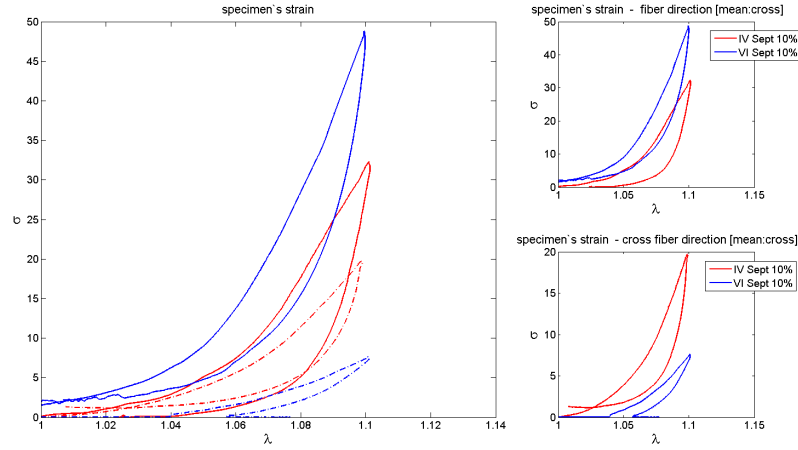


Figure 3.4: Stress-stretch datasets from porcine hearts at fresh state. The plotted datasets are measured at a stretch level of 10% at a stretch ratio from 1:1 (see Chapt. 2.2.5.1). All plotted datasets are listed in Tab. 3.1 with its origin, the heart number and specimen number according to their legend index. Because of the large amount of data, the datasets are plotted as loading path.

Table 3.6: Calculating table for the porcine hearts tensile test from the septum at a stretch value of 10%. This table includes the calculated data for the hysteresis areas HA within the stress-stretch curve and the maximum Cauchy stresses for each direction (fiber direction FD and cross-fiber direction CFD) from the dataset shown in Fig. 3.4.

Curve index	maximum CFD	maximum FD	HA CFD	HA FD
	[kPa]	[kPa]	[J/m ³]	[J/m ³]
IV Sept 10%	19.6784	32.307	0.2286	0.5437
VI Sept 10%	7.6312	48.7965	0.0789	0.5448
Mean	13.6584	40.5517	0.1538	0.5442
SD	8.5187	11.6598	0.1059	0.00077

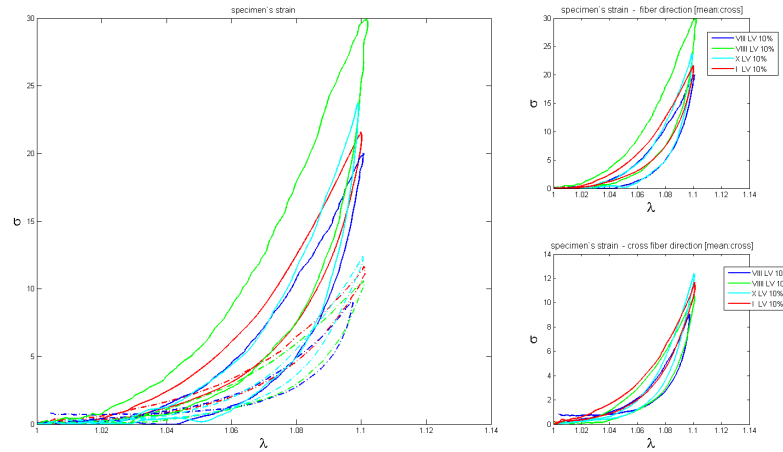


Figure 3.5: Stress-stretch datasets from porcine hearts at fresh state. The plotted datasets are measured at a stretch level of 15% at a Stretch ratio from 1:1 (see Chapt. 2.2.5.1). All plotted datasets are listed in Tab. 3.1 with its origin, the heart number and specimen number according to their legend index.

Table 3.7: Calculating table for the porcine hearts tensile test at defrosted state from the LV at a stretch value of 10% .This table includes the calculated data for the hysteresis areas HA within the stress-stretch curve and the maximum Cauchy stresses for each direction (fiber direction FD and cross-fiber direction CFD) from the dataset shown in Fig. 3.5.

Curve index	maximum CFD [kPa]	maximum FD [kPa]	HA CFD [J/m ³]	HA FD [J/m ³]
I LV 10%	21.622	11.663	0.2205	0.0912
VIII LV 10%	9.092	20.006	0.0616	0.2408
VIII LV 10%	10.565	29.927	0.1316	0.4880
X LV 10%	12.395	23.745	0.0064	0.2615
Mean	13.4185	21.3353	0.1050	0.2704
SD	5.6334	7.6364	0.0925	0.1637

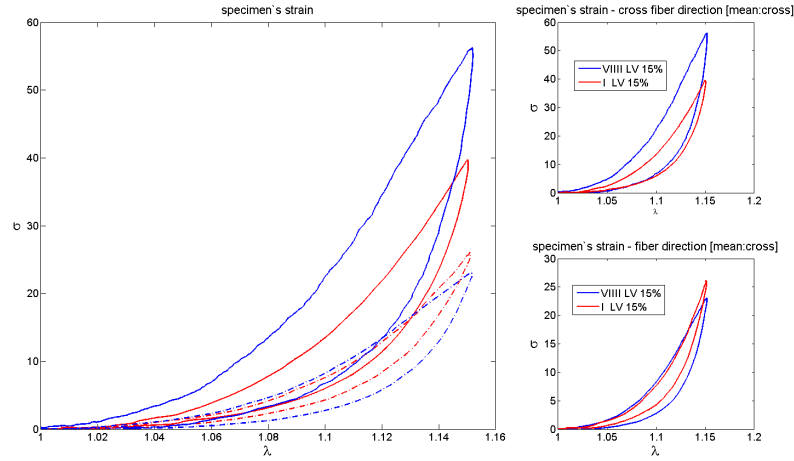


Figure 3.6: Stress-stretch datasets from porcine hearts at fresh state. The plotted datasets are measured at a stretch level of 15% at a Stretch ratio from 1:1 (see Chapt. 2.2.5.1). All plotted datasets are listed in Tab. 3.1 with its origin, the heart number and specimen number according to their legend index. Because of the large amount of data, the datasets are plottet as loading path.

Table 3.8: Calculating table for the porcine hearts tensile test at defrosted state from the LV at a stretch value of 15% .This table includes the calculated data for the hysteresis areas HA within the stress-stretch curve and the maximum Cauchy stresses for each direction (fiber direction FD and cross-fiber direction CFD) from the dataset shown in Fig. 3.6.

Curve index	maximum CFD	maximum FD	HA CFD	HA FD
	[kPa]	[kPa]	[J/m ³]	[J/m ³]
I LV 15%	39.702	26.0807	0.2945	0.6850
VIII LV 15%	23.0852	56.2885	0.5047	1.5030
Mean	31.3962	41.1846	0.5949	0.8968
SD	11.7535	21.3692	0.1275	0.8574

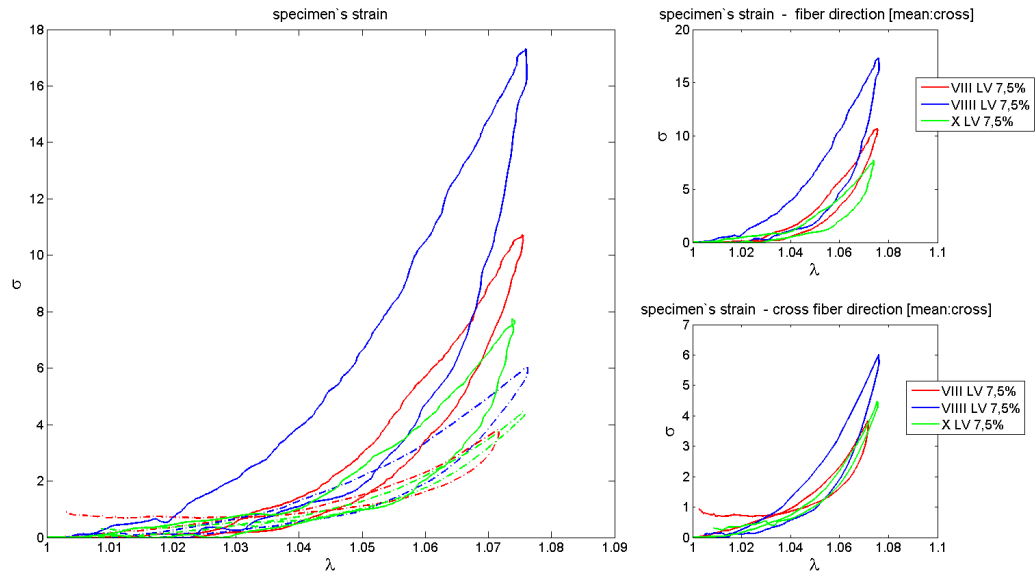


Figure 3.7: Stress-stretch datasets from porcine hearts at fresh state. The plotted datasets are measured at a stretch level of 7,5% at a Stretch ratio from 1:1 (see Chapt. 2.2.5.1). All plotted datasets are listed in Tab. 3.1 with its origin, the heart number and specimen number according to their legend index.

Table 3.9: Calculating table for the porcine hearts tensile test at defrosted state from the LV at a stretch value of 7.5%. This table includes the calculated data for the surface areas within the stress-stretch curve and the maximum Cauchy stresses for each direction (fiber direction FD and cross-fiber direction CFD) from the dataset shown in Fig. 3.7.

Curve index	maximum CFD [kPa]	maximum FD [kPa]	HA CFD [J/m ³]	HA FD [J/m ³]
VIII LV 7.5%	3.839	10.739	0.0045	0.071
VIII LV 7.5%	6.025	17.316	0.0478	0.2100
X LV 7.5%	4.472	7.741	0.0065	0.0695
Mean	4.7793	11.9322	0.0196	0.1168
SD	1.1249	4.8974	0.0244	0.0807

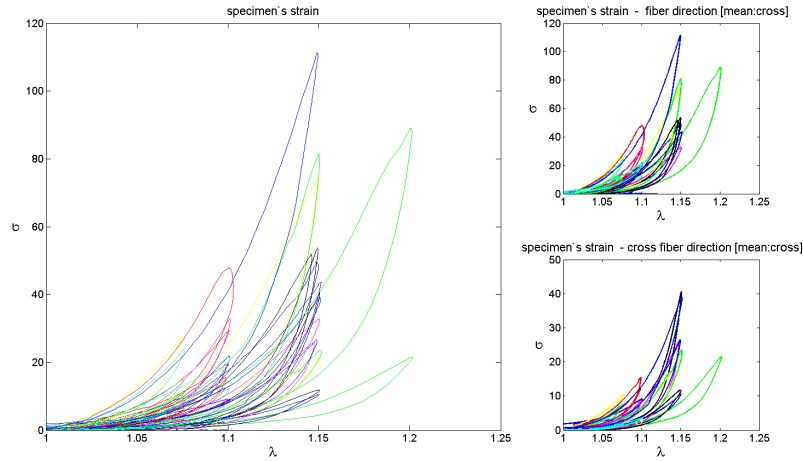


Figure 3.8: All datasets from porcine hearts at fresh state.

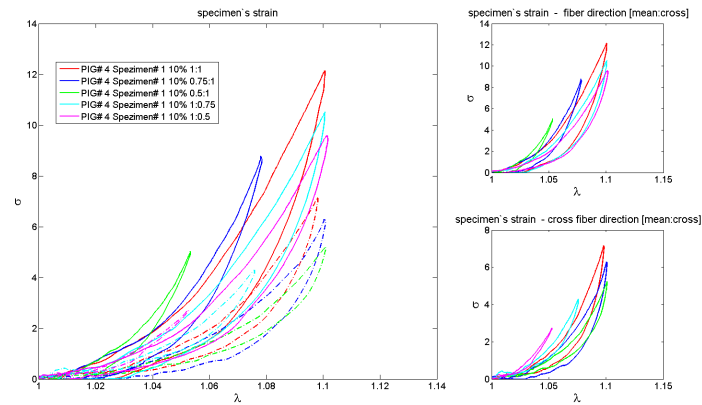


Figure 3.9: Stress-stretch datasets from porcine heart with the index PIG# 4. The plotted representative datasets are measured at a stretch level of 10% at different stretch ratios (see Chapt. 2.2.5.1).

3.2 Human heart tissue

According to the different Departments (Clinical Department of Transplantation Surgery and Institute of Pathology) the results are divided into two different parts. A list of all datasets according to their heart index (see Tab. 3.1) is shown for each human heart in the different chapters. For every heart the age of the donor and the used bath solution is very important, to be able to compare the different hearts in their mechanical behavior according to the biaxial tensile test results.

3.2.1 Human hearts from the Clinical department of Transplantation Surgery

To be able to classify the different results from the heart tissue received from the Clinical Department of Transplant Surgery, it is necessary to know basic informations about the donor of the heart. Significant values are the weight, the sex and the age of the donor. In Tab. 3.10 the necessary information are listed.

Table 3.10: Information about the donors according to the heart indexes, including the used solution during the tests. The index Pa stands for the additive of potassium, RFS for Ringer- Fresenius solution, SCS for standard cardioplegical solution, hypo for hypotrophy, ad for adipose, ddf for dyastolic dysfunction, sc for coronar sclerose.

Heart index	Age	Weight	Sex	Solution	Diseases
	[Years]	[kg]			
Transplant#1	74	116	male	PA RFS	hypo, adp
Transplant#2	41	82	male	SCS	ddf
Transplant#3	30	65	female	PA SCS	
Transplant#4	69	55	female	PA SCS	

3.2.1.1 Heart with the index Transplant# 1

In Tab. 3.11 all available datasets of human heart with the Index Transplant#1 are shown. In Fig. 3.10 and Fig. 3.11 the datasets are plotted according to their specific stretch values.

3.2.1.2 Heart with the index Transplant# 2

In Tab. 3.12 all available datasets of human heart with the Index Transplant#2 are shown. In Fig. 3.12 and Fig. 3.13 the datasets are plotted according to their specific stretch values.

Table 3.11: Index of plotting curves of human heart with the heart index Transplant#1.

Heart index	Specimen	Origin	Layer	Curve index	Thickness
Transplant #1	# 1	LV	central	<i>I</i> LV 5% 1:1	4.8mm
				<i>I</i> LV 5% 0.75:1	
				<i>I</i> LV 5% 0.5:1	
				<i>I</i> LV 5% 1:0.75	
				<i>I</i> LV 5% 1:0.5	
				<i>I</i> LV 7.5% 1:1	
				<i>I</i> LV 7.5% 0.75:1	
				<i>I</i> LV 7.5% 0.5:1	
				<i>I</i> LV 7.5% 1:0.75	
				<i>I</i> LV 7.5% 1:0.5	

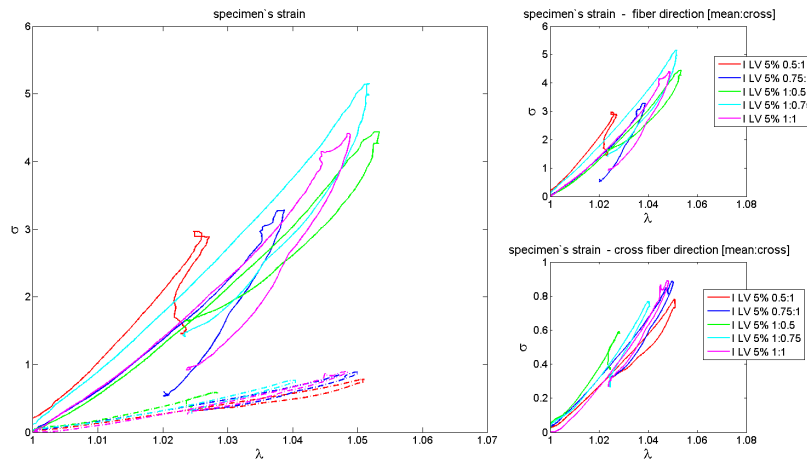


Figure 3.10: Stress-stretch datasets from Heart Transplant#1 at a stretch level of 5% including all different ratios (see Chapt. 2.2.5.1).

3.2.1.3 Heart with the index Transplant# 3

In Tab. 3.13 all available datasets of human heart with the Index Transplant#3 are shown. In Fig. 3.14, Fig. 3.15, Fig. 3.16 and Fig. 3.17 the datasets are plotted according to their specific stretch values.

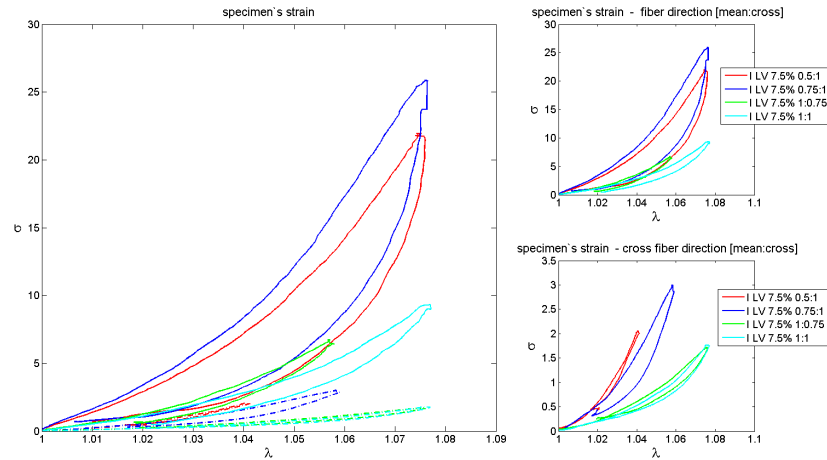


Figure 3.11: Stress-stretch datasets from Heart Transplant#1 at a stretch level of 7.5% including all different ratios (see Chapt. 2.2.5.1).

Table 3.12: Index of plotting curves of human heart with the heart index Transplant#2.

Heart index	Specimen	Origin	Layer	Curve index	Thickness
Transplant #2	# 1	LV	central	<i>II</i> LV 5% 1:1 <i>II</i> LV 5% 0.75:1 <i>II</i> LV 5% 0.5:1 <i>II</i> LV 5% 1:0.75 <i>II</i> LV 5% 1:0.5 <hr/> <i>II</i> LV 7.5% 1:1 <i>II</i> LV 7.5% 0.75:1 <i>II</i> LV 7.5% 0.5:1 <i>II</i> LV 7.5% 1:0.75 <i>II</i> LV 7.5% 1:0.5	3.5mm

3.2.1.4 Heart with the index Transplant# 4

In Tab. 3.14 all available datasets of human heart with the Index Transplant#4 are shown. In Fig. 3.18, Fig. 3.19, Fig. 3.21, Fig. 3.20 and Fig. 3.21 the datasets for specimen #1 are plotted according to their specific stretch values. Figure 3.22, Fig. 3.23 and Fig. 3.24 show the same plots for specimen #2.

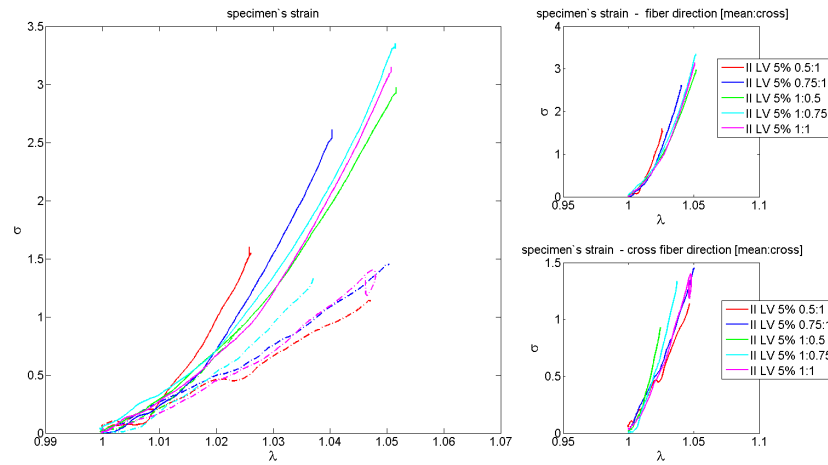


Figure 3.12: Stress-stretch datasets from Heart Transplant#2 at a stretch level of 5% including all different ratios (see Chapt. 2.2.5.1).

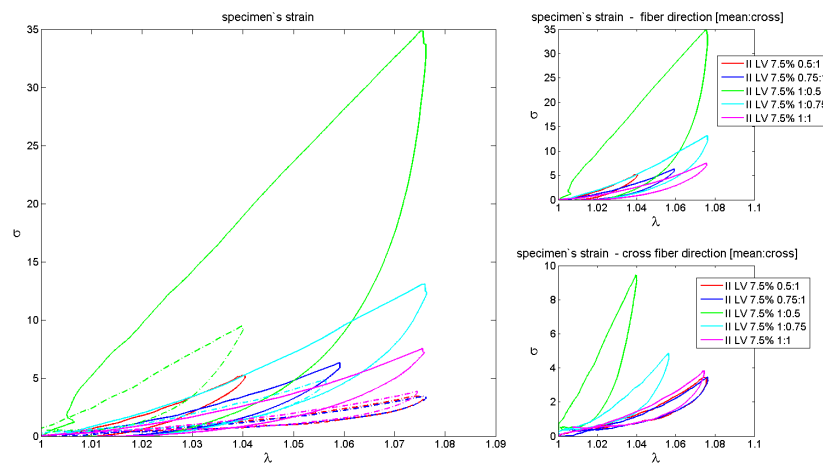


Figure 3.13: Stress-stretch datasets from Heart Transplant#2 at a stretch level of 7.5% including all different ratios (see Chapt. 2.2.5.1).

3.2.2 Human heart tissue from the Institute of Pathology

For human heart tissue received from the Institute of Pathology the important information for classifying the mechanical properties of the specimen the information about the autolysis time is very important. Furthermore, informations about the donors weight, sex, and age. The relevant information is shown in Tab. 3.15

Table 3.13: Index of plotting curves of human heart with the heart index Transplant#3.

Heart index	Specimen	Origin	Layer	Curve index	Thickness
Transplant #3	# 1	Septum	central	<i>I Sept 5% 1 : 1</i>	4.8mm
				<i>I Sept 5% 0.75:1</i>	
				<i>I Sept 5% 0.5:1</i>	
				<i>I Sept 5% 1:0.75</i>	
				<i>I Sept 5% 1:0.5</i>	
				<i>I Sept 7.5% 1:1</i>	
				<i>I Sept 7.5% 0.75:1</i>	
				<i>I Sept 7.5% 0.5:1</i>	
				<i>I Sept 7.5% 1:0.75</i>	
				<i>I Sept 7.5% 1:0.5</i>	
				<i>I Sept 10% 1:1</i>	
				<i>I Sept 10% 0.75:1</i>	
				<i>I Sept 10% 0.5:1</i>	
				<i>I Sept 10% 1:0.75</i>	
				<i>I Sept 10% 1:0.5</i>	
				<i>I Sept 12.5% 1:1</i>	
<i>I Sept 12.5% 0.75:1</i>					
<i>I Sept 12.5% 0.5:1</i>					
<i>I Sept 12.5% 1:0.75</i>					
<i>I Sept 12.5% 1:0.5</i>					

3.2.3 Heart with the index MYO 1/12

In Tab. 3.16 all available datasets of human heart with the Index Myo 1/12 are shown. In Fig. 3.25 and Fig. 3.26 the datasets are plotted according to their specific stretch values. Because of the high softening of the tissue according to the age of the donor and the time of autolysis, the stretch curves at 5% , 7.5% and 10% stretch are very noisy and not evaluable.

3.2.4 Heart with the index MYO 2/12

In Tab. 3.17 all available datasets of human heart with the Index Myo 2/12 are shown. In Fig. 3.27, Fig. 3.28, Fig. 3.29, Fig. 3.30 the datasets are plotted according to their specific stretch values.

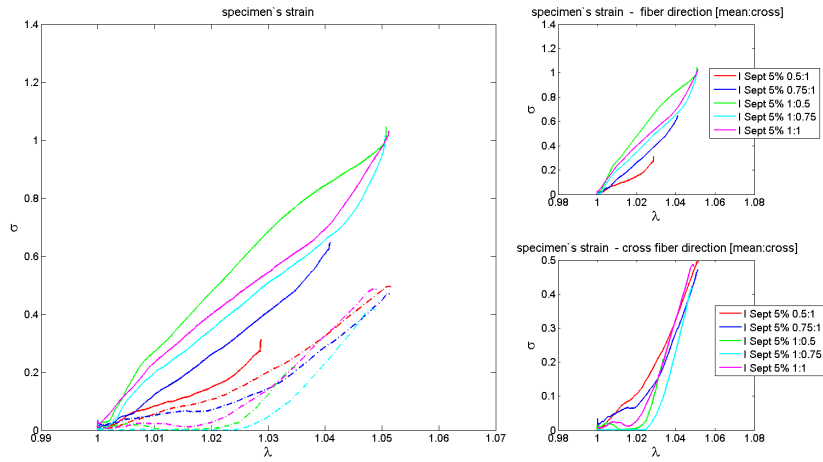


Figure 3.14: Stress-stretch datasets from Heart Transplant#3 at a stretch level of 5% including all different ratios (see Chapt. 2.2.5.1).

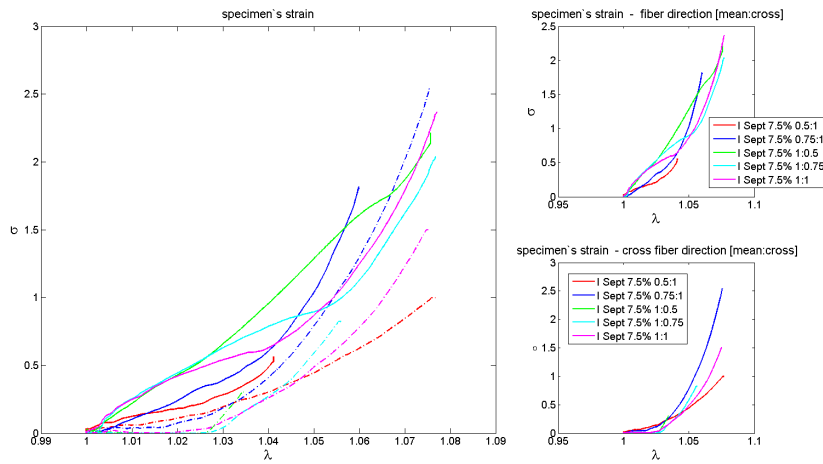


Figure 3.15: Stress-stretch datasets from Heart Transplant#3 at a stretch level of 7.5% including all different ratios (see Chapt. 2.2.5.1).

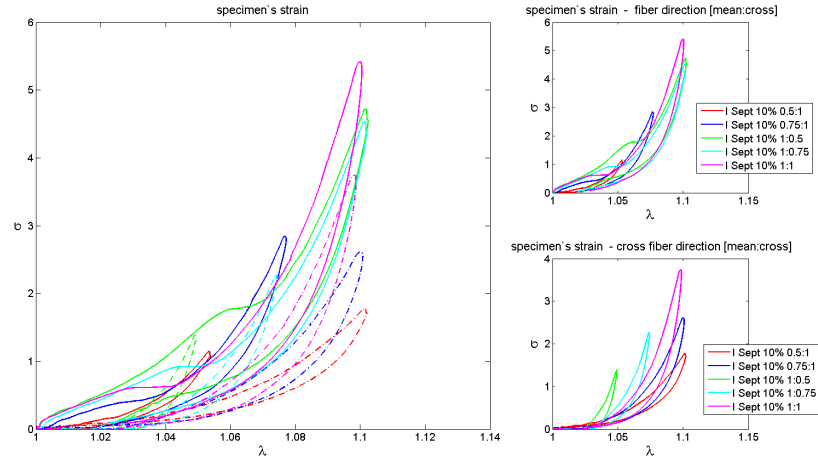


Figure 3.16: Stress-stretch datasets from Heart Transplant#3 at a stretch level of 10% including all different ratios (see Chapt. 2.2.5.1).

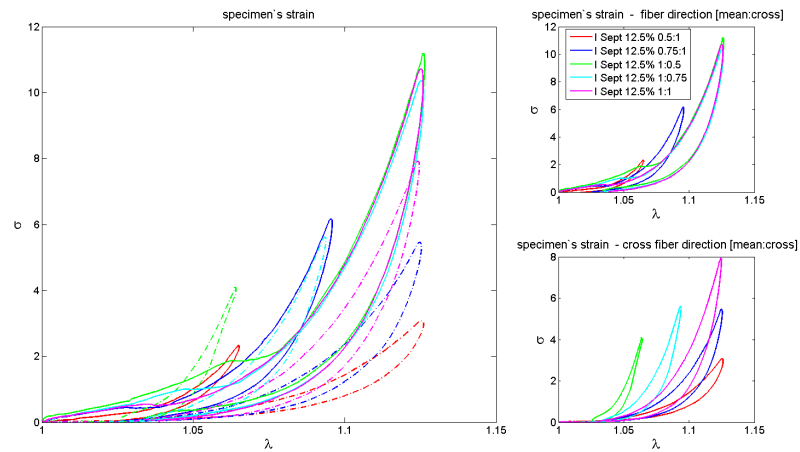


Figure 3.17: Stress-stretch datasets from Heart Transplant#3 at a stretch level of 12.5% including all different ratios (see Chapt. 2.2.5.1).

Table 3.14: Index of plotting curves of human heart with the heart index Transplant#4.

Heart index	Specimen	Origin	Layer	Curve index	Thickness
Transplant #4	# 1	Septum	central	<i>II Sept 5% 1 : 1</i>	5mm
				<i>II Sept 5% 0.75:1</i>	
				<i>II Sept 5% 0.5:1</i>	
				<i>II Sept 5% 1:0.75</i>	
				<i>II Sept 5% 1:0.5</i>	
				<i>II Sept 7.5% 1:1</i>	
				<i>II Sept 7.5% 0.75:1</i>	
				<i>II Sept 7.5% 0.5:1</i>	
				<i>II Sept 7.5% 1:0.75</i>	
				<i>II Sept 7.5% 1:0.5</i>	
				<i>II Sept 10% 1:1</i>	
				<i>II Sept 10% 0.75:1</i>	
	<i>II Sept 10% 0.5:1</i>				
	<i>II Sept 10% 1:0.75</i>				
<i>II Sept 10% 1:0.5</i>					
	# 2	LV	central	<i>II Sept 12.5% 1:1</i>	4.5mm
<i>II Sept 12.5% 0.75:1</i>					
	# 2	LV	central	<i>II Sept 12.5% 0.5:1</i>	4.5mm
<i>II Sept 12.5% 1:0.75</i>					
<i>II Sept 12.5% 1:0.5</i>					
<i>I Sept 5% 1 : 1</i>					
<i>III LV 5% 0.75:1</i>					
<i>III LV 5% 0.5:1</i>					
<i>III LV 5% 1:0.75</i>					
<i>III LV 5% 1:0.5</i>					
<i>III LV 7.5% 1:1</i>					
<i>III LV 7.5% 0.75:1</i>					
<i>III LV 7.5% 0.5:1</i>					
<i>III LV 7.5% 1:0.75</i>					
<i>III LV 7.5% 1:0.5</i>					
	# 2	LV	central	<i>III LV 10% 1:1</i>	4.5mm
<i>III LV 10% 0.75:1</i>					
<i>III LV 10% 0.5:1</i>					
<i>III LV 10% 1:0.75</i>					
	# 2	LV	central	<i>III LV 10% 1:0.5</i>	4.5mm
<i>III LV 10% 1:1</i>					
<i>III LV 10% 0.75:1</i>					
<i>III LV 10% 0.5:1</i>					

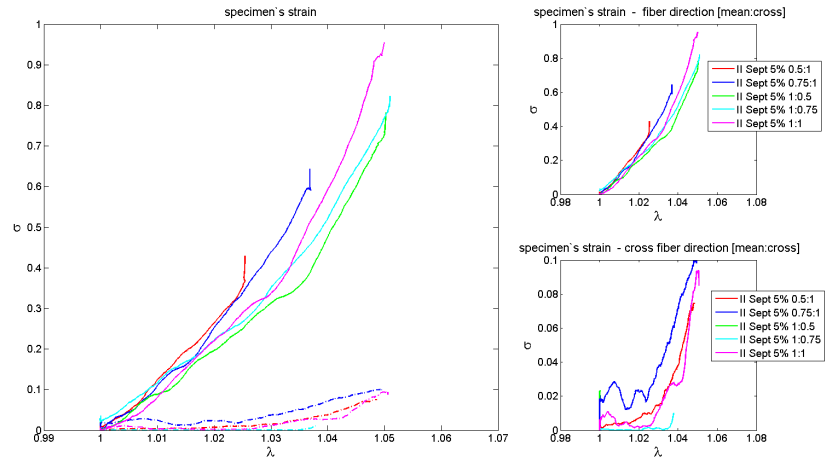


Figure 3.18: Stress-stretch datasets from Specimen #1 of the Heart Transplant#4 at a stretch level of 5% including all different ratios (see Chapt. 2.2.5.1).

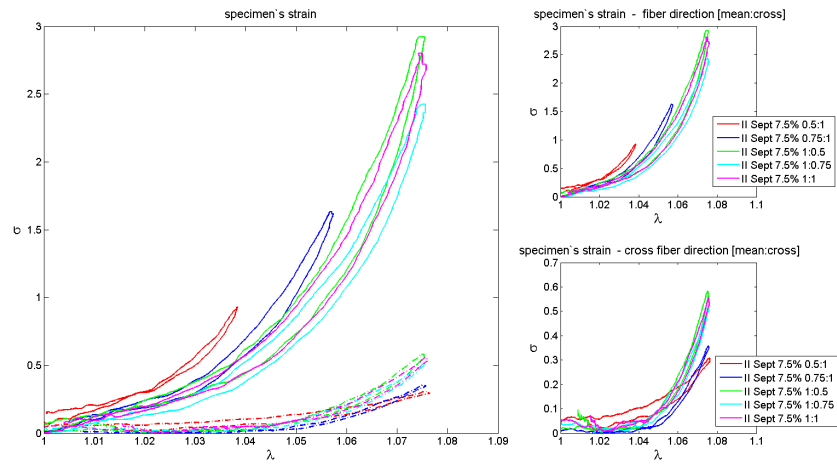


Figure 3.19: Stress-stretch datasets from Specimen #1 of the Heart Transplant#4 at a stretch level of 7.5% including all different ratios (see Chapt. 2.2.5.1).

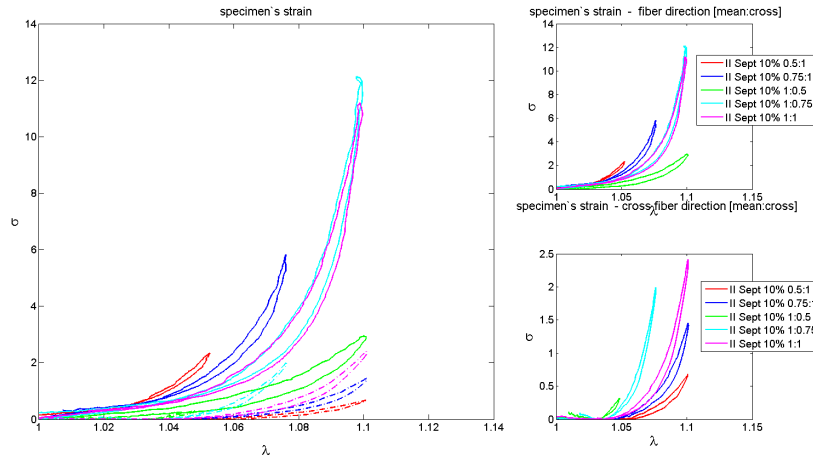


Figure 3.20: Stress-stretch datasets from Specimen #1 of the Heart Transplant#4 at a stretch level of 10% including all different ratios (see Chapt. 2.2.5.1).

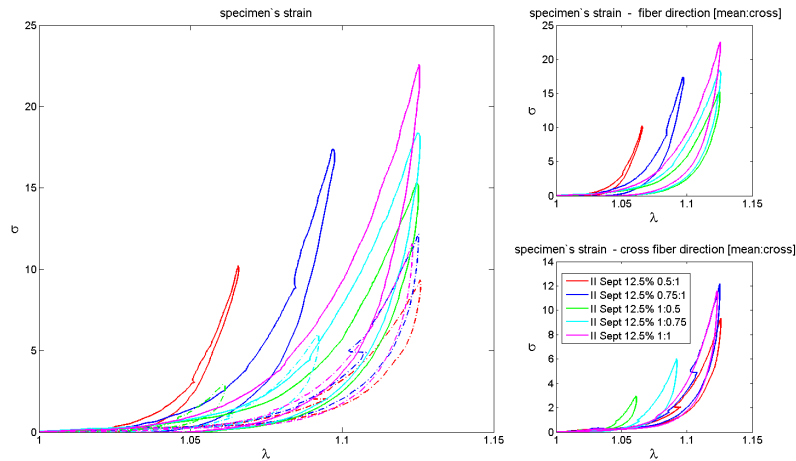


Figure 3.21: Stress-stretch datasets from Specimen #1 of the Heart Transplant#4 at a stretch level of 12.5% including all different ratios (see Chapt. 2.2.5.1).

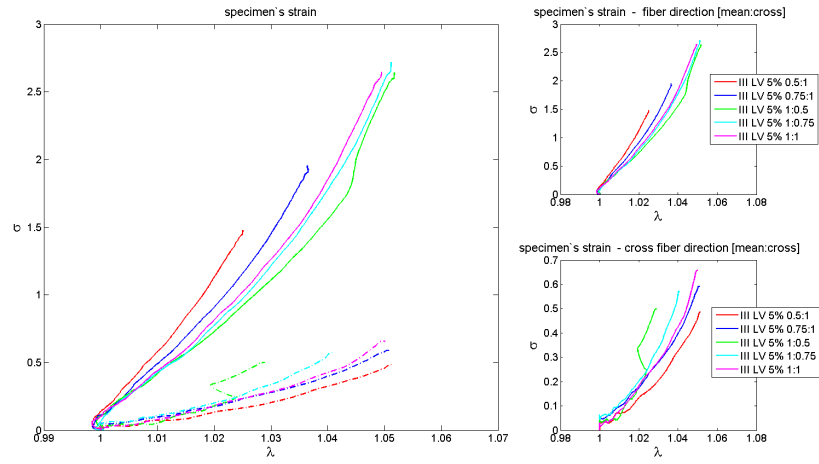


Figure 3.22: Stress-stretch datasets from Specimen #2 of the Heart Transplant#4 at a stretch level of 5% including all different ratios (see Chapt. 2.2.5.1).

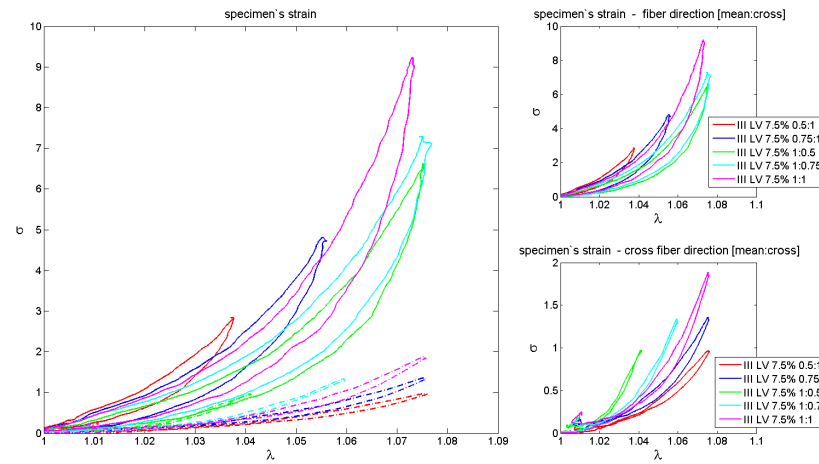


Figure 3.23: Stress-stretch datasets from Specimen #2 of the Heart Transplant#4 at a stretch level of 7.5% including all different ratios (see Chapt. 2.2.5.1).

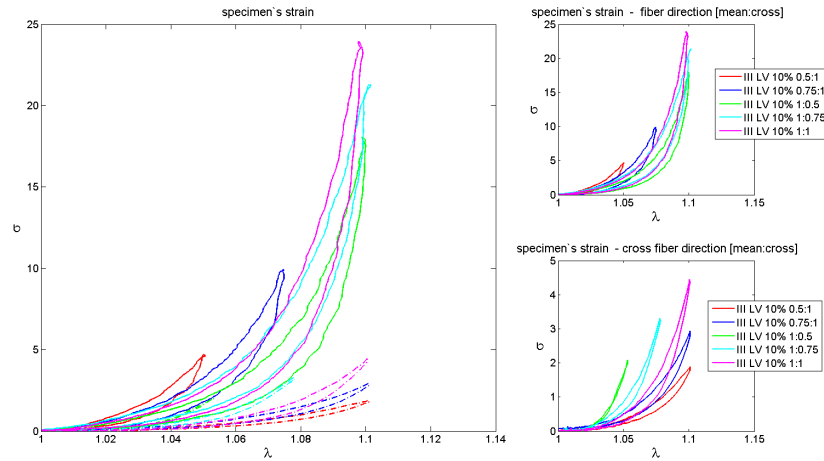


Figure 3.24: Stress-stretch datasets from Specimen #2 of the Heart Transplant#4 at a stretch level of 10% including all different ratios (see Chapt. 2.2.5.1).

Table 3.15: Information about the donors according to the heart indexes, including the used solution during the tests. The index Pa stands for the additive of potassium, RFS for Ringer- Fresenius solution, SCS for standard cardioplegical solution, hypo for hypotrophy, ad for adipose, ddf for dyastolic dysfunction, sc for coronar sclerose.

Heart index	Age	Weight	Sex	Solution	Autolysis	Diseases
	[Years]	[kg]			[Hours]	
Myo 1/12	77	55	male	PB RFS	26	cs
Myo 2/12	32	65	male	SCS	19	hypo
Myo 3/12	93	55	female	PB SCS	12.5	hypo, cs

Table 3.16: Index of plotting curves of human heart with the heart index Myo 1/12.

Heart index	Specimen	Origin	Layer	Curve index	Thickness
Myo 1/12	# 1	LV	central	<i>IV LV 15% 1:1</i>	3.5mm
				<i>IV LV 12.5% 0.75:1</i>	
				<i>IV LV 12.5% 0.5:1</i>	
				<i>IV LV 12.5% 1:0.75</i>	
				<i>IV LV 12.5% 1:0.5</i>	
				<i>IV LV 15% 1:1</i>	
				<i>IV LV 15% 0.75:1</i>	
				<i>IV LV 15% 0.5:1</i>	
				<i>IV LV 15% 1:0.75</i>	
				<i>IV LV 15% 1:0.5</i>	

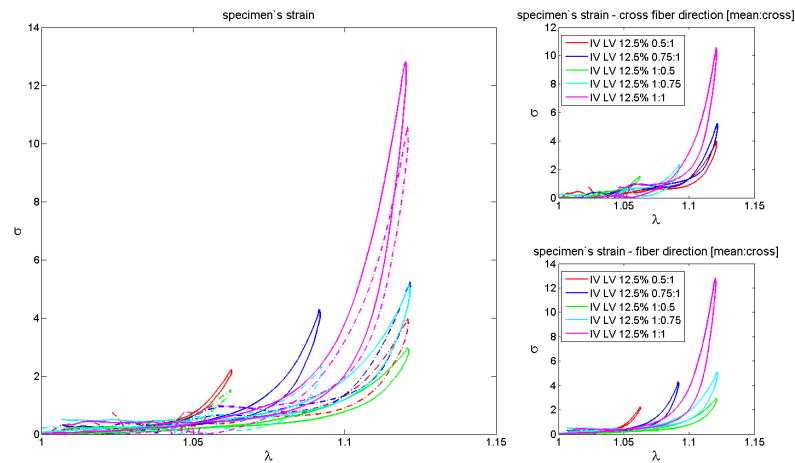


Figure 3.25: Stress-stretch datasets from the Heart with the index Myo 1/12 at a stretch level of 12.5% including all different ratios (see Chapt. 2.2.5.1).

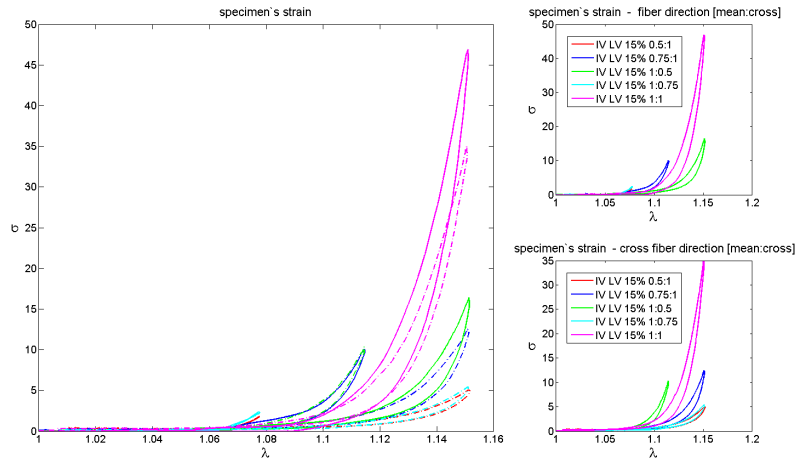


Figure 3.26: Stress-stretch datasets from the Heart with the index Myo 1/12 at a stretch level of 15% including all different ratios (see Chapt. 2.2.5.1).

Table 3.17: Index of plotting curves of human heart with the heart index Myo 2/12.

Heart index	Specimen	Origin	Layer	Curve index	Thickness
Myo 2/12	# 1	LV	central	V LV 5% 1:1	3.1mm
				V LV 5% 0.75:1	
				V LV 5% 0.5:1	
				V LV 5% 1:0.75	
				V LV 5% 1:0.5	
				V LV 7.5% 1:1	
				V LV 7.5% 0.75:1	
				V LV 7.5% 0.5:1	
				V LV 7.5% 1:0.75	
				V LV 7.5% 1:0.5	
				V LV 10% 1:1	
				V LV 10% 0.75:1	
				V LV 10% 0.5:1	
				V LV 10% 1:0.75	
				V LV 10% 1:0.5	
				V LV 12.5% 1:1	
				V LV 12.5% 0.75:1	
				V LV 12.5% 0.5:1	
				V LV 12.5% 1:0.75	
				V LV 12.5% 1:0.5	

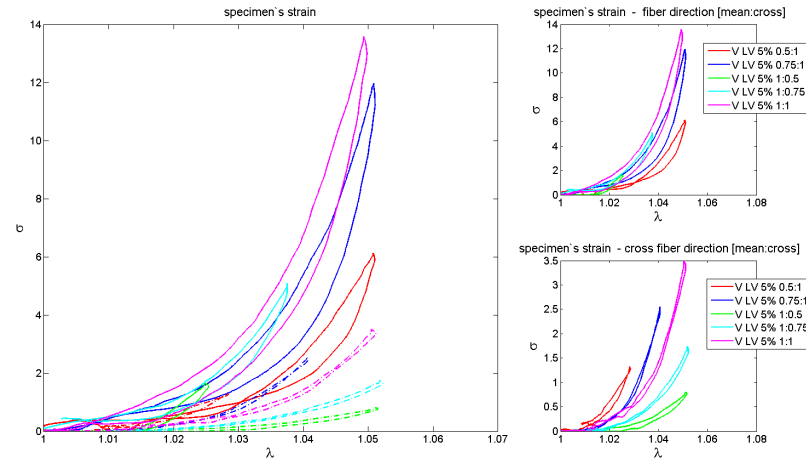


Figure 3.27: Stress-stretch datasets from the Heart with the index Myo 2/12 at a stretch level of 5% including all different ratios (see Chapt. 2.2.5.1).

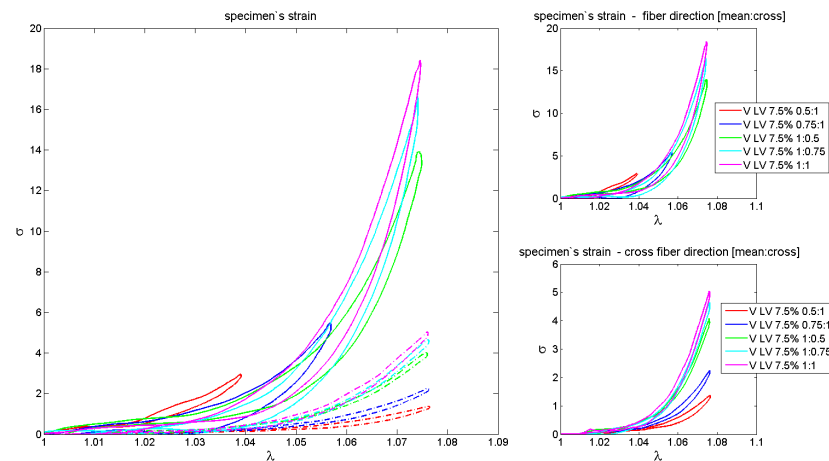


Figure 3.28: Stress-stretch datasets from the Heart with the index Myo 2/12 at a stretch level of 7.5% including all different ratios (see Chapt. 2.2.5.1).

3.2.5 Heart with the index MYO 3/12

In Tab. 3.18 all available datasets of human heart with the Index Myo 2/12 are shown. In Fig. 3.31, Fig. 3.32 and Fig. 3.33 the datasets are plotted according to their specific stretch values. According to the very soft state of the tissue, no evaluateable stress-stretch curves are available for the stretch level of 5% and 7.5%.

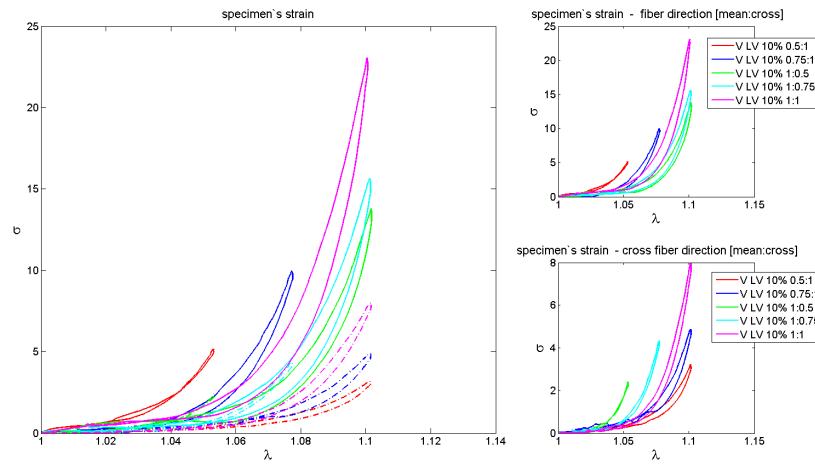


Figure 3.29: Stress-stretch datasets from the Heart with the index Myo 2/12 at a stretch level of 10% including all different ratios (see Chapt. 2.2.5.1).

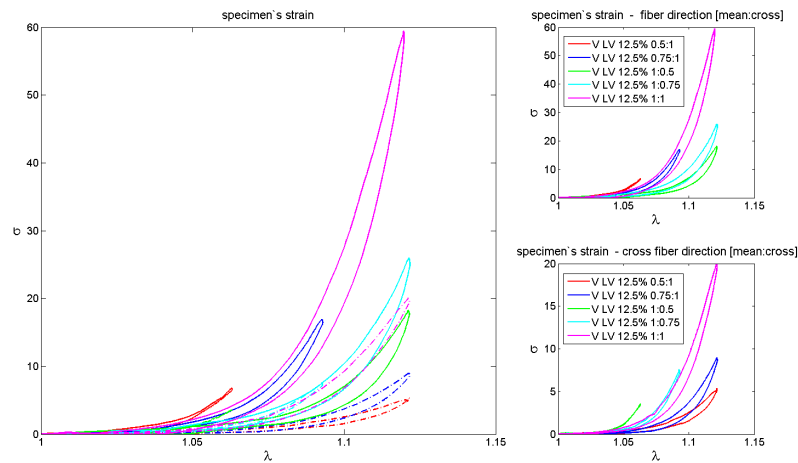


Figure 3.30: Stress-stretch datasets from the Heart with the index Myo 2/12 at a stretch level of 12.5% including all different ratios (see Chapt. 2.2.5.1).

3.2.6 Calculating tables for human hearts

In this chapter the maximum strain-value and the region area for each datasets are listed. The evaluation table is created separately for each heart.

Table 3.18: Information about the donors according to the heart indexes, including the used solution during the tests

Myo 3/12	# 1	LV	central	V LV 12.5% 1:1	4.9mm
				V LV 12.5% 0.75:1	
				V LV 12.5% 0.5:1	
				V LV 12.5% 1:0.75	
				V LV 12.5% 1:0.5	
				V LV 15% 1:1	
				V LV 15% 0.75:1	
				V LV 15% 0.5:1	
				V LV 15% 1:0.75	
				V LV 15% 1:0.5	

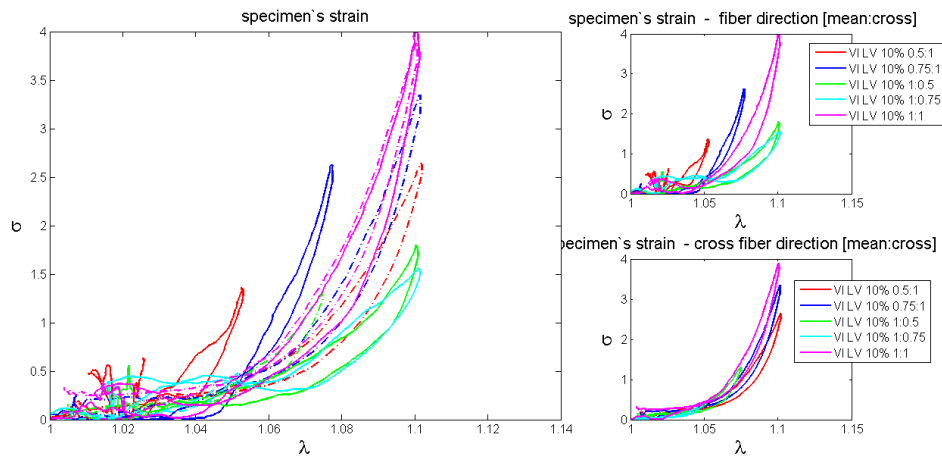


Figure 3.31: Stress-stretch datasets from the Heart with the index Myo 3/12 at a stretch level of 10% including all different ratios (see Chapt. 2.2.5.1).

3.2.6.1 Calculating table of Heart with the index Transplant#1

Because the activation of the heart tissue during the biaxial tensile tests at a stretch level of 7.5% (see Fig. 3.11) only the the values from the 5% stretch test are evaluable. The results are shown in Tab.3.19.

3.2.6.2 Calculating table of Heart with the index Transplant#2

Because the activation of the heart tissue during the biaxial tensile tests at a stretch level of 7.5% (see Fig. 3.11) only the the values from the 5% stretch test are evaluable. The results

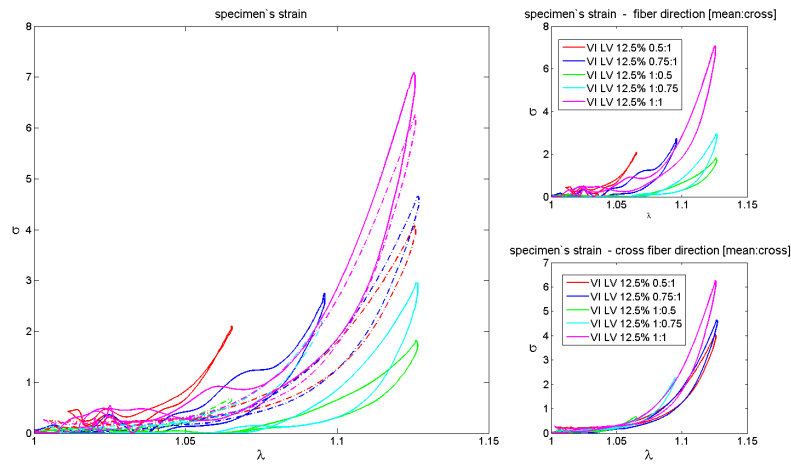


Figure 3.32: Stress-stretch datasets from the Heart with the index Myo 3/12 at a stretch level of 12.5% including all different ratios (see Chapt. 2.2.5.1).

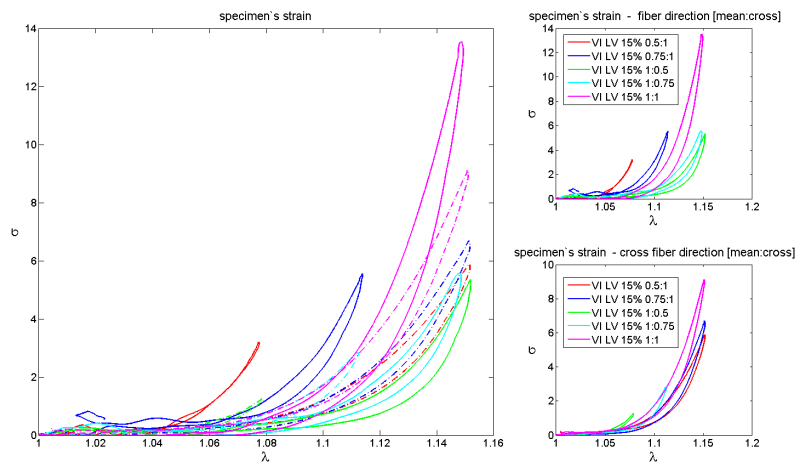


Figure 3.33: Stress-stretch datasets from the Heart with the index Myo 3/12 at a stretch level of 15% including all different ratios (see Chapt. 2.2.5.1).

ares shown in Tab.3.12.

3.2.6.3 Calculating table of Heart with the index Transplant#3

The results for the heart with the index Transplant#3 are listed in Tab.3.21.

Table 3.19: Calculating table for the datasets of specimen #1 of the heart with the index Transplant#1. This table includes the calculated data for the surface areas within the stress-stretch curve and the maximum Cauchy stresses for each direction (fiber direction FD and cross-fiber direction CFD) from the datasets listed in Tab. 3.11.

Curve index	maximum CFD [kPa]	maximum FD [kPa]	Surface area CFD [J/m ³]	Surface area FD [J/m ³]
I LV 5% 1:1	0.9186	4.5006	0.0045	0.0376
I LV 5% 0.75:1	0.9169	3.3445	0.0071	0.0255
ILV 5% 0.5:1	0.7923	3.0432	0.0057	0.0270
I LV 5% 1:0.75	0.7663	5.2480	0.0054	0.0476
I LV 5% 1:0.5	0.6154	4.5606	0.0055	0.0281

Table 3.20: Calculating table for the datasets of specimen #1 of the heart with the index Transplant#2. This table includes the calculated data for the hysteresis areas HA within the stress-stretch curve and the maximum Cauchy stresses for each direction (fiber direction FD and cross-fiber direction CFD) from the datasets listed in Tab. 3.12.

Curve index	maximum CFD [kPa]	maximum FD [kPa]	HA CFD [J/m ³]	HA FD [J/m ³]
II LV 5% 0.5:1	1.1382	1.6011	0.0050	0.0050
II LV 5% 0.75:1	1.4498	2.6121	0.0045	0.0134
II LV 5% 1:0.5	0.9301	2.9733	0.0017	0.0236
II LV 5% 1:0.75	1.3339	3.3514	0.0006	0.0274
II LV 5% 1:1	1.4020	3.1479	0.0051	0.0255

3.2.6.4 Calculating table of Heart with the index Transplant#4

The relevant values are calculated in Tab. 3.22 for specimen#1 and in Tab. 3.23 for specimen#2 of the Heart with the index Transplant#4.

3.2.6.5 Calculating table of Heart with the index Myo1/12

For the human heart with the index Myo1/12 only datasets from the 12.5% and 15% tensile test are evaluable. The relevant values are calculated in Tab. 3.16 for specimen#1 of the Heart with the index Myo1/12.

Table 3.21: Calculating table for the datasets of specimen #1 of the heart with the index Transplant#3. This table includes the calculated data for the surface areas within the stress-stretch curve and the maximum Cauchy stresses for each direction (fiber direction FD and cross-fiber direction CFD) from the datasets listed in Tab. 3.13.

Curve index	maximum CFD	maximum FD	HA CFD	HA FD
	[kPa]	[kPa]	[J/m ³]	[J/m ³]
I Sept 5% 0.5:1	0.4954	0.3117	0.0016	0.0022
I Sept 5% 0.75:1	0.4696	0.6480	0.0014	0.0049
I Sept 5% 1:0.5	0.2168	1.0455	0.0008	0.0124
I Sept 5% 1:0.75	0.4166	1.0154	0.0095	0.0084
I Sept 5% 1:1	0.4857	1.0370	0.0015	0.0108
I Sept 7.5% 0.5:1	0.9971	0.5627	0.0084	0.0054
I Sept 7.5% 0.75:1	2.5407	1.8182	0.0201	0.0134
I Sept 7.5% 1:0.5	0.3030	2.2133	0.0049	0.0323
I Sept 7.5% 1:0.75	0.8228	2.0394	0.0030	0.0282
I Sept 7.5% 1:1	1.4960	2.3659	0.0074	0.0253
I Sept 10% 0.5:1	1.7654	1.143	0.0166	0.0052
I Sept 10% 0.75:1	2.6088	2.8421	0.0245	0.0249
I Sept 10% 1:0.5	1.3805	4.7215	0.0061	0.0713
I Sept 10% 1:0.75	2.1717	4.5233	0.0122	0.0577
I Sept 10% 1:1	3.741	5.4119	0.0337	0.0691
I Sept 12.5% 0.5:1	3.0730	2.3292	0.0349	0.0138
I Sept 12.5% 0.75:1	5.4622	6.1648	0.0612	0.0604
I Sept 12.5% 1:0.5	4.1046	11.1851	0.0176	0.1701
I Sept 12.5% 1:0.75	5.6151	10.3574	0.0421	0.15558
I Sept 12.5% 1:1	7.9272	10.7171	0.0870	0.1513

3.2.6.6 Calculating table of Heart with the index Myo2/12

The relevant values are calculated in Tab. 3.17 for specimen#1 of the Heart with the index Myo2/12.

3.2.6.7 Calculating table of Heart with the index Myo3/12

The results of the evaluated datasets from specimen#1 from the heart with the Index Myo3/12 are listed in 3.26.

Table 3.22: Calculating table for the datasets of specimen #1 of the heart with the index Transplant#4. This table includes the calculated data for the hysteresis areas HA within the stress-stretch curve and the maximum Cauchy stresses for each direction (fiber direction FD and cross-fiber direction CFD) from the datasets listed in Tab. 3.14.

Curve index	maximum CFD	maximum FD	HA CFD	HA FD
	[kPa]	[kPa]	[J/m ³]	[J/m ³]
II Sept 5% 0.5:1	0.0745	0.4287	0.0003	0.0001
II Sept 5% 0.75:1	0.1	0.6434	0.0001	0.0018
II Sept 5% 1:0.5	0.0231	0.7820	0.0004	0.0023
II Sept 5% 1:0.75	0.0098	0.8221	0.0001	0.0037
II Sept 5% 1:1	0.0093	0.9546	0.0005	0.0027
II Sept 7.5% 0.5:1	0.3072	0.9302	0.0032	0.0009
II Sept 7.5% 0.75:1	0.3568	1.6299	0.0007	0.0041
II Sept 7.5% 1:0.5	0.5815	2.9213	0.0013	0.0121
II Sept 7.5% 1:0.75	0.5132	2.4321	0.0021	0.0101
II Sept 7.5% 1:1	0.5580	2.7989	0.0012	0.0107
II Sept 10% 0.5:1	0.6839	2.3353	0.0030	0.0014
II Sept 10% 0.75:1	1.4155	5.8345	0.0056	0.0111
II Sept 10% 1:0.5	0.3174	2.9492	0.0005	0.0289
II Sept 10% 1:0.75	1.9876	12.1147	0.0030	0.0246
II Sept 10% 1:1	2.4131	11.2096	0.0081	0.0423
II Sept 12.5% 0.5:1	9.3574	10.2265	0.0716	0.0290
II Sept 12.5% 0.75:1	12.1956	17.4049	0.0931	0.1211
II Sept 12.5% 1:0.5	2.9484	15.2949	0.0122	0.1928
II Sept 12.5% 1:0.75	5.9879	18.3626	0.0408	0.2579
II Sept 12.5% 1:1	11.5851	22.5748	0.1059	0.2959

Table 3.23: Calculating table for the datasets of specimen #2 of the heart with the index Transplant#4. This table includes the calculated data for the hysteresis areas HA within the stress-stretch curve and the maximum Cauchy stresses for each direction (fiber direction FD and cross-fiber direction CFD) from the datasets listed in Tab. 3.14.

Curve index	maximum CFD	maximum FD	HA CFD	HA FD
	[kPa]	[kPa]	[J/m ³]	[J/m ³]
III LV 7.5% 0.5:1	0.9606	2.8364	0.0027	0.0138
III LV 7.5% 0.75:1	1.3523	4.7893	0.0049	0.0311
III LV 7.5% 1:0.5	0.9701	6.6152	0.0009	0.0570
III LV 7.5% 1:0.75	1,3323	7.2893	0.0017	0.0668
III LV 7.5% 1:1	1.8859	9.2237	0.0047	0.0695
III LV 10% 0.5:1	1.8900	4.7138	0.0131	0.0256
III LV 10% 0.75:1	2.9340	9.9555	0.0198	0.0746
III LV 10% 1:0.5	2.0887	18.0871	0.0007	0.1513
III LV 10% 1:0.75	3.3064	21.3073	0.0110	0.1811
III LV 10% 1:1	4.4386	23.9261	0.0248	0.1888

Table 3.24: Calculating table for the datasets of specimen #1 of the heart with the index Myo1/12. This table includes the calculated data for the hysteresis areas HA within the stress-stretch curve and the maximum Cauchy stresses for each direction (fiber direction FD and cross-fiber direction CFD) from the datasets listed in Tab. 3.24.

Curve index	maximum CFD	maximum FD	HA CFD	HA FD
	[kPa]	[kPa]	[J/m ³]	[J/m ³]
IV LV 12.5% 0.5:1	3.9842	2.2180	0.0177	0.0003
IV LV 12.5% 0.75:1	5.2440	4.2961	0.0197	0.0099
IV LV 12.5% 1:0.5	1.5285	2.9668	0.0076	0.0117
IV LV 12.5% 1:0.75	2.3427	5.1135	0.0260	0.0191
IV LV 12.5% 1:1	10.5892	12.8137	0.0238	0.0630
IV LV 15% 0.5:1	1.8099	5.0710	0.0007	0.0207
IV LV 15% 0.75:1	10.0955	12.4758	0.0484	0.0792
IV LV 15% 1:0.5	16.4188	10.3150	0.1033	0.0373
IV LV 15% 1:0.75	2.4017	5.4284	0.0011	0.0306
IV LV 15% 1:1	34.9891	46.8092	0.1802	0.3074

Table 3.25: Calculating table for the datasets of specimen #1 of the heart with the index Myo2/12. This table includes the calculated data for the hysteresis areas HA within the stress-stretch curve and the maximum Cauchy stresses for each direction (fiber direction FD and cross-fiber direction CFD) from the datasets listed in Tab. 3.17.

Curve index	maximum CFD	maximum FD	HA CFD	HA FD
	[kPa]	[kPa]	[J/m ³]	[J/m ³]
V LV 5% 0.5:1	1.3187	6.1090	0.0014	0.0196
V LV 5% 0.75:1	2.5491	11.9642	0.0011	0.0450
V LV 5% 1:0.5	0.7973	1.6432	0.0031	0.0028
V LV 5% 1:0.75	1.7333	5.0896	0.0025	0.0132
V LV 5% 1:1	3.4960	13.5737	0.0027	0.0525
V LV 7.5% 0.5:1	1.3711	2.9466	0.0054	0.0087
V LV 7.5% 0.75:1	2.2519	5.6422	0.0060	0.0412
V LV 7.5% 1:0.5	4.0711	13.8914	0.0020	0.0673
V LV 7.5% 1:0.75	4.6405	16.6517	0.0096	0.0797
V LV 7.5% 1:1	5.0401	18.4153	0.0128	0.0769
V LV 10% 0.5:1	3.2162	5.1388	0.0159	0.0067
V LV 10% 0.75:1	4.8860	9.9717	0.0157	0.0374
V LV 10% 1:0.5	2.3934	13.7815	0.0019	0.0635
V LV 10% 1:0.75	4.3359	15.6475	0.0047	0.0902
V LV 10% 1:1	7.9983	23.0605	0.0268	0.1118
V LV 12.5% 0.5:1	5.3878	6.7590	0.0596	0.0207
V LV 12.5% 0.75:1	8.9964	19.9652	0.0611	0.0614
V LV 12.5% 1:0.5	3.5552	18.2243	0.0046	0.1546
V LV 12.5% 1:0.75	7.7563	25.9962	0.0189	0.1794
V LV 12.5% 1:1	19.9834	59.5296	0.1124	0.3802

Table 3.26: Calculating table for the datasets of specimen #1 of the heart with the index Myo3/12. This table includes the calculated data for the hysteresis areas HA within the stress-stretch curve and the maximum Cauchy stresses for each direction (fiber direction FD and cross-fiber direction CFD) from the datasets listed in Tab. 3.18.

Curve index	maximum CFD	maximum FD	HA CFD	HA FD
	[kPa]	[kPa]	[J/m ³]	[J/m ³]
VI LV 12.5% 0.5:1	4.0987	2.1087	0.0236	0.0007
VI LV 12.5% 0.75:1	4.6561	2.7506	0.0280	0.0246
VI LV 12.5% 1:0.5	0.6821	1.8169	0.0017	0.0174
VI LV 12.5% 1:0.75	2.6827	2.9529	0.0062	0.2221
VI LV 12.5% 1:1	6.2625	7.0854	0.0362	0.0575
VI LV 15% 0.5:1	5.9016	3.2066	0.0399	0.0004
VI LV 15% 0.75:1	6.6888	5.5462	0.0500	0.0210
VI LV 15% 1:0.5	1.2807	5.3454	0.0019	0.0515
VI LV 15% 1:0.75	2.8327	5.5718	0.0209	0.0708
VI LV 15% 1:1	9.1296	13.5138	0.0583	0.1053

4 Discussion

4.1 Porcine myocardial tissue

The main aim of this thesis is the investigation of the human myocardial tissue. Due to this, the results for porcine myocardium tissue is discussed briefly. Referring to the results obtained from the biaxial tensile tests, there is a need to compare the different datasets to each other, to conduct a meaningful statement about the mechanical behavior of porcine myocardial tissue. A qualitative method for comparing the stress-stretch curves is to contrast them according to their maximum values and surface areas. In Tab. 4.1 the calculated mean values and corresponding standard deviation from the datasets of the fresh LV are listed. Comparing the mean values at a ratio from 1:1 (CFD:FD) of the maximum for both directions (CFD and the MFD) at the different stretches, makes it possible to formulate an accurate factor that describes the relationship between the CFD and FD with an relationship factor of 3 as shown in Eq. 4.1.

$$CFD_{7.5} : FD_{7.5} = 2.952 \quad CFD_{10} : FD_{10} = 3.048 \quad CFD_{15} : FD_{15} = 2.58 \quad (4.1) \\ \implies CFD : FD \sim 3$$

For the mean values of the septum the same relationship between the CFD and FD can be established (see Tab.4.2) as shown in Eq.4.2.

$$CFD_{10} : FD_{10} = 2.952 \quad (4.2) \\ \implies CFD : FD \sim 3$$

The assessment of the relationship factor for the septum of the porcine heart is not as meaningful as the relationship factor of the LV because of the much fewer data collected from the septum ($n_{LV}=13$, $n_{Septum} = 5$). Comparing the maximum mean Cauchy stress values from the septum at 10% stretch with the corresponding mean values from the LV, it can be shown, that the stiffness of the septum is considerably larger. The relation factor is 45%.

By comparing the mean hysteresis areas of the septum and the LV, it turns out that the septum's hysteresis is much bigger (45%), which is probably due to a higher amount of cardiomyocytes. This in turn suggests the bigger stiffness of the porcine myocardium from the septum.

Table 4.1: Mean value (mean) and standard deviation (SD) of datasets from porcine heart tissue separated from the LV at fresh state according to their maximum values for each direction and hysteresis areas HA.

Stretch value	statistic	maximum CFD	maximum FD	HA CFD	HA FD
		[kPa]	[kPa]	[J/m ³]	[J/m ³]
7.5%	Mean	5.2034	15.364	0.0324	0.1435
	SD	2.9918	7.1831	0.0247	0.0623
10%	Mean	8.9917	27.4109	0.0745	0.3419
	SD	4.1701	12.8814	0.0525	0.2206
15%	Mean	24.7039	63.7538	0.3159	1.1768
	SD	10.2722	23.9999	0.1609	0.4936

Table 4.2: Mean value (mean) and standard deviation (SD) of datasets from porcine heart tissue separated from the septum at fresh state according to their maximum values for each direction and hysteresis areas HA.

Stretch value	statistic	maximum CFD	maximum FD	HA CFD	HA FD
		[kPa]	[kPa]	[J/m ³]	[J/m ³]
10%	Mean	13.6584	40.5517	0.1538	0.5442
	SD	8.5187	11.6598	0.1059	0.0007

4.2 Human myocardial tissue

For the investigation of the mechanical behavior of human myocardial tissue an amount of seven human heart was available, whereas three hearts were derived from the Institute of Pathology and four hearts from the Clinical Department of Transplant Surgery. Referring to the origin of the tissue, different results are expected. Pathological heart tissue, which is exposed to an uncooled and unbuffered state before achieved, is getting modified according to the autolysis process (see Chapt.4.2.2). Due to this, a softening of the tissue should be noticed. In comparison, human heart tissue from the Department of Transplant Surgery is buffered in cardioplegical solution before and immediately after separation from the donor, which continues the supply of nutrients other relevant substances to the cardiomyocytes after the removal, and keeps the myocardial tissue at a passive state. Based on this statement it can be assumed that the stiffness of the myocardial tissue from the Department of Transplant Surgery should show a higher stiffness.

Furthermore, heart related diseases like hypertrophy, cardiac adipose and coronary sclerosis influence the heart tissue already during the lifetime of the donor, and take effect on the mechanical behavior of the tissue (see Chapt. 4.2.3).

There are also other factors, that are not heart dependent, that might influence the measured data during the biaxial tensile tests. The circumstances, that the amount of received myocardial tissue was quite small, the separation of the specimen under consideration of the exact defined directions (CFD and FD) was not always possible. Another problem were the inhomogeneous regions (like little fat storages) on the separated specimen.

In the following chapter the test results are listed and compared for both type of heart origin.

4.2.1 Result and comparison of the different datasets

Comparable values for the hearts referring to their origin and location are the stress-stretch curves at the same ratios. In Tab. 4.3 the relevant datasets for Hearts of the Clinical Department of Transplant Surgery, and in Tab. 4.4 are listed for discussion.

Table 4.3: Relevant datasets from hearts of the Department of Transplant Surgery showing their maximum values for each direction and hysteresis areas HA.

Heart index	Curve index	maximum CFD [kPa]	maximum FD [kPa]	HA CFD [J/m ³]	HA FD [J/m ³]
Transplant#1	I LV 5% 1:1	0.9186	4.5006	0.0045	0.0376
	I LV 7.5% 1:1	1.8479	9.5343	0.0093	0.0756
Transplant#2	II LV 5% 1:1	1.4020	3.1479	0.0051	0.0255
	II LV 7.5% 1:1	4.2495	7.5983	0.0369	0.0983
Transplant#3	I Sept 5% 1:1	0.4857	1.0370	0.0015	0.0108
	I Sept 7.5% 1:1	1.4960	2.3659	0.0074	0.0253
	I Sept 10% 1:1	3.741	5.4119	0.0337	0.0691
	I Sept 12.5% 1:1	7.9272	10.7171	0.0870	0.1513
Transplant#4	II Sept 5% 1:1	0.0093	0.9546	0.0005	0.0027
	II Sept 7.5% 1:1	0.5580	2.7989	0.0012	0.0107
	II Sept 10% 1:1	2.4131	11.2096	0.0081	0.0423
	II Sept 12.5% 1:1	11.5851	22.5748	0.1059	0.2959
	III LV 7.5% 1:1	1.8859	9.2237	0.0047	0.0695
	III LV 10% 1:1	4.4386	23.9261	0.0248	0.1888

Table 4.4: Relevant datasets from Hearts of the Institute of Pathology showing their maximum values for each direction and hysteresis areas HA.

Heart index	Curve index	maximum CFD	maximum FD	HA CFD	HA FD
		[kPa]	[kPa]	[J/m ³]	[J/m ³]
Myo1/12	IV LV 12.5% 1:1	10.5892	12.8137	0.0238	0.0630
	IV LV 15% 1:1	34.9891	46.8092	0.1802	0.3074
Myo2/12	V LV 5% 1:1	3.4960	13.5737	0.0027	0.0525
	V LV 7.5% 1:1	5.0401	18.4153	0.0128	0.0769
	V LV 10% 1:1	7.9983	23.0605	0.0268	0.1118
	V LV 12.5% 1:1	19.9834	59.5296	0.1124	0.3802
Myo3/12	VI LV 12.5% 1:1	6.2625	7.0854	0.0362	0.0575
	VI LV 15% 1:1	9.1296	13.5138	0.0583	0.1053

The ratio between the FD (fiber direction) and CFD (cross-fiber direction) of the heart Transplant#1, Transplant#2 and Transplant #4 from the LV at a stretch ratio from 7.5% shows similar behavior. The maximum of the strain from CFD of both varies considerably but the maximum strain is nearly the same. Facts comparing the mean values for the maximum strain at the different stretch ratios (5% and 7.5%) are shown in Tab. 4.5.

Table 4.5: Mean value (mean) and standard deviation (SD) of datasets from Transplant heart tissue according to their maximum values for each direction and hysteresis areas HA.

Stretch value	statistic	maximum CFD	maximum FD	HA CFD	HA FD
		[kPa]	[kPa]	[J/m ³]	[J/m ³]
5%	Mean	1.208	3.7855	0.0048	0.03
	SD	0.4334	0.9559	0.00005	0.0104
7.5%	Mean	2.6363	8.6429	0.0169	0.097
	SD	1.3973	0.9771	0.0175	0.0169

Under the fact, that different solutions were used as bath during the test (see Tab. 3.10), the results of the proceeded test are not as different as expected. During the 7.5% stretch test of the Transplant#1 and Transplant#2 at body milieu temperature of 37°C an activation occurred as shown in Fig.3.11 and Fig.3.13. Different than anticipated, potassium concentration in the solution plays not a so important role as expected. This means that only the increasing of potassium concentration can not prevent the activation of the tissue. During the test it was recognized, that the temperature component of the used bath solutions play

at least an as big role as the potassium concentration. So, to prevent the activation of the tissue during the test, the hypothermia and the concentration of cardioplegical components in the solution play the major roles. This fact will be discussed in 4.2.2. Biaxial tensile tests on the heart Transplant#3 and Transplant#4 were done under consideration of the new insights discussed in 4.2.2 at a temperature of 17°C.

The results from Transplant #3 is not comparable with the other 3 from the Department of Transplant Surgery hearts, because of the fact that the cells were frozen, and so the cardiomyocytes were dead after defrosting. This heart shows a stiffer behavior than the ones from the Institute of Pathology, but a softer behavior than the other transplant hearts if comparing the values. It would not be meaningful to discuss the statistic values of the hearts Myo1/12, Myo2/12, and Myo3/12 from the Institute of Pathology in the same way as done for received hearts from the Department of Transplant Surgery, because the cardiomyocytes of those hearts are already dead and so the measured values are mostly references from the collageneous components of the ECM. This phenomenon will be discussed in Chapt. 4.2.2. As shown in Myo1/12 and Myo3/12 the ratio between CFD and FD is very small.

The ratio between the CFD and FD from the heart Myo 2/12 (a factor of about 4) was quite high. This heart can not be compared directly with the other two hearts from the Institute of Pathology, because the age of the human donor (32 years) in this case was very small in comparison to the other two. So, the natural decay of cardiomyocytes during lifetime of the donor was much lower. Due to this, it can be concluded, that the tissue was basically stiffer when received, and the autolysis due to the young heart tissue was proceeded very hardly because of the greater amount of cardiomyocytes.

4.2.2 Autolysis and activation

Autolysis is known as the self-decomposition of already dead cardiac myocytes. If a certain period of autolysis (> 20 h) is exceeded, cells are already destroyed and mainly collageneous components from the extracellular matrix and cell deposits remain (endomysial collagen as seen in Fig. 1.3). Due to this, it can be assumed, that the highly anisotropic mechanical behavior of the human myocardial tissue with progression of autolysis, is getting more isotropic (only hypothesis).

Therefore, only small maximum values of Myo1/12 and Myo3/12 according to each direction are recognized, due the destroyed myofibers, the decay of endomysial collagen and the associated decrease in stiffness in the direction of them.

Activation of the myocardial tissue occurred during the tensile tests of the hearts Transplant#1 and Transplant#2. Generally the activation of the myocardial tissue should be prevented while using cardioplegical solutions containing potassium. The higher potassium concentration of such a cardioplegical solution increases the permeability of the cell mem-

brane for potassium. Further, the resting potential is decreased due to the minimized K^+ -concentration-gradient. Hence, the cell is depolarized, which immobilizes the cell membrane. Due to the immobilization, ion exchange is inhibited. Mechanical stress acting on the cardiomyocytes of the tissue can cancel this depolarization and cause an activation (contraction). Another reason for activating the depolarized membrane is the mechanotransductive activation, initiated by the unleashing of the internal Ca^{2+} reservoirs out of the mitochondria from the cardiomyocytes via the acting mechanical stress on the cell. During the biaxial tensile tests it has been established, that this effect is increasing due to the rising temperature of the solution bath (hypothermia component of cardioplegia).

4.2.3 Heart related diseases and age related changes in structure

Due to the investigation of human hearts containing heart related diseases like the hypertrophy, coronary sclerosis and the diastolic dysfunction, only anatomical changes according to the wall thickness of the ventricles were detected. During this thesis it was not possible to determine the impact of these diseases according to the mechanical behavior, because of the small amount of human specimens tested.

The donor's age was greatly influencing the mechanical behavior of the myocardial tissue. Biaxial tensile tests have shown, that with the increasing age of the donor the stiffness of the myocardial tissue is decreasing. As seen in the results of Myo2/12 the influence of the natural decay of cardiomyocytes during the lifetime of the donor has much more influence than the autolysis. Because only one specimen at a younger age was derived from each department, this statement can only be seen as a hypothesis.

5 Appendix

5 Appendix

Antrag	
Version 6.3 vom 25.03.2011	Bitte immer die <u>aktuelle</u> Version verwenden (http://ethikkommissionen.at)!

Dieses Formular soll für Einreichungen bei österreichischen Ethikkommissionen verwendet werden.
 Es setzt sich aus einem allgemeinen **Teil A** - Angaben zur Studie und zum Sponsor -
 und aus einem speziellen **Teil B** - Angaben zu der/den einzelnen Prüfstelle(n) - zusammen.
 Bei Einreichungen für mehrere Zentren (Prüfer/innen) muss nur der Teil B an das jeweilige Zentrum angepasst werden.

Adresse der Ethikkommission (optional) An die Ethikkommission der Medizinischen Universität Graz LKH Universitätsklinikum Auenbruggerplatz 2, 3. OG A-8036 Graz	Raum für Eingangsstempel, EK-Nummer, etc. Bitte Freilassen!
---	--

ANTRAG AUF BEURTEILUNG EINES KLINISCHEN FORSCHUNGSPROJEKTES

für folgende Prüfer/innen bei folgenden österreichischen Ethikkommissionen:

- ▶ Bitte **alle** Ethikkommissionen eintragen, an die der Antrag gesendet wird (**Kurzbezeichnung!**) ◀
- ▶ Im Falle einer **multizentrischen Arzneimittelstudie** ist die **Leitethikkommission** als erste anzuführen! ◀

Zuständige Ethikkommission	Prüferin/Prüfer (lokale Studienleitung)
Ethikkommission Graz	Dr. med.univ. Michaela Schwarz

Teil A

1. Allgemeines:

- 1.1 Projekttitel: **Biomechanik des humanen ventrikulären Myokards**
- 1.2 Protokollnummer/-bezeichnung: **BiomechMyocard V2.0** 1.2.1 EudraCT-Nr.:
- 1.3 Datum des Protokolls: **14.12.2011** 1.3.1 ISRCTN-Nr.:
- 1.4 Daten der beiliegenden Amendments: 1.4.1 Nr. 1.4.2 Datum:
- 1.4.3 Nr. 1.4.4 Datum:
- 1.4.5 Nr. 1.4.6 Datum:

1.5 Sponsor / RechnungsempfängerIn (Kontaktperson in der Buchhaltung):

- | | | | |
|----------------------|----------------|--|-----------------------------|
| | <u>Sponsor</u> | | <u>RechnungsempfängerIn</u> |
| 1.5.1 Name: | keine | | |
| 1.5.2 Adresse: | | | |
| 1.5.3 Kontaktperson: | | | |
| 1.5.4 Telefon: | | | |
| 1.5.5 FAX: | | | |
| 1.5.6 e-mail: | | | |
| 1.5.7 UID-Nummer | | | |

(wenn nicht gleich wie „Sponsor“)

2. Eckdaten der Studie

- 2.1 Art des Projektes: 2.1.1 Klinische Prüfung eines nicht registrierten **Arzneimittels**
 2.1.2 Klinische Prüfung eines registrierten **Arzneimittels**
 2.1.2.1 gemäß der Indikation 2.1.2.2 nicht gemäß der Indikation
 2.1.3 Klinische Prüfung einer neuen **medizinischen Methode**
 2.1.4 Klinische Prüfung eines **Medizinproduktes**
 2.1.4.1 mit CE-Kennzeichnung 2.1.4.2 ohne CE-Kennzeichnung
 2.1.4.3 Leistungsbewertungsprüfung (In-vitro-Diagnostika)
 2.1.5 **Nicht-therapeutische biomedizinische Forschung** am Menschen
(Grundlagenforschung)
 2.1.6 **Genetische Untersuchung**
 2.1.10 **Register**
 2.1.11 **Biobank**
 2.1.12 **Retrospektive Datenauswertung**
 2.1.13 **Fragebogen Untersuchung**
 2.1.14 **Psychologische Studie**
 2.1.15 **Pflegewissenschaftliche Studie**
 2.1.16 **Nicht-interventionelle Studie (NIS)**
 2.1.7 **Sonstiges** (z.B. Diätetik, Epidemiologie, etc.), bitte spezifizieren:

Zusatzinformation: 2.1.8 **Dissertation** 2.1.9 **Diplomarbeit**

2.2 Fachgebiet: **Transplantchirurgie, Biomechanik**

2.3 Arzneimittelstudie (wenn zutreffend)

2.4 Medizinproduktstudie (wenn zutreffend)

2.3.1 Prüfsubstanz(en):

2.4.1 Prüfprodukt(e):

2.3.2 Referenzsubstanz:

2.4.2 Referenzprodukt:

2.5 Klinische Phase: _____ (unbedingt angeben, bei Medizinprodukten die am ehesten zutreffende Phase)

2.6 Nehmen andere Zentren an der Studie teil: ja nein. Wenn **ja**:

2.6.1 im Inland

2.6.2 im Ausland

2.7 Liste der Zentren: **Klinische Abteilung für Transplantationschirurgie, Medizinische Universität
Graz
Institut für Biomechanik, Technische Universität Graz**

2.8 Liegen bereits Voten anderer Ethikkommissionen vor?

ja nein. Wenn **ja**, **Voten beilegen!**

2.9 Geplante **Gesamtzahl** der **Prüfungsteilnehmer/innen** (in allen teilnehmenden Zentren):

30

5 Appendix

- 2.10 Charakterisierung der Prüfungsteilnehmer/innen: 2.10.1 Mindestalter: _____ 2.10.2 Höchstalter: _____
2.10.3 Sind auch nicht persönlich Einwilligungsfähige einschließbar? ja nein
2.10.4 Einschließbar sind weibliche (und/oder) männliche Teilnehmer/innen.
2.10.5 Sind gebärfähige Frauen einschließbar? ja nein. Wenn **nein**: Begründung unter 7.5

- 2.11 Dauer der Teilnahme der einzelnen Prüfungsteilnehmer/innen an der Studie: **nicht zutreffend**
2.11.1 Aktive Phase: _____ 2.11.2 Nachkontrollen: _____

- 2.12 Voraussichtliche Gesamtdauer der Studie: **2.5 Jahre**

3a. Betrifft nur Studien gemäß AMG: Angaben zur Prüfsubstanz (falls nicht in Österreich registriert):

- 3.1 Registrierung in anderen Staaten? ja nein. Wenn **ja**, geben Sie an, in welchen:

3.2 Liegen über das zu prüfende Arzneimittel bereits aussagekräftige Ergebnisse von klinischen Prüfungen vor? ja nein
Wenn **ja**, bitte geben Sie folgende Daten an:
3.2.1 In welchen Staaten wurden die Prüfungen durchgeführt:
3.2.2 Phase: _____ (Wenn Studien in mehreren Phasen angeführt sind, die höchste Phase angeben)
3.2.3 Zeitraum:
3.2.4 Anwendungsart(en):
3.2.5 Wurde(n) die klinische(n) Prüfung(en) gemäß GCP-Richtlinien durchgeführt? ja nein
3.2.6 Liegt ein Abschlußbericht vor? ja nein
Wenn **ja**, bitte legen Sie die **Investigator's Brochure, relevante Daten** oder ein **Gutachten des Arzneimittelbeirates** bei.

3b. Sonstige im Rahmen der Studie verabreichte Medikamente, deren Wirksamkeit und/oder Sicherheit nicht Gegenstand der Prüfung sind:

Generic Name	Darreichungsform	Dosis

4. Betrifft nur Studien gemäß MPG: Angaben zum Medizinprodukt:

- 4.1 Bezeichnung des Produktes:
4.2 Hersteller:
4.3 Zertifiziert für diese Indikation: ja nein
4.4 Zertifiziert, aber für eine andere Indikation: ja nein
4.5 Das Medizinprodukt trägt ein CE-Zeichen ja nein
4.6 Die Produktbroschüre liegt bei.
4.7 Welche Bestimmungen bzw. Normen sind für die Konstruktion und Prüfung des Medizinproduktes herangezogen worden (Technische Sicherheit):

4.8 Allfällige Abweichungen von den o.a. Bestimmungen (Normen):

5. Angaben zur Versicherung (gemäß §32 Abs.1 Z.11 und Z.12 und Abs.2 AMG; §§47 und 48 MPG)

5.1 Eine Versicherung ist erforderlich: ja nein. Wenn ja:

5.1.1 Versicherungsgesellschaft

5.1.2 Adresse:

5.1.3 Telefon:

5.1.4 Polizzenummer:

5.1.5 Gültigkeitsdauer:

Diese Angaben müssen in der Patienten- / Probandeninformation enthalten sein!

6. Angaben zur durchzuführenden Therapie und Diagnostik

6.1. Welche Maßnahmen bzw. Behandlungen werden **ausschließlich studienbezogen** durchgeführt?

Art	Anzahl/Dosis	Zeitraum	Insgesamt
Entnahme von Myokardproben von all denjenigen Herzen , die aufgrund des erhoehten Alters oder anderer Kontraindikationen NICHT für die Herztransplantation geeignet sind. Die Proben werden im Rahmen der Organexplantation entnommen. Anschließend biomechanische, histologische und polarisationsmikroskopische Untersuchungen an den Myokardgewebeproben. Die Myokardproben werden unterschiedlich sowohl für den biaxialen Zugversuch als auch für den triaxialen Scherversuch präpariert, mechanisch vermessen und analysiert, um ein bestmögliches Resultat zu erhalten.	Aus den beiden Herzventrikeln werden pro Herz mind. 8 Herzmuskelproben entnommen.		2.5 Jahre

6.2. Welche speziellen Untersuchungen (**nur invasive und strahlenbelastende**) werden während des Studienzeitraumes **zu Routinezwecken** durchgeführt:

Art	Anzahl/Dosis	Zeitraum	Insgesamt

7. Strukturierte Kurzfassung des Projektes (*in deutscher Sprache, kein Verweis auf das Protokoll*)

<p>7.1 Wenn Original-Projekttitle nicht in Deutsch: Deutsche Übersetzung des Titels: Biomechanik des humanem ventrikulärem Myokardiums (Biaxiale und triaxiale mechanische Untersuchung)</p>
<p>7.2 Zusammenfassung des Projektes (Rechtfertigung, Relevanz, Design, Maßnahmen und Vorgehensweise): Das mechanische Verhalten der Ventrikel des menschlichen Myokards (linker Ventrikel, rechter Ventrikel und Septum), im Speziellen der Muskelzellen und der umliegenden kollagenen Faserkomponenten, ist bis dato noch sehr dürtig erforscht. Eine systematische, biomechanische, mikrostrukturelle und histologische Untersuchung des humanen Herzmuskels soll daher durchgeführt werden. Daten aus biaxialen Zugversuchen am menschlichen Myokardgewebe existieren bis heute nur in sehr geringem Ausmaß, Daten aus triaxialen Scherversuchen existieren de facto gar nicht. Insbesondere sind die Einflüsse der zu Verbänden von mehrlagig angeordneten Muskelfasern zusammengesetzten sogenannten Sheet-Strukturen zu erfassen. Dazu werden Gewebescheiben in Hauptmuskelfaserrichtung mittels biaxialen Zugversuchen unter verschiedenen Lastprotokollen biomechanisch getestet. Neben den biaxialen Zugversuchen sollen die Schereigenschaften des Myokards auch mit Hilfe eines triaxialen Kraftaufnehmers, entsprechend der Koordinatenachsen die sich aus der Muskelfaserrichtung und Sheets ergeben, gemessen werden. Die daraus resultierenden Ergebnisse, sollen vorallem auch einer späteren mathematischen Modellierung dienen, welche die Einhaltung der drei Dimensionen unbedingt voraussetzt. Anschließend werden die laminare Struktur und Komponenten der geprüften Bereiche histologisch untersucht. Die folglich erhaltene räumliche Mikrostruktur der mechanisch relevanten Komponenten soll Aufschluss über noch nicht verstandene Einflüsse der Sheet-Strukturen auf die Stabilität des Herzwandgewebes geben. Derartig kombinierte biomechanische Daten von humanen Herzmuskelgeweben existieren bis heute nur in sehr geringem Ausmaß. Das Projekt erstreckt sich weniger über eine geplante Dauer, als über ein Versuchskontingent von mindestens 30 menschlichen Herzen. Dabei sollen jeweils beide Ventrikel eines menschlichen Herzens post-mortem getestet werden. Für die biaxialen mechanischen Untersuchungen sind die Herzen so zu beschneiden, dass sich je 3 Proben aus der lateralen Wand des linken Ventrikels, sowie je 2 Proben aus dem Septum und der medialen Wand des rechten Ventrikels extrahieren lassen. Für Untersuchungen der triaxialen Schereigenschaften werden, jeweils 3 Würfel vom linken und rechten Ventrikel in einem Winkel von 45° zur Base entnommen. Es sind keine Atria, Herzohren, Klappen oder versorgende Gefäße zur Untersuchung nötig. Die Proben werden im Rahmen der Organexplantation entnommen und in einer kardioplegischen Lösung bis zu den Präparationen und den Tests bei 2-4°C gelagert. Selbige dient dazu, fortschreitende Autolyse zu minimieren. Die Tests an den Proben aus dem Herzgewebe finden aufgrund der Autolyse auch innerhalb 24h statt. Nach Abschluss werden die Gewebeproben in Formalin fixiert, um die mikroskopischen Struktur-Untersuchungen durchführen zu können. Folgende Maßnahmen bzw. Voraussetzungen werden bei der Präparateentnahme berücksichtigt (die klinische Transplantation wird durch die Probenentnahme nicht beeinträchtigt - siehe auch 7.6.): 1) Die Ventrikelproben werden sofort nach der Gewinnung aus dem Herzen in kardioplegischer Lösung bei 4°C eingelegt. 2) Extraktion der quadratischen Proben für den biaxialen Zugversuch aus dem spezifizierten Herzgewebe der Ventrikel und zusätzliche Extraktion von würfelförmigen Proben aus den Ventrikel für den triaxialen Scherversuch. 3) Erfassung der Hauptfaserrichtungen der Gewebeober- und Gewebegrundflächen durch mikroskopische Untersuchung für die biaxialen Zugversuche. (biaxial) Erfassung der Sheet-Strukturen und Muskelfaserrichtung durch eine mikroskopische Untersuchung bzw. mit Hilfe eines Vergrößerungsglases für die triaxialen Scherversuche. (triaxial) 4) Zuschneiden der Proben in definierter Größe (25x25x2,5mm) (LxBxT) in der mittleren Hauptfaserrichtung. (biaxial) Zuschneiden der Proben in definierter Größe (4x4x4mm) (LxBxH) entsprechend eines definierten Koordinatensystems. (triaxial) 5) Biaxial: Proben mit quadratischem Grundriss für die biaxialen mechanischen Untersuchungen</p>

<p>werden aus dem Herzgewebe präpariert. Biaxiale Zugversuche mit verschiedenen Lastprotokollen bezüglich der Axial- und Umfangsrichtung werden an den Proben durchgeführt, wobei die Deformation der Probe berührungsfrei mit einem Videoextensometer bestimmt wird.</p> <p>Triaxial: Die extrahierten würfelförmigen Proben werden mit Hilfe eines Videoextensometers nachgemessen und deren Spannungs-Dehnungs-Kurven durch die Scherversuchsanlage aufgezeichnet.</p> <p>6) Histologische Untersuchungen der getesteten Proben hinsichtlich der Verteilung und des Vorkommens besagter Herzfaserverbände (den sog. Sheets) mit Spezialfärbung der elastischen und kollagenen Fasern.</p>
<p>7.3 Ergebnisse der prä-klinischen Tests oder Begründung für den Verzicht auf prä-klinischen Tests: In einer Pilot-Studie konnte gezeigt werden, dass biaxiale und triaxiale Tests an 15 frischen Schweineherzen eine deutliche Relevanz der Sheet-Struktur auf die biomechanischen Eigenschaften des ventrikulären Myokards erkennen lassen. Da diese Eigenschaften bei verschiedenen Spezies deutliche Unterschiede aufweisen, soll diese Abhängigkeit nun auch am humanen Myokard überprüft bzw. nachgewiesen werden.</p>
<p>7.4 Primäre Hypothese der Studie (wenn relevant auch sekundäre Hypothesen): Die biaxiale und triaxiale Untersuchung der biomechanischen Eigenschaften und deren Variation in Zusammenhang mit den erhaltenen Sheet-Strukturen der Gewebeprobe, soll den wesentlichen Einfluss der Herzmuskelfaserverbände (Sheets) auf die Systemeigenschaften des Myokardiums nachweisen und beschreiben. Dadurch werden grundlegende, mechanische und bis dato nicht existente Daten der Mechanik des ventrikulären Herzmuskelgewebes gewonnen und diese für computerunterstützte Simulationen nutzbar gemacht.</p>
<p>7.5 Relevante Ein- und Ausschlusskriterien:</p>
<p>7.6 Ethische Überlegungen (Identifizieren und beschreiben Sie alle möglicherweise auftretenden Probleme. Beschreiben Sie den möglichen Wissenszuwachs, der durch die Studie erzielt werden soll und seine Bedeutung, sowie mögliche Risiken für Schädigungen oder Belastungen der Prüfungsteilnehmer/innen. Legen Sie Ihre eigene Bewertung des Nutzen/Risiko-Verhältnisses dar):</p> <ol style="list-style-type: none"> 1. Die Probengewinnung wird nur an Herzen durchgeführt, die für Transplantationen ungeeignet sind. 2. Die Probengewinnung wird sorgfältig von einem Transplantationschirurgen im Rahmen Explantation durchgeführt. 3. Während der Probengewinnung wird ein Protokoll geführt, das die Daten des Patienten sowie die Art und Zweck der Herzmanipulation beinhaltet. 4. Die Probengewinnung erfolgt in pietätvoller Weise. 5. Die Probengewinnung dient keinem finanziellen Zweck. 6. Die Probengewinnung dient einer klaren Zielsetzung, die zukünftig der ärztlichen Betreuung von Patienten dient.
<p>7.7 Begründung für den Einschluss von Personen aus geschützten Gruppen (z.B. Minderjährige, temporär oder permanent nicht-einwilligungsfähige Personen; wenn zutreffend):</p>
<p>7.8 Beschreibung des Rekrutierungsverfahrens (alle zur Verwendung bestimmte Materialien, z.B. Insete inkl. Layout müssen beigelegt werden): Entnahme von Gewebeprobe nach einer erforderlichen Herztransplantation an der klinischen Abteilung für Transplantationschirurgie der Medizinischen Universität Graz.</p>
<p>7.9 Vorgehensweise an der/den Prüfstelle(n) zur Information und Erlangung der informierten Einwilligung von Prüfungsteilnehmer/innen/n, bzw. Eltern oder gesetzlichen Vertreter/innen/n, wenn zutreffend (wer wird informieren und wann, Erfordernis für gesetzliche Vertretung, Zeugen, etc.):</p>
<p>7.10 Risikoabschätzung, vorhersehbare Risiken der Behandlung und sonstiger Verfahren, die verwendet werden sollen (inkl. Schmerzen, Unannehmlichkeiten, Verletzung der persönlichen Integrität und Maßnahmen zur Vermeidung und/oder Versorgung von unvorhergesehenen / unerwünschten Ereignissen):</p>

5 Appendix

7.11 Voraussichtliche Vorteile für die eingeschlossenen Prüfungsteilnehmer/innen:
7.12 Relation zwischen Prüfungsteilnehmer/in und Prüfer/in (z.B. Patient/in - Ärztin/Arzt, Student/in - Lehrer/in, Dienstnehmer/in - Dienstgeber/in, etc.):
7.13 Verfahren an der/den Prüfstelle(n) zur Feststellung, ob eine einzuschließende Person gleichzeitig an einer anderen Studie teilnimmt oder ob eine erforderliche Zeitspanne seit einer Teilnahme an einer anderen Studie verstrichen ist (von besonderer Bedeutung, wenn gesunde Proband/inn/en in pharmakologische Studien eingeschlossen werden):
7.14 Methoden, um unerwünschte Effekte ausfindig zu machen, sie aufzuzeichnen und zu berichten (Beschreiben Sie wann, von wem und wie, z.B. freies Befragen und/oder an Hand von Listen):
7.15 Optional: Statistische Überlegungen und Gründe für die Anzahl der Personen, die in die Studie eingeschlossen werden sollen (ergänzende Informationen zu Punkt 8, wenn erforderlich): In bekannter Literatur weisen Studien dieses Umfanges an tierischem Gewebe bereits gute Aussagekraft über die biomechanischen Zusammenhänge auf.
7.16 Optional: Verwendete Verfahren zum Schutz der Vertraulichkeit der erhobenen Daten, der Quelldokumente und von Proben (ergänzende Informationen zu Punkt 8, wenn erforderlich): Patientenbezogene Daten (Alter, Geschlecht, Krankheiten) werden nur in anonymisierter Form mit den Analyseergebnissen verglichen, so dass keine Beziehung zwischen den Daten einerseits und der Identität der Patienten andererseits hergestellt werden kann.
7.17 Plan zur Behandlung oder Versorgung nachdem die Personen ihre Teilnahme an der Studie beendet haben (wer wird verantwortlich sein und wo): -
7.18 Betrag und Verfahren der Entschädigung oder Vergütung an die Prüfungsteilnehmer/innen (Beschreibung des Betrages, der während der Prüfungsteilnahme bezahlt wird und wofür, z.B. Fahrtspesen, Einkommensverlust, Schmerzen und Unannehmlichkeiten, etc.): -
7.19 Regeln für das Aussetzen oder vorzeitige Beenden der Studie an der/den Prüfstelle(n) in diesem Mitgliedstaat oder der gesamten Studie: -
7.20 Vereinbarung über den Zugriff der Prüferin/des Prüfers/der Prüfer auf Daten, Publikationsrichtlinien, etc. (wenn nicht im Protokoll dargestellt): Daten die in Publikationen veröffentlicht werden unterliegen den strengen Kriterien der Journals und sind anonymisiert.
7.21 Finanzierung der Studie (wenn nicht im Protokoll dargestellt) und Informationen über finanzielle oder andere Interessen der Prüferin/des Prüfers/der Prüfer: Institutseigene Mittel, FWF Einzelprojekt-Forschungsförderung
7.22 Weitere Informationen (wenn erforderlich): -

8. Biometrie, Datenschutz:

(Hier nur Kurzinformationen in Stichworten, ausführlicher - wenn erforderlich - unter Punkt 7.15 und 7.16)

8.1 Studiendesign (z.B. doppelblind, randomisiert, kontrolliert, Placebo, Parallelgruppen, multizentrisch)

- 8.1.1 offen 8.1.2 randomisiert 8.1.3 Parallelgruppen 8.1.4 monozentrisch
 8.1.5 blind 8.1.6 kontrolliert 8.1.7 cross-over 8.1.8 multizentrisch
 8.1.9 doppelblind 8.1.10 Placebo 8.1.11 faktoriell 8.1.12 Pilotprojekt
 8.1.13 observer-blinded 8.1.14 Äquivalenzprüfung
 8.1.15 sonstiges:

8.1.16 Anzahl der Gruppen:

8.1.17 Stratifizierung: nein ja: Kriterien:8.1.18 Messwiederholungen: nein ja: Zeitpunkte:

8.1.19 Hauptzielgröße:

8.1.20 Nullhypothese(n): -

8.1.21 Alternativhypothese(n): -

8.1.22 Nebenzielgrößen:

8.2 Studienplanung

Die Fallzahlberechnung basiert auf (Alpha = Fehler 1. Art, Power = 1 – Beta = 1 – Fehler 2. Art):

8.2.1 Alpha: 8.2.2 Power: 8.2.3 Stat.Verfahren:

8.2.4 Multiples Testen: nein ja: Korrekturverfahren.:

8.2.5 Erwartete Anzahl von Studienabbrecher/inne/n (Drop-out-Quote):

8.3 Geplante statistische Analyse

Population: 8.3.1 Intention-to-treat 8.3.2 Per protocol8.3.3 Zwischenauswertung: nein ja: Abbruchkriterien:

8.3.4 Geplante statistische Verfahren: **deskriptive Statistik, Mittelwert, Standardabweichung, Korrelationstests (Korrelationskoeffizienten nach Pearson), stat. Auswertung werden mittels spezieller Software (OriginLab) durchgeführt, siehe auch Studienprotokoll.**

8.4 Dokumentationsbögen / Datenmanagement

8.4.1 Angaben zur Datenqualitätsprüfung

8.4.2 Angaben zum Datenmanagement

Patientenbezogene Daten werden nur in anonymisierter / codierter Form mit den Analyseergebnissen verglichen. (Eurotransplant Nummer) Die relevanten Daten werden unmittelbar nach der Explantation auf Dokumentationsbögen übertragen, so dass keine Beziehung zwischen den Daten einerseits und der Identität der Patienten andererseits hergestellt werden kann. Da die zu erwartenden Ergebnisse derzeit nicht unmittelbar für die Therapie (von Blutsverwandten) relevant sind, ist eine Weiterleitung der erzielten wissenschaftlichen Ergebnisse an die jeweiligen Angehörigen im Rahmen der Studie nicht vorgesehen. Die Sammlung der anonymisierten Daten und das Datenmanagement, sowie statistische Berechnungen erfolgen am Institut für Biomechanik, Technische Universität Graz.

8.5 Verantwortliche und Qualifikation

8.5.1 Wer führte die biometrische Planung durch (ggf. Nachweis der Qualifikation)?

DI Dr. Gerhard Sommer, Prof. Dr. Gerhard A. Holzapfel

8.5.2 Wer wird die statistische Auswertung durchführen (ggf. Nachweis der Qualifikation)?

Michael Kutschera (triaxiale Scherversuche), Roland Kresnik (biaxiale Zugversuche), Statistiker des Institutes für Biomechanik, TU Graz

5 Appendix

8.6 Datenschutz

8.6.1 Die Datenverarbeitung erfolgt a) personenbezogen b) indirekt personenbezogen
c) nicht personenbezogen

8.6.2 Wenn a): Begründung:

DVR-Nummer:

8.6.3 Wenn b): Wie erfolgt die Verschlüsselung?

Sämtliche Daten werden im Datenblatt anonym geführt.

9. Liste der eingereichten Unterlagen (wenn nicht gesondert dem Antrag beiliegend):

Dokument	Version/Identifikation	Datum
Protokoll	BiomechMyocard V2.0	14.12.11
Kurzfassung		
Patienteninformation / Einwilligungserklärung		
Prüfbogen (Case Report Form, CRF)		
Versicherungsbestätigung		
Amendment Nr.		
Amendment Nr.		
Amendment Nr.		
Lokales Amendment Nr.		

Name und Unterschrift der Antragstellerin/des Antragstellers

- 9.1 Name: **Dr. med.univ. Michaela Schwarz**
 9.2 Institution/ Firma: **Klinische Abteilung für Transplantationschirurgie**
 9.3 Position: **Assistenzärztin in Ausbildung**
 9.4 Antragsteller/in ist 9.4.1 koordinierende/r Prüfer/in (multizentrische Studie)
 (nur AMG-Studien) 9.4.2 Hauptprüfer/in (monozentrische Studie)
 9.4.3 Sponsor bzw. Vertreter/in des Sponsors
 9.4.4 vom Sponsor autorisierte Person/Organisation

Ich bestätige hiermit, dass die in diesem Antrag gemachten Angaben korrekt sind und dass ich der Meinung bin, dass die Durchführung der Studie in Übereinstimmung mit dem Protokoll, nationalen Regelungen und mit den Prinzipien der Guten Klinischen Praxis möglich sein wird.

Weiters stimme ich mit meiner Unterschrift zu, dass folgende Daten aus meinem Antrag ggf. durch die Ethikkommission veröffentlicht werden, um die Anträge nach Zahl und Inhalt transparent zu machen: EK-Nummer, Einreich-Datum, Projekttitel, Hauptprüfer, Sponsor/CRO, weitere Zentren.
(Im Falle der Nicht-Zustimmung bitte diesen Absatz durchzustreichen)

.....
 Unterschrift der Antragstellerin/des Antragstellers

.....
 Datum

!!! Achtung: Diese Unterschrift ist in jedem Fall erforderlich !!!

Teil B

Studienkurzbezeichnung: Biomechanik des humanen Ventrikels

10. Angaben zur Prüferin/zum Prüfer

10.1 Name: **Dr. med.univ. Michaela Schwarz**

10.2 Krankenanstalt/Institut/Abteilung: **Klinische Abteilung für Transplantationschirurgie**

10.3 Telefon	10.4 „Pieps“/Mobil	10.5 Fax	10.6 e-mail-Adresse:
385 84444	385 80678	385 14446	michaela.schwarz@medunigraz.at

10.7 Jus practicandi: ja nein 10.8 Facharzt für:

10.9 Prüfärztekurs: ja nein

10.10 Sofern relevant: Präklinische Qualifikation (z.B. Labordiagnostik) bzw. Name der Verantwortlichen:

11. Geplante Anzahl der PatientInnen bzw. ProbandInnen an dieser Prüfstelle 30

12. Verantwortliche MitarbeiterInnen an der klinischen Studie (an Ihrer Prüfstelle)

Fr/Hr	Titel	Vorname	Name	Institution
Hr.	Dr.	Gerhard	Sommer	Inst. f. Biomechanik, TU Graz
Hr.	Prof. Dr.	Gerhard A.	Holzapfel	Inst. f. Biomechanik, TU Graz

13. Unterschrift der Prüferin/des Prüfers

Ich bestätige hiermit, dass die in diesem Antrag gemachten Angaben korrekt sind und dass ich der Meinung bin, dass die Durchführung der Studie in Übereinstimmung mit dem Protokoll, nationalen Regelungen und mit den Prinzipien der Guten Klinischen Praxis möglich sein wird.

.....
 Unterschrift der Prüferin/des Prüfers Datum

Bei multizentrischen AMG-Studien sind die Teile B von der Hauptprüferin/dem Hauptprüfer des jeweiligen Zentrums zu unterzeichnen. Alternativ zur Unterschrift auf den Teilen B können die Unterschriften der Hauptprüfer/innen auch auf den Unterschriftenseiten des Protokolls oder der Prüfärzterträge vorgelegt werden. Es muss jedenfalls eine eindeutige - durch Unterschrift dokumentierte - Zustimmung aller Hauptprüfer/innen zum Protokoll vorliegen.

14. Name und Unterschrift der Leiterin/des Leiters der Einrichtung* des Pflegedienstes*

14.1 Name: **Univ. Prof. Dr. Karlheinz Tscheliessnigg**

.....
 Unterschrift der Leiterin/des Leiters Datum

** Die Unterschrift der Leiterin/des Leiters des Pflegedienstes ist für Pflegeforschungsprojekte und die Anwendung neuer Pflegekonzepte und -methoden erforderlich, ansonsten die Unterschrift der Leiterin/des Leiters der jeweiligen Einrichtung. Einrichtung: die Klinik (wenn gegliedert: die klinische Abteilung), die Abteilung oder die gemeinsame Einrichtung*

!!! Achtung: Teil B ist in jedem Fall vollständig auszufüllen, bei multizentrischen klinischen Prüfungen nach AMG für jedes in Österreich teilnehmende Zentrum separat !!!

Ethikkommission



Medizinische Universität Graz

Auenbruggerplatz 2, A-8036 Graz
ethikkommission@medunigraz.at
Tel.: +43 / 316 / 385-13928, Fax: -14348

VOTUM
gültig bis 16.12.2012

EK-Nummer: 24-107 ex 11/12
Studientitel: Biomechanik menschlicher ventrikulärer Myokarde (biaxialer Zugversuch, triaxialer Scherversuch)
Prüfer: *) Dr. Michaela Schwarz
Univ.Klinik für Chirurgie
Sponsor: (Prüfer)
CRO: -

*) Antragsteller

Die o.a. Studie wurde von der Ethikkommission erstmals in der Sitzung 03-11/12 am 12.12.2011 behandelt.

Die Ethikkommission ist zu folgendem Schluss gekommen:

Es besteht kein Einwand gegen die Durchführung der Studie in der vorliegenden Form.

Stimmberechtigte bzw. anwesende Mitglieder bei der Behandlung waren: Siehe beiliegende Liste vom 12.12.2011.

Kommissionsmitglieder, die für diesen Tagesordnungspunkt als befangen anzusehen waren und daher gemäß Geschäftsordnung an der Entscheidungsfindung und Abstimmung nicht teilgenommen haben: keine

Zur Beurteilung vorliegende Dokumente:

Dokumente eingegangen am 18.11.2011, begutachtet in der Sitzung 03-11/12 am 12.12.2011	
✓ Antragsformular	18.11.2011
Originalprotokoll November 2011	
Dokumente eingegangen am 30.11.2011, begutachtet in der Sitzung 03-11/12 am 12.12.2011	
Originalprotokoll November 2011	
Dokumente eingegangen am 05.12.2011, begutachtet in der Sitzung 03-11/12 am 12.12.2011	
✓ Sonstiges: Stellungnahme Prof. Pieske	01.12.2011
Dokumente eingegangen am 14.12.2011, begutachtet im 'expedited Review' am 16.12.2011	
✓ Originalprotokoll 2.0	14.12.2011

Es handelt sich um eine Studie im Rahmen einer Diplomarbeit.

Das Votum der Ethikkommission berührt in keiner Weise die alleinige Verantwortung der Prüferin / des Prüfers / der Prüfer für die ordnungsgemäße Durchführung der Studie unter Einhaltung aller einschlägiger gesetzlicher Bestimmungen und Richtlinien.

Weiters machen wir darauf aufmerksam, dass der Kommission unverzüglich zu melden sind:

- Abweichungen vom Protokoll aus Sicherheitsgründen oder Protokolländerungen
- Änderungen, die das Risiko der Teilnehmer/-innen erhöhen oder die Durchführung der Studie wesentlich beeinflussen
- Mutmaßliche unerwartete schwerwiegende Nebenwirkungen - SUSARs (AMG-Studien ab 1.5.2004)

EK-Nummer: 24-107 ex 11/12

Votum

Seite 1 von 2

Medizinische Universität Graz, Universitätsplatz 3, A-8010 Graz. www.medunigraz.at

Rechtsform: Juristische Person öffentlichen Rechts gem. Universitätsgesetz 2002. Information: Mitteilungsblatt der Universität und www.medunigraz.at. DVR-Nr. 210 9494.
UID: ATU 575 111 79. Bankverbindung: Bank Austria Creditanstalt BLZ 12000 Konto-Nr. 500 948 400 04, Raiffeisen Landesbank Steiermark BLZ 38000 Konto-Nr. 49510.


5 Appendix

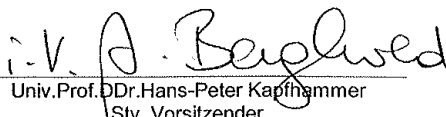
oder schwerwiegende unerwünschte Ereignisse - SAEs (andere Studien)

- Jegliche Information über sonstige Umstände, die die Sicherheit der Teilnehmer/-innen oder die Durchführung der Studie beeinträchtigen können

Dieses Votum gilt für ein Jahr ab dem Datum der Ausstellung. Bei längerer Studiendauer ist rechtzeitig vor Ablauf der Gültigkeit des Votums ein Zwischenbericht vorzulegen (Berichtsformular), um eine etwaige Verlängerung zu erlangen.

Graz, 16. Dezember 2011


Univ.-Prof. Dr. Peter H. Renak
Vorsitzender


Univ.-Prof. Dr. Hans-Peter Kapfhammer
Stv. Vorsitzender

Achtung: Bitte bei allen das Projekt betreffende Schreiben oder telefonischen Anfragen die EK-Nummer angeben!

Ethikkommission



Medizinische Universität Graz

Auenbruggerplatz 2, A-8036 Graz
ethikkommission@medunigraz.at
Tel.: +43 / 316 / 385-13928, Fax: -14348

Liste der stimmberechtigten bzw. anwesenden Mitglieder

am 12. Dezember 2011

Univ.Prof.DI Dr.Andrea Berghold
Univ.Prof.Dr.Josef Donnerer
Univ.Prof.Mag.Dr.H.Jesser-Huß
Univ.Prof.Dr.Elisabeth Mahla
Univ.Prof.Dr. Leopold Neuhold
Univ.Prof.DI Dr.Peter H. Rehak
Univ.Prof.Dr.Ekkehard Ring
OPfl. DGKP Thomas Schelischansky, MSc
Univ.Prof.Dr. Michael Speicher
Univ.Prof.Dr.Rudolf Stauber
Mag.Monika Steinwender
Univ.Prof.Dr.Hermann Toplak
Ursula Vennemann
Univ.Prof.Dr.Kurt Weber
Univ.Prof.Dr.Andreas Zimmer
Ing.Franz Deutschmann
Doz.Dr.Christian Fazekas
Univ.Prof.DI Dr.Josef Haas
Univ.Prof.DDr.Hans-Peter Kapfhammer

Beigezogene Fachärzte

PD Dr.Philipp Klaritsch

EK-Nummer: 24-107 ex 11/12

Mitgliederliste

Medizinische Universität Graz, Universitätsplatz 3, A-8010 Graz. www.medunigraz.at

Rechtsform: Juristische Person öffentlichen Rechts gem. Universitätsgesetz 2002. Information: Mitteilungsblatt der Universität und www.medunigraz.at. DVR-Nr. 210 9494.
UID: ATU 575 111 79. Bankverbindung: Bank Austria Creditanstalt BLZ 12000 Konto-Nr. 500 948 400 04, Raiffeisen Landesbank Steiermark BLZ 38000 Konto-Nr. 49510.

Bibliography

- Akiyama, N., Ohnuki, Y., Kunioka, Y., Saeki, Y., and Yamada, T. (2006). Transverse stiffness of myofibrils of skeletal and cardiac muscles studied by atomic force microscopy. *The Journal of Physiological Sciences*, 56(2):145–151.
- Anversa, P. (2000). Myocyte death in the pathological heart. *Circ. Res.*, 86:121–124.
- Baldock, C., Oberhauser, A. F., Ma, L., Lammie, D., Siegler, V., Mithieux, S. M., Tu, Y., Chow, J. Y., Suleman, F., Malfois, M., Rogers, S., Guo, L., Irving, T. C., Wess, T. J., and Weiss, A. S. (2011). Shape of tropoelastin, the highly extensible protein that controls human tissue elasticity. *Proc. Natl. Acad. Sci. U.S.A.*, 108:4322–4327.
- Caulfield, J. B. and Borg, T. K. (1979). The collagen network of the heart. *Lab. Invest.*, 40:364–372.
- Costa, K. D., Hunter, P. J., Wayne, J. S., Waldman, L. K., Guccione, J. M., and McCulloch, A. D. (1996). A three-dimensional finite element method for large elastic deformations of ventricular myocardium: II—prolate spheroidal coordinates. *J Biomech Eng*, 118:464–472.
- Demer, L. L. and Yin, F. C. (1983). Passive biaxial mechanical properties of isolated canine myocardium. *J. Physiol. (Lond.)*, 339:615–630.
- Demiray, H. (1976). Large deformation analysis of some basic problems in biophysics. *Bull. Math. Biol.*, 38:701–712.
- Dokos, S., Smaill, B. H., Young, A. A., and LeGrice, I. J. (2002). Shear properties of passive ventricular myocardium. *Am. J. Physiol. Heart Circ. Physiol.*, 283:H2650–2659.
- Downing, B. P. (2009). Using optical tweezers to probe the elasticity of short molecules. In *The American Physical Society*.
- Fujii, T., Sun, Y.-L., An, K.-N., and Luo, Z.-P. (2002). Mechanical properties of single hyaluronan molecules. *Journal of Biomechanics*, 35(4):527 – 531.
- Fung, Y. (1993). *Biomechanics: mechanical properties of living tissues*. Springer, ISBN 978-0-387-97947-2, Hardcover.
- Gittes, F., Mickey, B., Nettleton, J., and Howard, J. (1993). Flexural rigidity of microtubules and actin filaments measured from thermal fluctuations in shape. *J. Cell Biol.*, 120:923–934.

- Greenbaum, R. A. and Gibson, D. G. (1981). Regional non-uniformity of left ventricular wall movement in man. *Br Heart J*, 45:29–34.
- Greenbaum, R. A., Ho, S. Y., Gibson, D. G., Becker, A. E., and Anderson, R. H. (1981). Left ventricular fibre architecture in man. *Br Heart J*, 45(hello):248–263.
- Guccione, J. M., McCulloch, A. D., and Waldman, L. K. (1991). Passive material properties of intact ventricular myocardium determined from a cylindrical model. *J Biomech Eng*, 113:42–55.
- Hohenadl, M., Storz, T., Kirpal, H., Kroy, K., and Merkel, R. (1999). Desmin filaments studied by quasi-elastic light scattering. *Biophys. J.*, 77:2199–2209.
- Holzapfel, A. and Ogden, R. W. (2006). *Mechanics of biological tissue*. Springer-Verlag Berlin Heidelberg.
- Holzapfel, G. A. (2010). Lecture at graz university of technology on biomechanik biologischer gewebe 450.001, wintersemester 2009/10, institute of biomechanics. Graz University of Technology, Institute of Biomechanics.
- Holzapfel, G. A. and Ogden, R. W. (2009). Constitutive modelling of passive myocardium: a structurally based framework for material characterization. *Philos Transact A Math Phys Eng Sci*, 367:3445–3475.
- Holzapfel, G. A., Sommer, G., and Regitnig, P. (2004). Anisotropic mechanical properties of tissue components in human atherosclerotic plaques. *J Biomech Eng*, 126:657–665.
- Hooks, D. A. (2007). Myocardial segment-specific model generation for simulating the electrical action of the heart. *Biomed Eng Online*, 6:21.
- Humphrey, J. D. (2002). *Cardiovascular Solid Mechanics: Cells, Tissues, and Organs*. Springer, ISBN 978-0-387-95168-3, Hardcover.
- Humphrey, J. D., Strumpf, R. K., and Yin, F. C. (1990). Biaxial mechanical behavior of excised ventricular epicardium. *Am. J. Physiol.*, 259:H101–108.
- Humphrey, J. D. and Yin, F. C. (1987). On constitutive relations and finite deformations of passive cardiac tissue: I. a pseudostrain-energy function. *J Biomech Eng*, 109:298–304.
- Kauer, D. M.-I. E. M. (2001). *Inverse finite element characterization of soft tissue with aspiration elements*. Phd-thesis, ETH Zurich.
- Kuehnel, W. (2003). *Color atlas of cytology, histology, and microscopic anatomy*. Georg Thieme Verlag, ISBN 3-13-5562404-8 (GTV).
- Li, J., Dao, M., Lim, C. T., and Suresh, S. (2005). Spectrin-level modeling of the cytoskeleton and optical tweezers stretching of the erythrocyte. *Biophys. J.*, 88:3707–3719.

- Medic on Web, . (2012). Layers of the heart wall.
- Ng L., Patwari P., S. J. P. A. (2005). Aggrecan conformation, persistence length, and stiffness depend on the nanomolecular properties of its constituent gag chains.
- Nielsen, P. M., Le Grice, I. J., Smaill, B. H., and Hunter, P. J. (1991). Mathematical model of geometry and fibrous structure of the heart. *Am. J. Physiol.*, 260:H1365–1378.
- Novak, V. P., Yin, F. C., and Humphrey, J. D. (1994). Regional mechanical properties of passive myocardium. *J Biomech*, 27:403–412.
- Parry, D. A., Strelkov, S. V., Burkhard, P., Aebi, U., and Herrmann, H. (2007). Towards a molecular description of intermediate filament structure and assembly. *Exp. Cell Res.*, 313:2204–2216.
- Richfield, D. (2008). Picture of sacromere. Wikipedia, picture of sacromere.
- Rohmer, D., Sitek, A., and Gullberg, G. T. (2006). Reconstruction and visualization of fiber and sheet structure with regularized tensor diffusion mri in the human heart. Technical report, Lawrence Berkeley National Laboratory, LBNL-60277.
- Rossi, M. A., Abreu, M. A., and Santoro, L. B. (1998). Connective tissue skeleton of the human heart : A demonstration by cell-maceration scanning electron microscope method. *Circulation*, 97(9):934–935.
- Sacks, M. S. and Chuong, C. J. (1993). Biaxial mechanical properties of passive right ventricular free wall myocardium. *J Biomech Eng*, 115:202–205.
- Schleip, R., Naylor, I. L., Ursu, D., Melzer, W., Zorn, A., Wilke, H. J., Lehmann-Horn, F., and Klingler, W. (2006). Passive muscle stiffness may be influenced by active contractility of intramuscular connective tissue. *Med. Hypotheses*, 66:66–71.
- Stalhand, J., Klarbring, A., and Holzapfel, G. A. (2008). Smooth muscle contraction: mechanochemical formulation for homogeneous finite strains. *Prog. Biophys. Mol. Biol.*, 96:465–481.
- Stokke, B. T., Mikkelsen, A., and Elgsaeter, A. (1985). Human erythrocyte spectrin dimer intrinsic viscosity: temperature dependence and implications for the molecular basis of the erythrocyte membrane free energy. *Biochim. Biophys. Acta*, 816:102–110.
- Streeter, D. D. and Hanna, W. T. (1973). Engineering mechanics for successive states in canine left ventricular myocardium. fiber angle and sarcomere length. *Circ. Res.*, 33:656–664.
- Sun, Y. L., Luo, Z. P., Fertala, A., and An, K. N. (2004). Stretching type ii collagen with optical tweezers. *J Biomech*, 37:1665–1669.

- Svoboda, P., Kvapil, P., Insel, P. A., and Ransnas, L. A. (1992). Plasma-membrane-independent pool of the alpha subunit of the stimulatory guanine-nucleotide-binding regulatory protein in a low-density-membrane fraction of s49 lymphoma cells. *Eur. J. Biochem.*, 208:693–698.
- Texas-Heart-Institute (2012). Homepage of texas heart institute at st. luke’s episcopal hospital.
- The-Cardio-Researched-Web-Project (2012). Cardiomyocytes. The Cardio Research Web Project.
- Tyska, M. J. and Warshaw, D. M. (2002). The myosin power stroke. *Cell Motil. Cytoskeleton*, 51:1–15.
- Weber, K. T. (1989). Cardiac interstitium in health and disease: the fibrillar collagen network. *J. Am. Coll. Cardiol.*, 13:1637–1652.
- Weber, K. T., Brilla, C. G., and Janicki, J. S. (1993). Myocardial fibrosis: functional significance and regulatory factors. *Cardiovasc. Res.*, 27:341–348.
- Yin, F. C. (1981). Ventricular wall stress. *Circ. Res.*, 49:829–842.
- Yin, F. C., Strumpf, R. K., Chew, P. H., and Zeger, S. L. (1987). Quantification of the mechanical properties of noncontracting canine myocardium under simultaneous biaxial loading. *J Biomech*, 20:577–589.
- Zeng, W., Snedaker, A. K., Megee, S., Rathi, R., Chen, F., Honaramooz, A., and Dobrinski, I. (2009). Preservation and transplantation of porcine testis tissue. *Reprod. Fertil. Dev.*, 21:489–497.

Statutory Declaration

I declare that I have authored this Thesis independently, that I have not used other than the declared sources/resources, and that I have explicitly marked all material, which has been quoted by the relevant reference.

date

signature